Exploring the origins of multicellularity using experimental populations of *Pseudomonas fluorescens* SBW25: Deciphering the genetic basis of an environmentally-responsive developmental switch

A thesis presented in partial fulfillment of the requirements for the degree of

Master of Natural Sciences

at Massey University, Auckland, New Zealand

Joanna Amelia Summers

2018

Abstract

The evolution of multicellularity was a significant evolutionary event that occurred on numerous independent occasions in the history of life. It is useful to consider this in the Darwinian population framework: a population may participate in evolution by natural selection given that it satisfies the criteria of – variation, reproduction, and heredity. The transition from unicellular to multicellular life represented the emergence of Darwinian properties at a new hierarchical level, and the shift of Darwinian individuality from the level of the individual cell to the cooperating cell collective. This required a mechanism of reproduction of the collective; best conceived with nascent multicellular life cycles, likely manifest through clonal development and single-cell bottlenecks to mediate conflict between levels of selection. For the origin of multicellularity, transitioning between phases of the life cycle was also dependent on the evolution of developmental processes that integrate the activity of the individual cells and the collective. An experiment previously conducted in the Rainey laboratory explored the origins of multicellularity using *Pseudomonas fluorescens* SBW25, selecting for the evolution of a developmental program to transition between the soma-like SM and germ-like WS phases of the life cycle. Derived from this experiment was the TSS-f6 genotype, that demonstrates an environmentally-responsive capacity to change phenotype – resembling a primitive multicellular organism able to transition through the life cycle under developmental regulation. Whole-genome sequencing revealed the mutational history of TSS-f6, with a substitution in the *wspA* gene necessary for the phenotype; the WspA chemoreceptor hypothesised to sense environmental oxygen. Suppressor analysis of the TSS-f6 phenotype revealed the underlying activation pathways: for the WS phenotype – the *wsp* & *wss* operons, and *mut* genes; and the SM phenotype – *pflu5960*, *amrZ*, and *wspE*. From this genetic dissection a simple model was proposed for the TSS-f6 developmental switch, though the role of *wspE* and the DNA mismatch repair system remain unexplained. The TSS-f6 genotype provided the opportunity to gain mechanistic insight into the emergence of a nascent life cycle under the control of a developmental program, and thus the origins of multicellularity and development in itself.

Acknowledgements

Firstly, I would like to thank my supervisor Professor Paul Rainey for providing such an interesting and challenging project for my research. For putting his confidence in me to self direct my own work, whilst still providing constant wisdom and support when required.

I would like to acknowledge Michael Barnett for all his help, and for letting me constantly annoy him in the office. Also to the support from Philippe Remigi and Daniel Rexin, who were always there to answer my questions and troubleshoot experiments. And to the rest of the Rainey lab for providing a good atmosphere to complete my research in.

I highly appreciate the financial support from Massey University, my Masters fees funded under the Massey University Albany Vice Chancellor's Natural Sciences Excellence Award.

Lastly, I would like to thank my Mum and Dad for providing such a strong foundation and for supporting all my endeavours, allowing me to reach the place I am today. And to my friends and family for keeping me sane through the past two years; notably Davina, Elaine, and Ronald. I couldn't have done it without you all, so thank you.

Table of Contents

Table of Abbreviations

Abbreviation	Meaning
ALI	Air liquid interface
Amp	Ampicillin
AP-PCR	Arbitrary primed-polymerase chain reaction
BLAST	Basic local alignment search tool
bp	base pair
c-di-GMP	Cyclic-dimeric-guanosine monophosphate
DGC	Di-guanylate cyclase
DNA	Deoxyribonucleic acid
dNTP	dinucleotide triphosphate
g	gram or gravity
G	guanine
GPM	Genotype-phenotype map
hr	hour
kb	kilobase pair
KB	King's broth
Km	Kanamycin
LB	Lysogeny broth
LSWS	Large spreading wrinkly spreader
min	minute
Nf	Nitrofurantoin
PCR	Polymerase chain reaction
PDE	Phosphodiesterase
Rif	Rifampicin
rpm	revolutions per minute
sec	second
SM	Smooth morphology
Tet	Tetracycline
TSS	Temperature sensitive switcher
WS	Wrinkly spreader
WT	Wild type

Chapter 1: Introduction

Evolution is a remarkable process with more than spectacular consequence, producing the unity and diversity of life and phenotypic traits that we see around us. Since the introduction of Darwin's (1859) theory of evolution by natural selection understanding of this process has continued to grow, especially with the experimental observation of evolution in microorganisms in real time. As outlined by Lewontin (1970), it is useful to consider evolutionary change in the context of Darwinian populations: according to this framework a population participates in the process of evolution by natural selection provided that individuals differ from one another (there is variation), individuals reproduce, and offspring resemble parental types (there is heredity). It is increasingly evident that entities with these Darwinian characteristics exist at multiple levels of biological organisation, giving life a hierarchical structure. For example multicellular organisms are comprised of cells – the organism itself is an individual in a Darwinian sense and so too are the cells of which it is composed. The evolution of multicellular life from single cells marks a major evolutionary transition (Maynard Smith & Szathmáry, 1995), in which the lower level entity of cells came together to form the multicellular entity of the cell collective, that like the individual cells from which it is composed, manifests Darwinian properties (Godfrey-Smith, 2009). It is the emergence of these properties during the evolution of multicellularity that is of central concern. Central to this transition is reproduction: the evolution of mechanisms that allow simple cooperating groups to leave collective-level offspring. This requires a life cycle, the origins of which, while unclear, are expected to involve clonal development of a collective phase and passage through a single-cell bottleneck stage (Ratcliff et al., 2017). The transitioning between phases of the life cycle are dependent on developmental processes that integrate the activity of individual cells and the collective.

To preface: the work reported in this thesis concerns a bacterial genotype derived from an experimental investigation into the origins of multicellularity (Hammerschmidt et al., 2014), that has evolved a capacity to transition between phases of a life cycle in response to an environmental cue. My goal has been to understand the genetic basis of this ability and thus shed light on how developmental programs emerge. Understanding this topic requires the

presentation of a number of pertinent issues, including: evolution by natural selection, Darwinian populations, and major evolutionary transitions; the evolution of multicellularity and link to life cycles, developmental regulation, and phenotypic switching; the concept and variational properties of the genotype-phenotype map and the constraint of evolution by genetic architecture; and the *Pseudomonas fluorescens* SBW25 (*P. fluorescens* SBW25) model system, wrinkly-spreader (WS) phenotype, and the life cycle experiment.

1.1 Background Evolutionary Theory

1.1.1 Evolution by natural selection

To provide context for the ideas discussed in this thesis, the relevant evolutionary theory will first be presented. The breakthrough in the history of evolutionary theory may be attributed to ideas presented by Charles Darwin (1859) in his book entitled *On the Origin of Species*, as well as to the works of Alfred Wallace. Darwin (1859) conceived the theory of evolution by natural selection to explain the diversity of life on earth, providing a mechanism for evolutionary change within populations. According to Malthus' (1798) theory of population growth, populations grow at an exponential rate when resources are in abundance, and reach a point of crisis when these resources become insufficient to sustain the size of the population. From this theory, Darwin (1859) deduced a 'struggle for existence', where individuals in a population must compete against one another for limited resources, also facing pressure from changing environmental conditions (Continenza, 2009). There is genetic variation within populations, as a result of random mutation due to errors in DNA replication and repair, and consequently phenotypic variation. Darwin (1859) explains that due to variation in phenotype in a population, some individuals will have a higher fitness in a given environment, thus are more likely to survive and reproduce and pass on these favourable phenotypic traits to future generations. Therefore beneficial heritable traits will increase in frequency in a population over time, resulting in a population more suited to the given environment. Under the framework of Darwinian selection, the adaptive evolution of populations are driven solely by natural selection (Darwin, 1859).

1.1.2 Historical views on the nature of variation

In the history of evolutionary theory there were changing views regarding the nature of variation, this important to consider as variation is necessary for evolutionary innovation by natural selection. Darwin (1859) considered variation to be gradual in nature; selection alone acting on the accumulation of slight heritable modifications in phenotype, due to the struggle between organisms and their environment (Gould, 2002). Under this paradigm, heritable variation provides the raw material for natural selection in populations – it must accordingly be in high abundance, small in effect, and without directionality (or isotropic) (Gould, 2002). The views of gradualism deny the influence of teleological mechanisms in the production of variation, though Darwin (1859) still admit the lack of knowledge regarding the regulation of variability and a model for heredity, 'our ignorance of the laws of variation is profound'.

1.1.2.1 The modern evolutionary synthesis

The modern evolutionary synthesis (Fisher, 1930; Dobzhansky, 1937; Mayr, 1942; Simpson, 1944) later unified the ideas of Darwinian selection and Mendelian inheritance in a joint framework. This was based on the ideas of Ronald Fisher (1930) in the publication *The Genetical Theory of Natural Selection* – presenting a rational theory of natural selection based on the discrete character of heritable traits as described by Gregor Mendel (Bateson, 1909). This theory described continuous variation to be the result of the combined action of many discrete traits; natural selection acting on those beneficial mutations with small effect on phenotype, as the larger the magnitude of mutation the higher the chance of a decrease in fitness (Fisher, 1930). Established by Huxley (1942), the modern synthesis outlined adaptive evolution as a gradual process in which small effect genetic changes accumulate over time in populations with genetic variation, by means of natural selection acting on the phenotype of an individual in a given environment. This modern synthesis held natural selection as the primary driver of evolutionary change, but also allowed for additional evolutionary processes that may influence the production and maintenance of variation and thus restrict the possibilities of evolution (Gould, 2002).

1.1.2.2 Extended synthesis and developmental constraints

Gould and Eldredge (1977) argued that a strict Darwinian view to understanding adaptive evolution was not sufficient, as in the history of life evolutionary change occurred in large-scale events rather than by gradual changes. Stephen Jay Gould (2002) explained that variation must be considered as not strictly isotropic, with the possibility of developmental constraints acting as an internal force channeling the pathways of evolutionary change. This argument resulted in the call for an extension of the modern evolutionary synthesis, especially to include the relationship between evolution and developmental processes (Gould, 2002). Massimo Pigliucci (2007) outlined an extended evolutionary synthesis that accounts for sources of phenotypic variation other than genetic mutation, including development, ecological factors, properties of gene networks including epigenetic effects, and other biological phenomena such as phenotypic plasticity. Pigliucci (2007) described the modern synthesis as a 'theory of genes' to explain evolutionary phenomena, and that what is required is a 'theory of form' as evolution is realised at the morphological level. These historical views on the nature of variation, developmental constraints, and the significance for natural selection shaped the way in which adaptive evolution is understood and explored today; this should be kept in mind for later sections, including the discussion of the connection between genotype and phenotype.

1.1.3 Darwinian populations and natural selection

To comprehend evolution by natural selection, it is useful to consider this process from the perspective of Darwinian populations. Borrowing from Lewontin (1970) – under Godfrey-Smith's (2009) Darwinian framework, a population may participate in the process of evolution by natural selection provided that individuals satisfy the following conditions: (1) reproduction – entities form a new generation; (2) heredity – offspring resemble their parents; (3) variation in a trait; this resulting in (4) differential reproductive rates and fitness between individuals. These properties defining a Darwinian population are necessary and sufficient for evolution by natural selection, in that any collection of entities satisfying this criteria may be expected to participate in the process (Godfrey-Smith, 2009). From this framework, Lewontin (1970) identified the 'unit of selection' – whether at each hierarchical level of a biological system the individuals satisfy the criteria of being a Darwinian population, thus determining if natural selection may operate at this level to produce evolutionary change (Calcott &

Sterelny, 2011). This allows for multi-level selection, where a system has evolving Darwinian populations at different hierarchical levels; 'de-Darwinisation' may occur when evolution at the lower-level is suppressed by that at the higher-level (Godfrey-Smith, 2009). The shift in units of selection under the Darwinian population framework is significant to the major evolutionary transitions, in which there was a transition in Darwinian individuality from the lower-level to higher-level entity (Libby & Rainey, 2013a); these transitions will be subsequently discussed.

1.1.4 Major evolutionary transitions

The history of life has been defined by major evolutionary transition events, in which changes occurred to the storage and transmission of genetic information, allowing for a general increase in biological complexity over time (Maynard Smith & Szathmáry, 1995). Szathmáry and Maynard Smith (1995) outline the major transitions to include the origin of: compartmentalised molecules, chromosomes from independent replicators, the genetic code, the eukaryotic from prokaryotic cell, sexual from asexual populations, multicellular from unicellular organisms, eusocial colonies, and societies with language and culture. During these transitions – lower-level entities aggregate to form a higher-level entity, with the emergence of new Darwinian properties at this hierarchical level; thus giving rise to the hierarchical structure of biological organisation that is observed in nature (Calcott & Sterelny, 2011). The transition in Darwinian individuality occurs when a collective of individuals that each participate in Darwinian processes and act as units of selection in their own right, evolve the capacity for reproduction at the level of the group; the higher-level collective then becoming a Darwinian population and unit of selection in itself (Godfrey-Smith, 2009; Libby & Rainey, 2013a). This may result in individuals within the higher-level entity that are incapable of independent replication after the transition, only able to reproduce as part of the larger collective; for example in the origin of eukaryotes from initially free-living prokaryotic cells (Szathmáry & Maynard Smith, 1995). The major transitions in evolution distinguish the significant events in the origin of life, and thus are of great interest to investigate further.

1.1.5 The evolution of multicellularity

The evolution of multicellularity was a significant major evolutionary transition, in which the lower-level of single cells came together to form a higher-level multicellular organism (Maynard Smith & Szathmáry, 1995). Multicellularity provided organisms with the advantages of large size, including the formation of an internal environment and a longer life span, as well as allowing division of labour and cell differentiation for the specialisation of tissues (Michod & Roze, 2001). As a result of these advantages, multicellularity has been observed to evolve independently numerous times in the history of life, in both prokaryotes and eukaryotes (Rainey & Kerr, 2010). In the context of Darwinian populations, this transition represented a shift in the unit of selection from the individual cells to groups of cells, and emergence at the higher-level of the Darwinian properties – variation, reproduction, and heredity (Libby & Rainey, 2013a). The evolution of multicellularity therefore required the generation of benefit for the collective as a higher-level entity, sufficient for the lower-level cells to sacrifice Darwinian individuality; this benefit was provided by cooperation (Michod & Roze, 2001).

1.1.5.1 Cooperation and conflict

The cooperation between cells in a collective allows individuals to work together for common benefit, rather than competing amongst each other for selfish benefit; though it may be costly to the individual it results in an increase in fitness of the group as a whole (Godfrey-Smith, 2009). In the evolution of multicellular organisms, cooperation had a strong role; by increasing the fitness of the group this allowed a shift in the unit of selection from the individual to the higher-level cooperating group. Although this cooperation mediates conflict amongst the hierarchical levels to some extent, at the lower-level selection will also favour the evolution of 'cheaters' that avoid the cost of cooperating while still receiving the benefits of the collective (Rainey & Rainey, 2003; Hammerschmidt et al., 2014). It is not evident how cooperation is maintained in the face of destructive cheating types – therefore more than just cooperation is required, but also the evolution of cheat suppressing mechanisms to regulate conflict (Calcott & Sterelny, 2011). This is influenced by genetic relatedness, with cooperation more beneficial between individuals of high relatedness due to kin selection; thus rare cheating types are less likely to be selected for in genetically-similar populations

(Michod & Roze, 2001). It has been argued that in the origin of multicellularity, a single-cell bottleneck occurred to give a genetically-identical population, thus minimising the conflict within groups and selection for cheaters (Libby & Rainey, 2013a). This interplay between cooperation and conflict is an important factor to consider for the evolution of multicellularity.

1.1.6 Life cycles and group-level reproduction

In the transition from unicellular to multicellular life, this required under Lewontin's (1970) framework the emergence of Darwinian properties of the higher-level of the collective, including a mechanism of group-level reproduction. Although in primitive collectives of cells (that may later form multicellular life) the distinction between parent and offspring generations is not necessarily so defined, so relaxation of the properties of the Darwinian framework is useful to conceptualise the transition in Darwinian individuality (De Monte & Rainey, 2014). The aspect of reproduction at the collective-level is best envisioned within 'nascent life cycles', that may be defined as the process in which a multicellular organism or collective will form, grow and reproduce (Ratcliff et al., 2017). Libby and Rainey (2013a) describe the minimal requirement for a collective of cells to function as a primordial unit of evolution – firstly it must at some point in the life cycle exist and be identifiable in a group state, and secondly the group must have the capacity to multiply and share heritable information with new groups. De Monte and Rainey (2014) further elaborate that selection may potentially act at the level of the collective without complete manifestation of Darwinian properties; with the focus put on establishing genealogical connections between collectives for the transmission of information, rather than means of group-level reproduction. In the origin of multicellularity these nascent life cycles are required for the emergence of a mechanism of reproduction, providing the distinction between generations and the stages of the multicellular state.

1.1.6.1 Nascent multicellular life cycles

Three different nascent multicellular life cycles may be identified based on distinct modes of reproduction: (1) fragmentation – small cell groups grow to form larger groups, that fragment by fission to give offspring groups; (2) aggregation – individual cells come together to give a

small aggregate that grows to form a larger aggregate, that produce single cell offspring; and (3) clonal development – individual cells grow and divide to each give clonal cell groups, that produce single cell offspring (Michod & Roze, 2001; Libby & Rainey, 2013a; Ratcliff et al., 2017). These three reproductive modes differ in the form transitioning through the life cycle – with dominance of the multicellular state (fragmentation), unicellular state (aggregation), or alternating states (clonal development). The aggregative life cycle also differs in that groups are formed randomly from a mix of cells, while in the clonal development life cycle groups form through a single-cell bottleneck (Ratcliff et al., 2017). The other major difference between the life cycles is the partitioning of genetic variation at the level of the individual cells (within-group) and the cell collective (between-group) (Libby & Rainey, 2013a). Ratcliff et al. (2017) explain that the reduction of within-group variation (e.g. by bottlenecks) will limit conflict between the levels of selection thus allowing for the transition in Darwinian individuality, as well as to facilitate the emergence of heritable multicellular traits. The increase in between-group variation will also accelerate adaptive evolution of the collective, based on Fisher's (1930) fundamental theorem of natural selection (Ratcliff et al., 2017). Therefore clonal development and single-cell bottlenecks may have been essential to mediate conflict in nascent multicellular life cycles.

1.1.6.2 Developmental programs

The ability to sustain these nascent life cycles in the evolution of multicellularity is also dependent on the emergence of mechanisms that allow transitioning between phases of the life cycle, and thus coordinate the activity of the single cell and collective states. This integration is achieved by developmental programs – the mechanistic rules of development that regulate cellular activities and constrain evolutionary processes (Libby & Rainey, 2013b; Oster & Alberch, 1982). De Monte and Rainey (2014) suggest that these early developmental programs that generate self-sustaining life cycles may have also driven the evolution of development in itself, and the subsequent developmental division of labour and differentiation of cell types in complex multicellular organisms (including somatic and germline cells for sexual reproduction). Wolpert and Szathmáry (2002) compare this origin of development to a chicken or the egg scenario. From the previous discussion of historical views on the nature of variation, it is evident that developmental processes constrain morphological evolution by natural selection; the concept of development will also be further

discussed in Section 1.2.1, in relation to genotype-phenotype mapping. In the origin of early developmental programs, this may have taken the form of simply phenotypic noise under fluctuating environmental conditions; this leads also to deliberation of the link to stochastic phenotypic switching.

1.1.6.3 Link to phenotypic switching

The concept of phenotypic switching relates to that of life cycles and the development programs underpinning the evolution of multicellularity. Phenotypic plasticity is the ability of a genotype to express different phenotypic states in response to unpredictable environment conditions; and phenotypic switching the capacity to undergo reversible transitions between multiple different cell morphologies (West-Eberhard, 1989). There are two types of phenotypic switching to be considered: stochastic switching in which a phenotype changes spontaneously without influence from the environment, and responsive switching where the change in phenotypic state is a direct response to an environmental cue (Kussel & Leibler, 2005). The effect of stochastic switching may be contrasted to a 'bet-hedging' strategy – a population of genetically identical cells may increase their chance of survival in a fluctuating environment by spreading their risk phenotypically; at least some cells will express an advantageous phenotypic state and thrive in the environment, thus allowing the survival of the population (Beaumont et al., 2009; Gallie et al., 2015). Therefore given regular fluctuation in environmental conditions, stochastic mechanisms that enable switching of phenotype will be selected for and evolve in populations. The underlying mechanisms that allow phenotypic switching within clonal populations may have a genetic or epigenetic basis; genetic mechanisms often involving the elevation of mutation rate in relevant 'contingency loci', and epigenetic mechanisms often the result of transcriptional regulation of gene expression due to differential DNA methylation (Henderson et al., 1999). For example stochastic switching was observed in experimental populations of *P. fluorescens* SBW25, with the bistable ON/OFF expression of a colanic acid-based capsule hypothesised to have an epigenetic mechanism (Beaumont et al., 2009; Gallie, 2010; Gallie et al., 2015).

Libby and Rainey (2013b) explain that the mechanisms and environmental conditions that mediate the stabilisation of stochastic phenotypic switching may parallel those that allow the evolution of developmental programs in primitive multicellular life cycles. With irregular

fluctuating conditions the stabilisation of stochastic switches is unlikely; but if the population growth is coupled to the environmental change, this feedback may allow for the selection of the population to rapidly switch phenotype, and thus provide opportunity for the evolution of developmental processes (Libby & Rainey, 2013b). The ability to switch phenotypic states is likely to have first emerged with reliance on mutational change, therefore the switching itself not heritable, but perhaps the rate of switching (Beaumont et al. 2009; Libby & Rainey, 2013a). Libby and Rainey (2013a) envision that this strategy of switching by mutation may then provide the conditions necessary for later mutations that give the capacity to transition between states by heritable epigenetic mechanisms, and eventually come under developmental regulation. This was investigated in experimental populations of *P. fluorescens* SBW25 evolved to rapidly transition between phases of a life cycle with the selection for evolution of a developmental program (Hammerschmidt et al., 2014); this model system and experiment will be later discussed in Sections 1.3.2 and 1.4.2.

1.2 The Connection between Genotype and Phenotype

1.2.1. The genotype-phenotype map and development

Leading from discussion of the evolution of multicellularity and life cycles under developmental regulation, it is important to consider the connection between genotype and phenotype. The genotype-phenotype map (GPM) concept was introduced by Alberch (1991) to reflect the complex non-linear relationship between genotype and phenotype. This describes development as the function mapping genotype on to phenotype, with developmental processes the result of the expression of genes in a complex system, with interactions both between genes and with the environment (Alberch, 1991). The GPM defines phenotype in parameter space, where the parameters are developmental in nature; only a discrete set of phenotypes are possible due to the dynamics of interactions in developmental systems (Alberch, 1991). Alberch (1991) derives the following properties: the same phenotype may result from different combinations of parameter values; transitions in phenotypic state may occur at 'transformational boundaries' due to small perturbations in developmental parameters (both genetic and environmental); and the stability of a phenotype

is determined by the position of its domain in parameter space, with greater instability near transformational boundaries (Pigluicci, 2010). Based on these properties of the GPM – the evolvability of a dynamic system may be as described as a function of its global properties in parameter space: including the stability, topology of transformational boundaries, and ability to generate phenotypic variation. Therefore a balance may be observed in biological systems, between the stability of the system to perturbation (such as genetic mutation) and its evolutionary potential to produce sufficient heritable variation in phenotype (Alberch, 1991). Pigluicci (2010) asserts that adaptive evolution should be considered under this framework of the GPM, where phenotypic variation in biological systems is both genetically and developmentally encoded and has interaction with the environment.

1.2.1.1 Evolvability, modularity and robustness

Consideration of genotype-phenotype mapping requires further discussion of three important and related concepts – evolvability, modularity and robustness; these build on from the ideas proposed by Alberch (1991). Evolvability refers to the capacity of a biological system to generate beneficial mutations and accumulate genetic variation, and thereby undergo evolution by means of natural selection (Pigluicci, 2010). The modularity is the degree of interconnectedness between components in a gene network system, and robustness the ability of the system to remain functional whilst withstanding genetic and environmental perturbations (Pigluicci, 2010). Ciliberti et al. (2007) demonstrate that the robustness of a system is a precondition for its evolvability, as mediated by its modularity. There is a trade-off between the robustness and evolvability of a system – high robustness resulting in a limited ability to innovate due to lack of phenotypic variation, and low robustness giving too high susceptibility to perturbation (Ciliberti et al., 2007). The modularity of a biological system is the product of the two phenomenon: pleiotropy and epistasis. Pleiotropy refers to the effect in which one gene (or mutation) may influence multiple phenotypic traits, while epistasis is the inverse in which one trait is under the control of multiple interacting genes (Wagner & Altenberg, 1996). Pigluicci (2010) explains that gene networks with intermediate levels of modularity will maintain a balance between too high robustness and too low evolvability. These characteristics of the GPM demonstrate the tension found in biological systems, between the need to remain evolvable and produce phenotypic innovation under

dynamic environmental conditions, whilst maintaining robust to genetic perturbation including deleterious mutations.

1.2.2 Genetic architecture constrains evolution

The genotype-phenotype map and its variational properties describe how phenotypic variation maps onto genetic variation under developmental constraint (Wagner & Altenberg, 1996), this may also be termed the 'genetic architecture' of a trait. From the previous discussion of the modularity and robustness of the GPM, it is clear that genetic architecture will have an influence on the production of phenotypic variation, and consequently constrain adaptive evolution and the pathways it may take. With advances made in molecular biology and the availability of genome sequencing technology it is becoming more evident that phenotypic traits have complex genetic architecture (Farr, 2015). The observation of mutational bias and parallel evolution provide insight into the constraints posed on evolutionary pathways by genetic architecture. Parallel evolution refers to the independent evolution of similar phenotypic traits in different species, as a result of changes to homologous genes (Stern & Orgogozo, 2009). The commonly referenced example of parallel mutation is that of the *shavenbaby* gene – required for trichome formation in *Drosophila melanogaster*. Although hundreds of genes are involved in trichome regulation, only mutations in *shavenbaby* are observed to alter the patterns of this trait (Stern & Orgogozo, 2009). This hotspot *shavenbaby* gene exhibits mutational bias, the mutations that contribute to variation in this trait are non-randomly distributed across the genetic regions; some constraint of the genetic architecture is restricting the potential targets of evolution (Gompel & Prud'homme, 2009). Gompel and Prud'homme (2009) explain that the *shavenbaby* gene has a nodal position in the gene regulatory network, making it a good target for mutation as it causes minimal disruption to other developmental processes. Stern and Orgogozo (2009) propose that 'All genes are not equal in the eyes of evolution' – due to the complex genetic architecture underlying phenotypic traits, certain genes are more able to produce variation and thus contribute to adaptive evolution (Farr, 2015).

1.2.2.1 On the repeatability of evolution

Discussion of the constraints of genetic architecture on evolutionary pathways leads to deliberation of the repeatability of evolution. Gould (1989) proposed the metaphor of 'replaying life's tape' – if the history of life was rewound, whether or not replaying it would generate a similar result and diversity of life. For repeatability of evolution, the roles of adaptation, chance, and history in evolutionary change should be evaluated (Travisano et al., 1995). The effects of chance include the stochastic nature of mutation and genetic drift; Monod (1970) conferred that the origin of life may be attributed to natural selection acting on the product of random chance alone, and consequently that there are no predictable objects or events. Gould (1998) also argued for the importance of contingency, that historical events are dependent upon those random events preceding it, thus making patterns of evolution unpredictable. While Conway Morris (1998) contended the role of contingency in evolution, explaining that there are restrictions on organismal design due to the constraints of complex genetic architecture. The observance of parallel evolution gives support for the inevitability of evolutionary outcomes – if the tape of life was replayed there could in fact be a similar result (Conway Morris, 1998). This metaphor of replaying life's tape and the interplay between the roles of chance and contingency are worth keeping in mind when considering the evolution of complex phenotypic traits and the constraint of genetic architecture.

1.3 Pseudomonas fluorescens SBW25 Model System

1.3.1 Bacterial model systems and experimental evolution

To observe the dynamics and outcomes of evolution in real time, the application of bacterial model systems is fundamental. The use of microorganisms is based on the following advantages – short generation times, ability to produce large clonal populations, ease of replication, and the capacity to store cryogenic stocks indefinitely. Bacterial model systems therefore permit the running of long-term evolution experiments, such as those begun by Richard Lenski in 1988, observing the adaptive evolution of 12 parallel *Escherichia coli* (*E. coli*) populations. The investigation of evolution over many generations provides insight into evolutionary processes; it may also shed light on the repeatability of evolution by 'replaying life's tape' on a smaller scale. Advancement in DNA sequencing technology has trivialized

the identification of mutational changes within genomes of evolved lines, the small genome size and clonal reproduction of bacteria allowing for a comparatively straightforward use of molecular genetics techniques to reveal characteristics of the GPM of complex phenotypic traits.

1.3.2 *Pseudomonas fluorescens* SBW25 model

The use of *Pseudomonas fluorescens* SBW25 (*P. fluorescens* SBW25) as a model system was realised by Rainey and Travisano (1998), due to its ability to rapidly evolve phenotypic variants in heterogeneous environments. *P. fluorescens* SBW25 is a plant phyllosphere and rhizosphere-colonising organism, first isolated in 1989 from the leaf of sugar beet grown in Oxfordshire (Rainey & Bailey, 1996). Members of the *P. fluorescens* species are able to colonise a range of terrestrial niches including soil, water, and plant or animal surfaces; they also have the characteristics of being gram-negative, rod-shaped, saprophytic, strictly aerobic, and motile by multiple flagella (Rainey & Bailey, 1996). There has been extensive work completed on *P. fluorescens* SBW25, including the full genome sequencing and annotation (Silby et al., 2009). A reverse-evolution experiment performed by Bertus Beaumont observed the evolutionary trajectories of 12 parallel *P. fluorescens* SBW25 populations over 16 rounds of adaptive evolution, with alternation between static and shaking microcosms; at each round a single-cell bottleneck was imposed on each population, with selection for a change in colony morphology phenotype (Rainey & Travisano, 1998; Beaumont et al., 2009). The characteristics of the *P. fluorescens* SBW25 model will be discussed in the following sections, including the significance of the wrinkly spreader phenotype.

1.3.3 The wrinkly spreader phenotype

The *P. fluorescens* SBW25 genotype with an ancestral smooth (SM) colony morphology rapidly diversifies into numerous niche specialist types when inoculated into static broth microcosms; the unshaken microcosms providing a spatially structured environment (Rainey & Travisano, 1998). Over time as nutrients deplete – primarily oxygen, the competition for access to oxygen at the air-liquid interface (ALI) becomes intense, driving the evolution of niche specialist types including the wrinkly spreader (WS) phenotype. WS types colonise the

ALI by the overproduction of a cellulosic polymer, that allows cells to adhere to one another and form a self-supporting mat or 'biofilm' at the surface of the broth. The fitness advantage of the access to oxygen enables the WS type to readily invade the ancestral SM type in static microcosms. As the WS type becomes more common, the mat collapses under the weight and allows the SM type to reinvade (Rainey & Rainey, 2003). This niche preference may be observed at the colony morphology level on agar plates – the WS phenotype giving a wrinkled colony, and the ancestral SM phenotype a smooth rounded colony; see Figure 1.1 below.

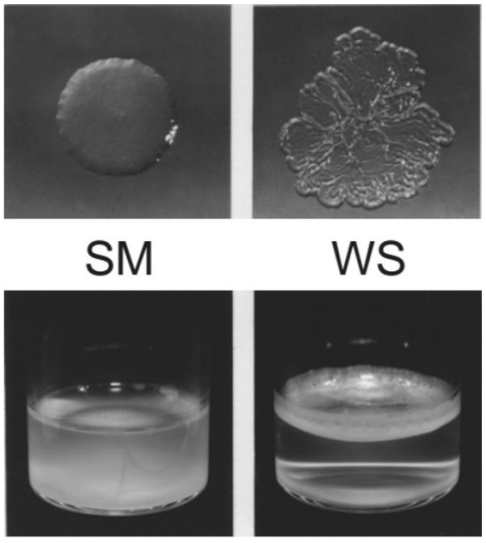

Figure 1.1: Niche specialisation and colony morphology of *P. fluorescens* SBW25 smooth (SM) and wrinkly spreader (WS) phenotypes. The ancestral SM type after growth in static microcosm diversifies to give the WS type that may colonise the ALI. These two phenotypes display specific niche specialisation (top) and colony morphology (bottom). Adapted from Rainey & Travisano (1998).

1.3.3.1 The structural basis of the WS phenotype

The underlying structural genes and mutational causes of the WS phenotype were identified using suppressor analysis. The WS type was mutagenised using a transposon (Tn5), and colonies screened for loss of the wrinkled morphology and ability to colonise the ALI (Spiers et al., 2002; Spiers et al., 2003; Goymer et al., 2006; Bantinaki et al., 2007; McDonald et al., 2009). The primary structural basis of WS was determined to be the *wss* (wrinkly spreader structural) operon, containing ten genes (*wss*A - *wss*J) that encode the machinery necessary for production of an acetylated cellulosic polymer (Spiers et al., 2002). Based on homology and genetic studies of mutants, the function of each gene product has been predicted: WssB, WssC & WssE as core subunits of cellulose synthase in association with WssD; WssF, WssG, WssH & WssI involved in the acetylation of cellulose; and WssA & WssJ involved in localisation of the cellulose synthase complex (Spiers et al., 2003). Further biochemical

analysis of the WS phenotype has confirmed that colonisation of the ALI is primarily enabled by the overproduction of acetylated cellulose as the product of the *wss* operon, that acts as a cell-cell glue (Spiers et al., 2003).

1.3.3.2 Mutational pathways involving DGCs and c-di-GMP

The mutational activation pathways that result in the WS phenotype all include genes that encode di-guanylate cyclases (DGCs). DGCs catalyse the biosynthesis of a secondary messenger cyclic-dimeric-guanosine monophosphate (c-di-GMP) (McDonald et al., 2009). c-di-GMP is an allosteric activator of cellulose synthase, and thus regulates biofilm formation; it is produced from two molecules of GTP by DGC enzymes, and broken down by specific phosphodiesterases (PDEs) (McDonald et al., 2009; Hengge, 2009). The activity of DGCs is associated with a GGDEF domain, and PDEs with an EAL domain; both domains containing conserved amino acid motifs essential for enzymatic activity (Hengge, 2009). The levels of intracellular c-di-GMP and DGC/PDE activity are controlled by one- or two-component signaling systems (Christen et al., 2006). An environmental signal is received by the respective GGDEF or EAL sensory domain (sensor kinase), this may then be transduced to a response regulator receiver, resulting in an increase or decrease in c-di-GMP levels (Hengge, 2009). A negative feedback loop also prevents the accumulation of c-di-GMP in the cell, at high concentrations of c-di-GMP it is able to bind noncompetitively to a secondary site of the GGDEF domain of DGCs and thus block enzymatic activity (Hengge, 2009; Christen et al., 2006).

The c-di-GMP signalling network is further complexed by the range of molecules c-di-GMP may bind, with numerous DGC and PDE encoding genes in *P. fluorescens* SBW25 as well as other effector molecules (Farr, 2015). The WS phenotype and underlying DGC mutational pathways are therefore a great candidate for investigation of how genetic architecture constrains the production of variation and pathways of evolution. Previous work has allowed construction of the basic genotype-phenotype map of the WS phenotype, and identification of three main activation pathways: the *wsp*, *aws* and *mws* DGC encoding loci (Spiers et al., 2002; McDonald et al., 2009).

1.3.3.3 **wsp, aws, & mws** *operons*

The *wsp* (wrinkly spreader phenotype) operon is the main mutational route for the WS phenotype, encoding seven genes (*wsp*A-E, & *wsp*R). The DGC-functioning WspR is activated predominantly by mutation to the *wspF* gene, encoding the negative regulator WspF (McDonald et al., 2009). The genes of the *wsp* operon encode a chemosensory pathway, demonstrating high homology to the *che* pathway of *E. coli* (Goymer et al., 2006). A model has been developed for the regulation of *wsp* in a two-component system – the predicted function and conserved protein domains of each gene product in this system is detailed in Table 1.1 below. Under this model the WspA methyl-acceptor detects a signal and activates the WspE histidine kinase and response regulator receiver (with WspB and WspD acting as linkers), resulting in the transfer of a phosphoryl group to the WspR DGC; the WspC methyltransferase and WspF methylesterase modulating the methylation and activity of WspA (Bantinaki et al., 2007; Coggan & Wolfgang, 2012; O'Connor et al., 2012). The phosphorylated WspR with DGC activity then synthesises c-di-GMP, activating the production of cellulose by the *wss* operon and thus biofilm formation.

Protein	Pflu	Size[a]	Predicted function	Conserved domains[b]
WspA	1219	540	Methyl-accepting chemoreceptor	HAMP (signaling); LBD (ligand-binding receptor); MCPsignal (methyl-acceptor)
WspB	1220	170	Scaffold protein	CheW (signal transduction)
WspC	1221	419	Methyltransferase	CheR (methyltransferase); TPR
WspD	1222	232	Scaffold protein	CheW (signal transduction)
WspE	1223	755	Histidine kinase; response regulator	CheA (histidine kinase) - HPT, HATPase & CheW; CheY (response regulator)
WspF	1224	336	Methylesterase; response regulator	CheB (methylesterase); CheY (response regulator)
WspR	1225	333	Diguanylate cyclase; response regulator	GGDEF; CheY (response regulator)

Table 1.1 The predicted function and domain characteristics of Wsp proteins encoded by the *wsp* operon. [a] Size refers to the number of amino acid residues. [b] Conserved domains refers to the conserved protein domains present (NCBI CDD, significant expect value). Adapted from Bantinaki et al. (2007) & Gallie (2010).

The *aws* (alternate wrinkly spreader) and *mws* (mike's wrinkly spreader) operons were later discovered to be additional mutational routes for the WS phenotype (McDonald et al., 2009). Models have been developed for the regulation of these operons in one-component systems. The *aws* operon encodes three genes (*awsX*, *awsR*, & *awsO*); the DGC AwsR activated

almost exclusively by mutation to the *awsX* gene, encoding AwsX presumably a negative regulator, in association with the outer membrane porin AwsO (McDonald et al., 2009). While the *mws* operon encodes a single gene *mwsR*; the multi-domain MwsR has both DGC and PDE activity, with mutation to the EAL domain resulting in an increase to c-di-GMP levels (McDonald et al., 2009). Other than these three common mutational routes, McDonald et al. (2009) hypothesised that there are many more potential pathways – the *P. fluorescens* SBW25 genome encoding 39 putative DGCs that may be involved in c-di-GMP regulation. Lind et al. (2015) confirmed this, by eliminating the *wsp*, *aws* and *mws* pathways, 13 alternative mutational pathways for the WS phenotype were identified with similar levels of fitness.

1.3.3.4 Constraint of WS evolutionary pathways

The WS phenotype of *P. fluorescens* SBW25 is derived from the SM ancestral phenotype, with mutations occurring exclusively in the three activation pathways *wsp*, *aws* and *mws*, involving the negative regulation of DGCs. This realisation of the WS phenotype through a limited number of the potential evolutionary pathways demonstrates the clear constraint on the pathways of evolution and production of variation due to underlying genetic architecture (McDonald et al., 2009). The strong preference for the three common pathways may not be explained by mutational bias as there is no evidence that these are hotspot genes, or a fitness advantage as the fitness was equivalent to that of the alternative pathways (Lind et al., 2015). An explanation may instead be given based on the WS genetic architecture – these mutational pathways are taken as a result of the high frequency of loss-of-function compared to gain-of-function mutations, and the large mutational target size of DGCs under negative regulation (McDonald et al., 2009; Lind et al., 2015). Based on this, Lind et al. (2015) proposed hierarchical principles for the mutational route of new phenotypes (arising by gene activation): evolution proceeding first by the loss-of-function mutation to extragenic regions mediating negative regulation, second by the activation of promoter activity as a result of gain-of-function mutation or gene fusion, and third by rare intragenic gain-of-function mutations. These hierarchical rules will help in understanding of the complex GPM and genetic architecture of the WS phenotype.

1.4 The Life Cycle Experiment

1.4.1 The WS phenotype and life cycles

The *P. fluorescens* SBW25 model may be used to explore the dynamics of the transition from unicellular to multicellular life forms. The ancestral SM phenotype diverges when propagated in a spatially structured environment, with the evolution of the niche specialist WS phenotype as a result of mutation selected for due to ability to colonise the ALI (Rainey & Travisano, 1998). The evolution of the WS phenotype may be compared to the evolution of multicellularity – the WS cells cooperate by over producing an acetylated cellulosic polymer that allows the cells to form a mat collective at the ALI with advantage of the access to oxygen, mediating a shift in the unit of selection to the higher hierarchical level of the collective (Rainey & Rainey, 2003). For this shift in the level of selection requires the group of cooperating cells to satisfy all criteria under the Darwinian framework: variation, reproduction, and heredity (Godfrey-Smith, 2009).

From the interaction between cooperation and conflict in the evolution of multicellularity, Rainey and Kerr (2010) hypothesised a means of collective reproduction in *P. fluorescens* SBW25 that embraces the cheating cells as propagules in a life cycle, rather than having a focus on cheat-suppression. Without a mechanism of reproduction the WS mat may be considered an 'evolutionary dead end', though the cheating cells may instead act as a primitive germ line for the somatic mat (Rainey & Kerr, 2010). Rainey and Kerr (2010) describe the life cycle proceeding as follows: WS cells that overproduce a cellulosic polymer form a mat at the ALI, over time mutation generates cheating types that result in the collapse of the mat, the cheaters liberated from the mat may then experience a back mutation allowing them to produce the adhesive again, and these cells may then reform the mat at a new location and thus complete the cycle. This proto-life cycle transitions between two phenotypic states by mutation, and though this is far from a developmentally-regulated life cycle it may provide the conditions necessary for the evolution of true life cycle phases in a multicellular organism in which the transitions are under regulation by developmental processes (Rainey & Kerr, 2010).

1.4.2 Hammerschmidt et al. (2014) life cycle experiment

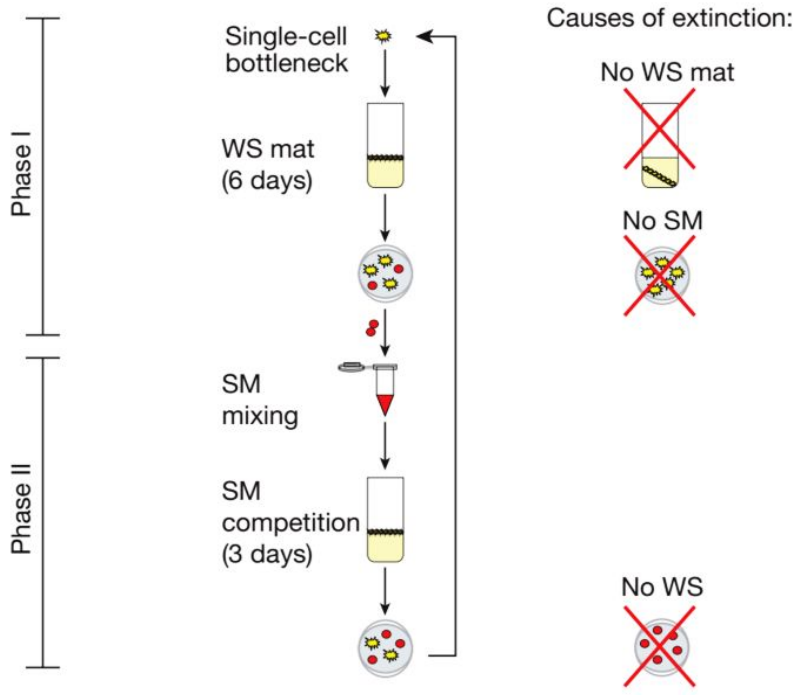

Figure 1.2 The cheat-purging regime of the life cycle experiment. Each line founded by a single WS cell, SM cheater types produced over the 6 days of phase I; an SM pool used to seed phase II in which over 3 days WS types are produced. Lines undergo extinction when they are unable to produce the WS mat or SM types in phase I, or the WS types in phase II. Figure reproduced from Hammerschmidt et al. (2014).

Hammerschmidt et al. (2014) developed an experiment to test the feasibility of a life cycle in *P. fluorescens* SBW25 in which SM cheating cells may act as propagules for the WS phenotype mat. The design of the life cycle experiment allowed for selection to be acting on the transition between the two phases of the life cycle – the SM cell and WS mat; and thus selection for a developmental program that mediates this transition. The life cycle experiment was completed as follows: each line was founded by a single WS cell (15 lines with 8 replicates of each, 120 total); over the 6 days of phase I the WS mat had to remain viable as well as produce SM types (cheaters); then over the 3 days of phase II these pooled SM types (or WS types for cheat purging) were required to revert back to the WS phenotype; a single cell bottleneck then used to seed the next generation (Hammerschmidt et al., 2014). For the cheat-embracing regime the SM type cheating cell was passed through the bottleneck between phase I and II, while for the cheat-purging regime the WS type cooperating cell was used instead. Extinction of a line occurred when it failed to complete the life cycle – so was unable to maintain a WS mat or produce the SM phenotype during phase I, or the WS phenotype during phase II. An extinct line was then replaced with another random viable line within the replicate (or from another replicate if all went extinct), thus allowing for

reproduction (Hammerschmidt et al., 2014). The design of the life cycle experiment cheat-embracing regime is shown in Figure 1.2 above.

Under the cheat-embracing regime the life cycle allowed the successful persistence of lines, as well an increase in the competitive performance of the evolved lines as compared to the ancestral lines (Hammerschmidt et al., 2014). Hammerschmidt et al. (2014) also observed fitness decoupling only when cheaters were embraced – an increase in fitness of the evolved lines with a decrease in the individual cell fitness. This fitness decoupling was the result of a shift in the Darwinian individuality and unit of selection, from the lower-level of individual cells to the higher-level of the collective. The improvement of evolved lineages under the cheat-embracing regime was attributed to an increased capacity to generate the phenotype necessary for each stage of the life cycle (SM in phase I, WS in phase II), indicating that selection was acting on the transition rate between the SM and WS phenotypes (Hammerschmidt et al., 2014).

1.4.2.1 Genetic switch in Line 17

To consider the genetics underlying the rapid transition rate between phases of the life cycle, the fittest lineage Line 17 was sequenced at generation 11 (Hammerschmidt et al., 2014). A mutation was identified in the *mutS* gene – *mutS* encoding a protein product of the DNA mismatch repair system, contributing to the correction of mutations due to errors in DNA replication. The ability for Line 17 to transition between the SM and WS phenotypic states was dependant on this mutation in *mutS*, directly or indirectly related to the resulting elevation of mutation rate. Hammerschmidt et al. (2014) also found in the mutational history of Line 17 a frameshift mutation in *wspR* within a guanine tract of 7 residues overlapping the active site; thus it was hypothesised that the hypermutability may mediate a genetic switch by changes to the tract of guanine residues (G tract) in the DGC encoding *wspR* gene. This was shown to be the case; when Line 17 at generation 10 was passed through additional life cycle rounds, many transitions correlated with changes to the G tract in *wspR* (Hammerschmidt et al., 2014). The hypermutable Line 17 was therefore found to switch between phenotypic states by the expansion (SM, *wspR* OFF) and contraction (WS, *wspR* ON) of this guanine tract in *wspR*. The *mutS*-dependent genetic switch in Line 17 allowed the rapid transition between SM and WS phenotypes, and integration of the two phases of the life cycle by a

mutational mechanism. Therefore the life cycle experiment and Line 17 genetic switch provided an approximation to a developmentally-regulated life cycle and means of collective reproduction.

1.4.2.2 The origin of TSS-f6

The TSS-f6 (temperature-sensitive switcher-f6) genotype of *P. fluorescens* SBW25 was derived from a continuation of the life cycle experiment with different size microcosms, to see the effect of mat size on the evolution of transitioning between SM and WS (P. Remigi & D. Rexin, unpublished data). This experiment used the Line 17 (L17) evolved lineage with the *mutS* gene restored to wild-type (L17-*mutS*wt) to prevent hypermutability, cycled through further generations of the life cycle. After 6 extra generations with L17-*mutS*wt in small microcosms, during cycle 7 in the line f6 a colony was selected in phase I as an SM cheater type and mistaken for producing the WS type in phase II; this line went extinct in the next generation due to an inability to produce the WS mat (P. Remigi & D. Rexin, unpublished data). By chance this line f6 was observed to change in colony morphology phenotype from SM at 28°C to WS at room temperature or 20°C (noticed by Paul Rainey by chance on a plate left at the lab bench).

This temperature-sensitive derived lineage was of interest as it demonstrated a mechanism of transitioning between the WS and SM phases of the life cycle that is responsive to the environment, perhaps more closely approximating a nascent multicellular life cycle under developmental regulation. It should be noted that the transitioning of phenotype observed in TSS-f6 may be termed a 'responsive switch' to an environmental cue; though the term switch will be used sparingly to prevent confusion with stochastic switching or bet-hedging, the words transition or environmentally-responsive developmental switch instead preferred. The temperature sensitivity of TSS-f6 is not relevant to the life cycle experiment in which it was derived; as the temperature was maintained at 28°C throughout the experiment it could not provide a significant selective force for adaptive evolution. Therefore temperature itself is unlikely to be the environmental cue that mediates transitioning between phases of the life cycle, but it may be associated with some other environmental factor – in particular the level of oxygen. It may be conceivable that the TSS-f6 genotype has evolved the capacity to

express the WS phenotype under oxygen rich conditions (e.g. at 20°C), while this is suppressed when oxygen is depleted (e.g. at 28°C) resulting in the SM phenotype.

The general aim of this study is to complete a phenotypic, genetic and evolutionary characterisation of the TSS-f6 genotype, to decipher the underlying genotype-phenotype map and mechanistic basis of the environmentally-responsive phenotype. There is also the aim to investigate the environmental cue eliciting the TSS-f6 phenotype, particularly of oxygen. The specific research objectives of this study are provided in the next section.

1.5 Research Objectives

1. To characterise the environmentally-responsive phenotype of the TSS-f6 genotype, including an investigation into the possible environmental cues mediating the transition between WS and SM – especially oxygen.
2. To analyse the evolutionary history of TSS-f6 in the context of the life cycle experiment, by whole genome sequencing of TSS-f6 and ancestral genotypes.
3. To perform suppressor analysis on TSS-f6 by transposon mutagenesis, suppressing the phenotype at the two environmental conditions of 28 and 20°C temperature.
4. To perform a second round of suppressor analysis by transposon mutagenesis, using select TSS-f6 transposon mutants derived from the first round.
5. To investigate the mutation rate of TSS-f6, with a focus on the expansion and contraction of guanine tracts in select TSS-f6 transposon mutants.

Chapter 2: Materials and Methods

2.1 Materials

2.1.1 Bacterial strains

The bacterial strains used in this study are listed in Table 2.1 below. All strains were stored indefinitely in 40% (w/v) glycerol at -80°C.

Strain	Characteristics and genotype	Reference
Pseudomonas fluorescens		
SBW25	Wild type isolate with SM genotype, ancestral strain to all *P. fluorescens* strains in this study	(Rainey & Bailey, 1996)
LSWS	Mutant evolved from SBW25, WS genotype due to mutation in *wspF* (A901C)	(Spiers et al., 2002)
Line 17 (L17)	Derived line from life cycle experiment, Line 17 (L17) with WS isolated at generation 11	(Hammerschmidt et al., 2014)
L17-*mutS*wt	Derived line from life cycle experiment, Line 17 with WS isolated at generation 11, *mutS* gene restored to wild type	(Hammerschmidt et al., 2014)
f2-5.2 [PE-6-WT]	Derived line from continuation of life cycle experiment with L17-*mutS*wt, WS isolated after 5 cycles (phase II) and used to seed cycle 6 (phase I)	(P. Remigi & D. Rexin, unpublished data)
f2-6.1 [PE-6-WT-SM]	Derived line from continuation of life cycle experiment with L17-*mutS*wt, SM pool of 8 replicates after 6 cycles (phase I) and used to seed cycle 6 (phase II)	(P. Remigi & D. Rexin, unpublished data)
f2 (f2-6.2) [PE-7-WT]	Derived line from continuation of life cycle experiment with L17-*mutS*wt, WS isolated after 6 cycles (phase II) and used to seed cycle 7 (phase I)	(P. Remigi & D. Rexin, unpublished data)
f2-7.1 [PE-7-WT-SM]	Derived line from continuation of life cycle experiment with L17-*mutS*wt, SM pool of 8 replicates after 7 cycles (phase I) and used to seed cycle 7 (phase II); origin of TSS-f6 strain	(P. Remigi & D. Rexin, unpublished data)
TSS-f6 (f6-7.2) [PE-8-WT]	Derived temperature-sensitive line from continuation of life cycle experiment with L17-*mutS*wt, isolated after 7 cycles (phase II)	(P. Remigi & D. Rexin, unpublished data)
JS: A1 - A29	29 x transposon mutants derived from TSS-f6 with SM suppressed at 28°C (Screen A), by transposon mutagenesis using IS-Ω-Km/hah	This study
JS: B1 - B36	36 x transposon mutants derived from TSS-f6 with WS	This study

	suppressed at 20°C (Screen B), by transposon mutagenesis using IS-Ω-Km/hah	
JS: A1ΔCre - A29ΔCre, JS: B1ΔCre - B36ΔCre	Select transposon mutants (derived from those above) that have undergone Cre recombinase-mediated excision of the transposon	This study
WS TSS-f6-*wspE*mut (JS:A9ΔCre)	Select WS transposon mutant with *wspE* mutation, derived from TSS-f6 (Screen A) and the transposon cre-deleted	This study
SM TSS-f6-*wspE*mut (JS:B22ΔCre)	Select SM transposon mutant with *wspE* mutation derived from TSS-f6 (Screen B) and the transposon cre-deleted	This study
JS: C1 - C28	28 x transposon mutants derived from WS TSS-f6- *wspE*mut (JS:A9ΔCre) with WS suppressed at 28°C (Screen C), by transposon mutagenesis using IS-Ω-Km/hah	This study
JS: D1 - D25	25 x transposon mutants derived from SM TSS-f6-*wspE*mut (JS:B22ΔCre) with SM suppressed at 20°C (Screen D), by transposon mutagenesis using IS-Ω-Km/hah	This study
JS: C1ΔCre - C28ΔCre, JS: D1ΔCre - D25ΔCre	Select transposon mutants (derived from those above) that have undergone Cre recombinase-mediated excision of the transposon	This study

Table 2.1 Designation and characteristics of bacterial strains used in this study

2.1.2 Plasmids and transposons

The plasmids and transposons used are listed in Table 2.2 below.

Name	Characteristics	Reference
Plasmids		
pRK2013	Helper plasmid used for tri-parental conjugation; Km^R, *tra*, *mob*	(Rainey, 1999)
pCre	Used to excise IS-Ω-Km/hah, derivative of pUT; Cm^R, *cre* (from pRH133)	(Rainey, 1999)
Transposons		
IS-Ω-Km/hah	Km^R, ColE1 *ori*, *npt*II promoter, *loxP*	(Giddens et al., 2007)

Table 2.2 Designations and characteristics of plasmids and transposons used in this study

2.1.3 Primers

The primers used are listed in Table 2.3 below. All primers were obtained from Integrated DNA Technologies, resuspended in ddH_2O to the concentration 100 pmol μL^{-1}, and used at the working concentration of 10 pmol μL^{-1}.

Name	Sequence 5' to 3'	Target
Transposon mutagenesis		
Tn*pho*A II	GTGCAGTAATATCGCCCTGAGCA	IS-Ω-Km/hah
CEKG 2A	GGCCACGCGTCGACTAGTACNNNNNNNNNNAGAG	Non specific
CEKG 2B	GGCCACGCGTCGACTAGTACNNNNNNNNNNACGCC	Non specific
CEKG 2C	GGCCACGCGTCGACTAGTACNNNNNNNNNNGATAT	Non specific
Hah-1	ATCCCCCTGGATGGAAAACGG	IS-Ω-Km/hah
CEKG 4	GGCCACGCGTCGACTAGTAC	5' end of CEKG 2 A/B/C
Guanine tract sequencing		
wssE_F	CTATCCTGCGTGACCGTACC	5' end of *wssE* G tract
wssE_R	GGGTTGTTACGCAGGTACCA	3' end of *wssE* G tract
wssJ_F	CGTTAAGCTTCGCCGTGATG	5' end of *wssJ* G tract
wssJ_R	ACGCTCAAGGCTTGATGGAA	3' end of *wssJ* G tract
wspC_F	AGGTGTTTTACTGGCTGGGG	5' end of *wspC* G tract
wspC_R	GCGGAACATCAAGAGCGAAC	3' end of *wspC* G tract
wspR_F	ATCACTCGCGCTCCTACATG	5' end of *wspR* G tract
wspR_R	CCTGATTGCGCCCATTATGC	3' end of *wspR* G tract

Table 2.3 Designations, sequences and target of primers used in this study

2.1.4 Antibiotics, reagents and enzymes

The water used throughout this study was double-distilled H_2O (ddH_2O, purified with the Millipore RiOs™ Essential 8 system and Millipore Synergy® system). All antibiotics and reagents unless specified, were obtained from Sigma-Aldrich. The antibiotics used were dissolved in ddH_2O and filter sterilised (pore size 0.22 μm), unless otherwise stated. The following concentrations were used: kanamycin (Km, Melford Biolaboratories) 100 μg mL^{-1},

ampicillin (Amp) 100 μg mL^{-1} (1M NaOH added to adjust pH), and tetracycline (Tet, Duchefa Biochemie) 12.5 μg mL^{-1} (dissolved in 50% (v/v) ethanol). Nitrofurantoin (Nf) was dissolved in dimethyl sulfoxide (DMSO) at a concentration of 100 μg mL^{-1}, and used to inhibit the growth of *E. coli*. For fluctuation analysis, rifampicin (Rif, Melford Laboratories) 50 μg mL^{-1} (dissolved in methanol) and nalidixic acid (Nal) 75 μg mL^{-1} were used. Other reagents were used as described in the text, including: Standard Taq polymerase (Invitrogen), Exonuclease I (ExoI, NEB) Calf Intestinal Phosphatase (CIP, NEB), and Antarctic Phosphatase (NEB).

2.1.5 Media and culture conditions

Unless stated otherwise, all *P. fluorescens* bacterial strains were cultured at 28°C in King's broth (KB). KB contained (1L total in ddH_2O, pH adjusted to 7.0): 10 g glycerol, 20 g proteose peptone no. 3 (BD Bacto), 1.5 g $K_2PO_4.3H_2O$, and 1.5 g $MgSO_4.7H_2O$. Unless stated otherwise, all *E. coli* bacterial strains were cultured at 37°C in Lysogeny broth (LB). LB contained (1L total in ddH_2O): 5 g yeast extract (HiMedia), 10 g tryptone (BD Bacto), and 10 g NaCl. For solid media, Bacteriological grade agar (AppliChem) was added at the concentration of 1.5% (w/v). Where detailed in the text, the following were added to media: Congo Red (CR) stain 40 μg mL^{-1} (dissolved in ddH_2O, filtered), 33% HCl (to adjust pH), and NaCl (to adjust salt concentration). All culture media was sterilised by autoclaving, to a temperature greater than 120°C. The solid media was cooled to 60°C before pouring; when required, antibiotics or other reagents were added just before the pouring of plates, and the plates dried inverted at room temperature for 3 days with minimal light exposure. Unless specified otherwise, all cultures were grown from a single isolated colony inoculated into 6 mL media in a glass microcosm. Overnight cultures were incubated shaking at 160 rpm for approximately 16-18 hours. Static broths for visually observing the mat formation ability of *P. fluorescens* strains were incubated without shaking for between 2 and 6 days. For dilution of cultures, Ringer's solution (Merck tablets) was often used due to its isotonic nature.

2.1.6 Gel electrophoresis

For standard gel electrophoresis, agarose gels were made with 1% (w/v) UltraPure™ agarose (Invitrogen) in 1x TBE buffer (Tris-Borate-EDTA, Invitrogen). For gel extraction, the gels contained 0.8% (w/v) UltraPure agarose in 1x TAE buffer (Tris-Acetate-EDTA, Thermo Scientific), as the borate in TBE may inhibit downstream enzymatic activity. The gels were run in TBE or TAE buffer as required. Samples were loaded with 1x DNA loading dye (Thermo Scientific), and run alongside the GeneRuler 1 kb (Thermo Scientific) DNA ladder. For visualisation of DNA, 1x SYBR® Safe DNA gel stain (Invitrogen) was added to the agarose gel, and viewed using a UV transilluminator, or Safe Imager™ 2.0 Blue-Light Transilluminator for gel extraction. The gels were imaged under UV light with the Canon Powershot G7, connected to the PS Remote software.

2.1.7 Photography and microscopy

The colony morphology phenotype of *P. fluorescens* SBW25 strains were viewed on solid agar plates from the underneath, with the naked eye or using a dissection microscope. All colony images were taken in a dark room with the ZEISS KL200 light source shining directly on the colony, using the Canon Powershot A640 attached to the Zeiss Stemi 2000-C dissection microscope. The mat formation ability of *P. fluorescens* SBW25 strains in static broth cultures were imaged with the Sony Xperia Z3 Compact or iPhone 6 camera. Time-lapse images of mat formation were obtained using the Canon Powershot G7, connected to the PS Remote software. For visualisation of cell capsulation, cell capsules were stained with 20% (v/v) India Ink (Graphic, Pébéo) and viewed using the Olympus BX61 fluorescence microscope. All cell-level images were taken with phase contrast microscopy using the Olympus F-view II camera attached to the Olympus BX61, connected to the cellSens Dimension software. The analysis of all images was completed in ImageJ (version 1.50i), and time-lapse videos produced using iMovie (version 9.0.9).

2.2 Methods

All methods used in this study were adapted from the theses of Barnett (2015), Farr (2015), and Gallie (2010), unless otherwise stated.

2.2.1 Phenotypic characterisation

The TSS-f6 genotype of *P. fluorescens* SBW25 exhibits a unique phenotype: transitioning from SM colony morphology at 28°C to the WS at 20°C. Therefore a thorough characterisation of this environmentally-responsive phenotype is necessary, to understand the underlying molecular mechanisms. It is also important to investigate the environmental cue that is eliciting the phenotype (observed as temperature) – especially the level of oxygen.

2.2.1.1 Colony morphology

The colony morphology of *P. fluorescens* SBW25 bacterial strains were observed on solid KB plates incubated for 3 days, or more where applicable. These were streaked directly from frozen stocks (1 μL) or overnight cultures spread with glass beads (10^{-7} dilution); with one colony composed of clones derived from a single parental cell. In some cases, the morphology was also observed not of single colonies but of a mass of colonies, to allow for sufficient growth in limiting environments; with 2-5 μL spots of overnight cultures made on KB plates. Congo red was used in KB plates to stain the WS colonies, with a strong red staining intensity indicating CR binding and a high cellulose content in the colony. The phenotype of TSS-f6 was compared to that of the smooth wild type SBW25, the wrinkly LSWS, as well as the wrinkly ancestral genotypes L17-*mutS*wt and f2 (f2-6.2) from the life cycle experiment. This was examined at the incubation temperature of 28 and 20°C where the TSS-f6 phenotype was first observed, as well as various intermediate (e.g. 25°C) and extreme temperatures.

The effect of other environmental cues on colony morphology was also investigated, including variations in media composition, pH level, and growth on depleted media. The use of depleted media was to indicate whether TSS-f6 is producing some form of extracellular signal that may be contributing to the phenotype. This depleted media was produced by

incubating static microcosms (6 or 30 μL) inoculated with TSS-f6 for 6 days at 28°C, spinning out the cells from the media by centrifugation, filtering it twice (pore size 0.22 μm), heating to 60°C (spin out any sediment by centrifugation), addition of 2x molten agarose, and pouring plates with different combinations of depleted and fresh media. Unfortunately no method was devised to investigate the effect of alteration to oxygen levels or oxygen deprivation.

2.2.1.2 Mat formation

The ability to form a mat or 'biofilm' at the air-liquid interface (ALI) of static microcosms demonstrates the niche preference of *P. fluorescens* SBW25 strains. In the static broth microcosm a spatially heterogeneous environment is produced, whereby cells collecting in a mat at the ALI have the collective advantage of access to oxygen. To assess mat formation ability, cultures were inoculated from a single colony or 10^{-3} dilution of overnight culture, vortexed to resuspend the cells, the lids loosened, and incubated without shaking at 28°C for 2 days (as mutations start to accumulate after 2 days). The presence of a mat at the surface of the broth was examined and photographed after 18, 24, and 48 hrs. The niche preference of TSS-f6 was compared to SBW25, and the ancestral genotypes L17-*mutS*wt and f2 (f2-6.2); as well as the difference at the temperatures of 28 and 20°C.

To understand the phenotype of TSS-f6 in the context of the life cycle experiment, mat formation was also examined over 6 days for TSS-f6 and SBW25, with time-lapse images of static microcosms taken every 15 mins. These 6 day cultures were also made in replicate, with a static microcosm plated after each 24 hr period, to demonstrate whether WS types were evolving. This was achieved by vigorous vortexing of the culture, and spreading on KB plates (10^{-6} & 10^{-7} dilution). These were incubated for 2 days at 28°C, and the colony morphology examined. The evolution of WS phenotypes in TSS-f6 was compared to SBW25, and the pooled SM f2 ancestor (f2-6.1).

2.2.1.3 Capsule staining

TSS-f6 was identified to form a mucoid coat over the WS colonies when incubated for more than 4 days at 20°C; due to the visual similarities it was hypothesised that this may be a form of colanic-acid capsulation observed previously in *P. fluorescens* SBW25 (Beaumont et al.,

2009; Gallie et al., 2015; Remigi et al., 2018). Therefore a capsule staining assay was completed to indicate capsulation in TSS-f6 and select TSS-f6 transposon mutants (transposon mutagenesis described in Section 2.2.4). Capsule staining of cells was achieved using the counter-stain India ink, capsules appearing colourless against a dark stained background. To normalise the bacterial growth phase of strains, cultures inoculated from a single colony were grown for 24 hrs in shaken microcosms, followed by a 10^{-3} dilution into fresh microcosms and growth for another 24 hours. 30 µL of culture was then added to an equal amount 20% (v/v) India ink, this was thoroughly mixed and incubated at room temperature for approximately 1 min. Microscope slides were prepared by adding ~0.8 µL of stained cells in a diagonal line on the slide, and a coverslip carefully placed on top. The slides were left at room temperature for 5 mins to minimise the movement of cells, before viewing under the microscope using 100x oil immersion objective lens.

2.2.2 Polymerase Chain Reaction

Polymerase Chain Reaction (PCR) was used to amplify specific sequences of DNA, with primers complementary to the target region. All reactions were carried out using the T100 Thermal Cycler (Bio-Rad).

2.2.2.1 Standard PCR

The standard reaction contained (25 µL total in ddH_2O): 2.5 µL 10x PCR buffer, 0.75 µL 50 mM $MgCl_2$, 0.5 µL 10 mM dNTP mix, 0.625 µL of each 10 pmol μL^{-1} primer, and 0.125 Taq polymerase (1 unit). Cells from overnight cultures (2 µL of 10^{-1} dilution per reaction) or taken directly from single-isolated colonies provided the template for PCR. The cycling conditions used were: initial denaturation for 10 mins at 94°C; 35 cycles of denaturation for 30 secs at 94°C, annealing for 30 secs at the primer-specific temperature (as calculated using the NEB Tm Calculator), and elongation for a size-specific time (1 min per kb of target DNA amplified) at 72°C; final elongation for 10 mins at 72°C; and the reaction product stored at 4°C indefinitely. In some cases 1.5 µL of DMSO was added to optimise the PCR reaction, and the annealing temperature decreased by 1°C to compensate.

2.2.2.2 Arbitrary Primed-PCR

The technique of Arbitrary Primed-PCR (AP-PCR) developed by Manoil (2000) may be used to easily map the location of a transposon insertion, allowing connection between an observed phenotype and the underlying genetic basis (Saavedra et al., 2017). AP-PCR was used in transposon mutagenesis to amplify the chromosome-transposon junction of IS-Ω-Km/hah insertions, which was followed by sequencing to identify the insertion location (Giddens et al., 2007). This was achieved through two successive rounds of PCR: the first round utilising a transposon-specific primer paired with a set of arbitrary primers that may bind to many sites in the genome; the product of this used as template for the second round that utilises a nested transposon-specific primer paired with a primer specific to the common 5' region of the arbitrary primers (Das et al., 2005).

The first reaction contained (25 µL total in ddH_2O): 3 µL template (colony scraping resuspended in 50 µL ddH_2O), 2.5 µL 10x PCR buffer, 0.8 µL 50 mM $MgCl_2$, 1 µL 10 mM dNTP mix, 2 µL of each 10 pmol μL^{-1} primer (*Tnpho*A II & CEKG 2 A/B/C mix), and 0.5 µL Taq polymerase. The cycling conditions used for PCR 1 were: initial denaturation for 10 mins at 94°C; amplification for 5 cycles of 94°C for 30 secs, 42°C for 30 secs (decreased by 1°C for each subsequent cycle), and 72°C for 3 mins; further amplification for 25 cycles of 94°C for 30 secs, 65°C for 30 secs, and 72°C for 3 mins; and a final elongation for 5 mins at 72°C. The product of the first PCR was diluted in 80 µL ddH_2O, and used as template for the second PCR. The second reaction contained (25 µL total in ddH_2O): 2 µL template (PCR 1 product), 2.5 µL 10x PCR buffer, 0.8 µL 50 mM $MgCl_2$, 1 µL 10 mM dNTP mix, 2 µL of each 10 pmol μL^{-1} primer (Hah-1 & CEKG 4), and 0.25 µL Taq polymerase. The cycling conditions used for PCR 2 were: initial denaturation for 3 mins at 94°C; amplification for 30 cycles of 94°C for 30 secs, 65°C for 30 secs, and 72°C for 3 mins; final elongation for 5 mins at 72°C. The final reaction product was stored at 4°C indefinitely, to be purified and sent for Sanger sequencing (see Section 2.2.6.1).

2.2.2.3 Enzymatic purification

All PCR products were purified before sending for sequencing. Enzymatic purification involved the addition of 0.1 µL ExoI (to remove remaining primer or template), and 0.2 µL Antarctic phosphatase (or CIP, to remove free dNTPs) to each 20 or 25 µL PCR product. This

was incubated for 60 mins at 37°C, then for 15 mins at 85°C to heat inactivate enzymes, and stored indefinitely at 4°C.

2.2.3 Gel electrophoresis

DNA was separated using gel electrophoresis, to verify the size of PCR products or for purification purposes. Samples were run on agarose gels alongside a 1 kb DNA ladder for size comparison, at 100-120 V until sufficient separation of DNA bands (as indicated by the loading dye), and visualised under UV light. When applicable, DNA was extracted using the QIAquick® Gel Extraction Kit (Qiagen); with bands cut from the gel using a sterile razor blade, and the DNA eluted into 20 µL ddH_2O.

2.2.4 Transposon mutagenesis

Suppressor analysis by transposon mutagenesis was used to gain insight into the underlying regulatory networks of the TSS-f6 environmentally-responsive phenotype, and specifically to identify the genes necessary for transitioning through the life cycle from WS to SM. This technique allows random mutagenesis of a bacterial genome by transposon insertion, where the resulting transposon mutants are screened for a reversion in colony morphology phenotype. For TSS-f6 this was run in parallel at two temperatures: at 28°C (SM suppressed) and 20°C (WS suppressed). Transposon mutagenesis was achieved using the IS-Ω-km/hah transposon (Giddens et al., 2007), and a tri-parental conjugation as described in Section 2.2.4.1 below. From the transposon mutants produced, the location of the transposon insertion was determined by AP-PCR and sequencing (detailed in Section 2.2.2.2).

2.2.4.1 Tri-parental conjugation

The tri-parental conjugation involved: the recipient *P. fluorescens* TSS-f6 (or other), the donor *E. coli* (containing IS-Ω-km/hah transposon), and the helper *E. coli* pRK2013 (encoding transfer and mobilisation genes). Overnight cultures of the recipient, donor, and helper strains were grown containing the appropriate antibiotics. Two 2 mL aliquots of recipient culture were heat shocked at 45°C for 20 mins, then pelleted by centrifugation (6,000 g for 2 mins), each resuspended in 0.5 mL KB and combined (1 mL total). 1 mL of

each donor and helper was pelleted and resuspended in 0.5 mL KB each; these were then both combined with the 1 mL of concentrated recipient. The recipient-donor-helper mix was then pelleted and resuspended in 60 µL KB. For conjugation: 15 µL spots of the mix were inoculated on a pre-warmed KB plate (each spot spread to ~1 cm^2), allowed to dry, and the plates incubated non-inverted at 28°C for 5 hrs. Each conjugation spot was then scraped and resuspended in 150 µL KB, and spread in replicate on KB plates (10^{-1} dilution) containing Nf (to counter-select for *E. coli*) and Km (to select for the transposon insertion). These plates were incubated at either 28 or 20°C respectively for 2-3 days, the colonies were then screened for a reversion in phenotype, and mutants re-streaked for purification.

The TSS-f6 transposon mutants were screened for a specific colony morphology: at 28°C the reversion from SM to WS, and at 20°C the reversion from WS to SM. More than 8,000 colonies were screened at each temperature; those with the required phenotype were re-streaked and incubated at the opposite temperature, to ensure the phenotype was maintained and no switching was occurring. Those mutants that had the true reversion of phenotype were stored at -80°C, and later prepared for sequencing to identify the transposon insertion location. A second round of transposon mutagenesis was also completed in the same manner as described previously, using select TSS-f6 transposon mutants obtained in the first round of screening, with the transposon cre-deleted (see Section 2.2.4.2). In this second round the reversed screen was completed: at 28°C the reversion from WS back to SM, and at 20°C the reversion back from SM to WS; with more than 4,000 colonies screened at each temperature.

2.2.4.2 Transposon excision

The excision of the IS-Ω-km/hah transposon from TSS-f6 transposon mutants produced by transposon mutagenesis was achieved by Cre recombinase-mediated excision. Using the *loxP* sites, Cre-recombinase removes most of the IS-Ω-km/hah transposon (including the Km^R gene) leaving an 189 bp scar at the insertion location (Giddens et al., 2007). This method allows an investigation into potential polar effects of the transposon insertion, indicating whether the effect on phenotype is a result of mutation to the gene in which the insertion occurred, or the polar effect of this on downstream genes.

Transposon excision involved a bi-parental conjugation between the recipient transposon mutant, and the donor *E. coli* (containing the pCre plasmid). Overnight cultures of the recipient, and donor strains were grown containing the appropriate antibiotics. A 2 mL aliquot of recipient culture was heat shocked at 45°C for 20 mins, and mixed with 0.4 mL of donor culture. This recipient-donor mix was then pelleted by centrifugation (6,000 g for 2 mins), resuspended in 30 µL KB, inoculated on the centre of a pre-warmed KB plate (spread to ~2 cm^2), and incubated non-inverted at 28°C for 24 hrs. The conjugation was then scraped and resuspended in 150 µL KB, spread on a KB plate (10^{-6} dilution) containing Nf, and incubated at 28°C for 2 days. To confirm excision of the transposon, selected colonies were re-streaked on KB plates containing Nf and Km, with those demonstrating sensitivity to Km kept and stored indefinitely at -80°C.

2.2.4.3 Phenotypic characterisation of transposon mutants

The phenotypes of select TSS-f6 (or other) transposon mutants were also characterised using the same methods as described for TSS-f6 in Section 2.2.1, including the colony morphology and mat formation ability.

2.2.5 Genomic DNA extraction

Genomic DNA was extracted from overnight cultures or colony scrapings, using the Wizard® Genomic DNA Purification Kit (Promega). The genomic DNA was resuspended in 100 µL DNA rehydration solution, and stored at -20°C. The concentration and quality of DNA was tested by spectrophotometry using the NanoDrop; concentration greater than 100 ng μL^{-1}, and 260/280 ratio of approximately 1.8-2.0.

For whole-genome sequencing, DNA was extracted from overnight cultures of TSS-f6, L17-*mutS*wt, and the f2 ancestor. DNA was also extracted from the scrapings of colonies grown at both 28 and 20°C of TSS-f6, SBW25, and select TSS-f6 transposon mutants (WS TSS-f6-*wspE*mut & SM TSS-f6-*wspE*mut).

2.2.6 DNA sequencing

2.2.6.1 Sanger sequencing

Purified PCR products were sent to Macrogen (Seoul, Korea) for Sanger sequencing. The DNA sequences were mapped to the *P. fluorescens* SBW25 genome (NC_012660, Pseudomonas Genome database; Winsor et al., 2016) using BLAST (NCBI), and aligned with Geneious (version 9.1.7). For transposon mutagenesis, the location of the transposon insertion was determined using BLAST and the graphic annotation of alignment. The gene and amino acid residue number was identified, and the corresponding gene ontology and protein domain identified using the Pseudomonas Genome database and NCBI Conserved Domain Database (Marchler-Bauer et al., 2015).

2.2.6.2 Whole-genome sequencing

Extracted genomic DNA (see Section 2.2.5) was whole-genome sequenced with Illumina to obtain short reads (50-300 bp) of high accuracy, allowing alignment of the genome and identification of mutations including SNPs. This was completed with DNA extracted from overnight cultures of TSS-f6, L17-*mutS*wt and the f2 ancestor (f2-6.2); and from colony scrapings grown at either 28 and 20°C of TSS-f6 and select TSS-f6 transposon mutants (WS TSS-f6-*wspE*mut & SM TSS-f6-*wspE*mut). The reads from Illumina for each sample were aligned to the *P. fluorescens* SBW25 genome (NC_012660, Pseudomonas Genome database; Winsor et al., 2016) with Geneious (version 9.1.7). The predicted mutations were identified using breseq (version 0.28.1; Deatherage & Barrick, 2014), as well as manually checked from the alignment in Geneious. Comparison of the mutations in TSS-f6, L17-*mutS*wt and the f2 ancestral genotypes enabled identification of the mutations unique to TSS-f6, and thus those necessary for the environmentally-responsive developmental switch.

2.2.7 Analysis of mutation rate

Due to the history of the hypermutator Line 17 in which TSS-f6 was derived (from L17-*mutS*wt), it was of interest to analyse the mutation rate of TSS-f6. Hammerschmidt et al. (2014) found Line 17 to have a genetic switch that allowed transition through the life cycle by expansion and contraction of a guanine tract in *wspR*, this mediated by the mutation in

mutS and elevated mutation rate. The environmentally-responsive phenotype in TSS-f6 may therefore also have some relation to changes in mutation rate. This was investigated with fluctuation tests (see Section 2.2.7.1), and specific guanine tracts of interest sequenced (see Section 2.2.7.2).

2.2.7.1 Fluctuation tests

Fluctuation tests may be used to analyse the mutation rate of bacterial strains, based on the Luria & Delbrück (1943) experiment. Mutation rate refers to the rate of spontaneous mutation per the mutational target per generation (Drake, et al., 1998). These mutations are all heritable changes to the nucleotide sequence of DNA in an organism in the absence of DNA damaging agents; including base pair substitutions, deletions, insertions, duplications or frameshifts (Rosche & Foster, 2000). The fluctuation analysis method determines mutation rate (per cell per generation) by analysing the distribution of mutant numbers in parallel cultures, dependent on the Luria and Delbrück distribution (Foster, 2006). The Lea-Coulson model assumes that the probability of mutation is constant, the proportion of mutants is small, the initial number of cells are negligible compared to the final number, growth rates are the same in mutants and non-mutants, reverse mutations and death are negligible, all mutants are detected, and no mutants arise after the selection is inflicted (Rosche & Foster, 2000). Based on this model the MSS-maximum likelihood method may be used to estimate the number of mutations (m) and mutation rate (μ), from the number of mutants (r) and the total number of cells (N) obtained in the experiment. Although fluctuation tests only investigate the general mutation rate of an organism using a representative antibiotic resistance gene, so are not useful in identifying for example hypermutable loci.

The method used for fluctuation analysis of mutation rate was based on the protocol by the Barrick Lab (2017). The mutation rate was estimated for TSS-f6 and the controls of SBW25 and the f2 ancestor. Overnight cultures of each bacterial strain were used to inoculate replicate parallel cultures; 10 μl of a 10^{-4} dilution (~1000 cells) was used to start each culture, incubated at 28°C shaking for 24 hours to reach saturation. The initial overnight culture was also plated on KB (10^{-7} dilution) to count the exact number of cells used for the inoculation; this had to be approximately equal between strains to allow comparison of results. After incubation, each 24 hour culture was then plated in replicate on selective KB plates

containing rifampicin (Rif, no dilution), and non-selective KB plates (10^{-7} dilution). These plates were incubated at 28°C for exactly 48 hours, and the number of colonies counted; the selective plates providing the number of Rif resistant (Rif^R) mutants (r) and the non-selective plates the total number of cells (N). In the case that there was variety in colony size on selective plates, a size cut off was used in which colonies smaller than a certain size were not included. This experiment was also repeated using nalidixic acid (Nal) instead of rifampicin, for a comparison of the effectiveness of the antibiotic. From the replicate numbers for r and N, the mutation rate (μ, per 10^{-7} mutations/genome/generation) was then calculated for each strain using the FALCOR fluctuation analysis calculator and MSS-Maximum Likelihood Estimator Method (MSS-MLE) (Hall et al., 2009). For statistical analysis of the estimated mutation rates obtained, the 95% confidence intervals (95% CI) for each strain were compared.

2.2.7.2 Guanine tract sequencing

Specific guanine tracts (G tracts) were sequenced to observe the mutational expansion or contraction of these loci in TSS-f6 and select TSS-f6 transposon mutants. The sequencing was achieved using PCR with DMSO (see Section 2.2.2.1) and primer pairs specific to known G tracts in the *wss* and *wsp* operon, specifically: *wssE* (5 G's), *wssJ* (5 G's), *wspC* (5 G's), & *wspR* (7 G's). This was completed using the DNA template from overnight cultures of TSS-f6 and select TSS-f6 transposon mutants, as well as from colony scrapings grown at 28 and 20°C of TSS-f6, L17-*mutS*wt, f2, and select TSS-f6 transposon mutants. The PCR products were sequenced by Sanger sequencing (see Section 2.2.6.1), and the G tracts analysed for any expansion or contraction in length by alignment to the respective gene using Geneious (version 9.1.7). The DNA base calling of the individual bases within G tracts were also checked on the raw .AB1 files, a strong and differentiated peak indicating a high accuracy of sequencing and base calling.

Chapter 3: Results

3.1 Phenotypic Characterisation of TSS-f6

3.1.1 Colony morphology

3.1.1.1 TSS-f6 temperature-sensitivity

The colony morphology phenotype was observed on KB agar plates as described in Section 2.2.1.1. The phenotype of TSS-f6 was compared with SBW25 and LSWS that exhibit the typical SM and WS phenotypes respectively, as well as the WS ancestral genotype L17-*mutS*wt. As seen in Figure 3.1 below there is a distinct difference in the phenotype of TSS-f6 at different incubation temperatures: SM at 28°C and WS at 20°C (or 25°C). For TSS-f6, the SM at 28°C highly resembles SBW25 though it has a slightly larger colony size; the WS at 20°C resembles the L17-*mutS*wt ancestor, and differs from the type of wrinkly of LSWS in that it is significantly smaller (approximately one-third the colony size). Therefore TSS-f6 exhibits an environmentally-responsive change in phenotype between WS and SM, likely dependant on the environmental cue of oxygen (though observed as temperature).

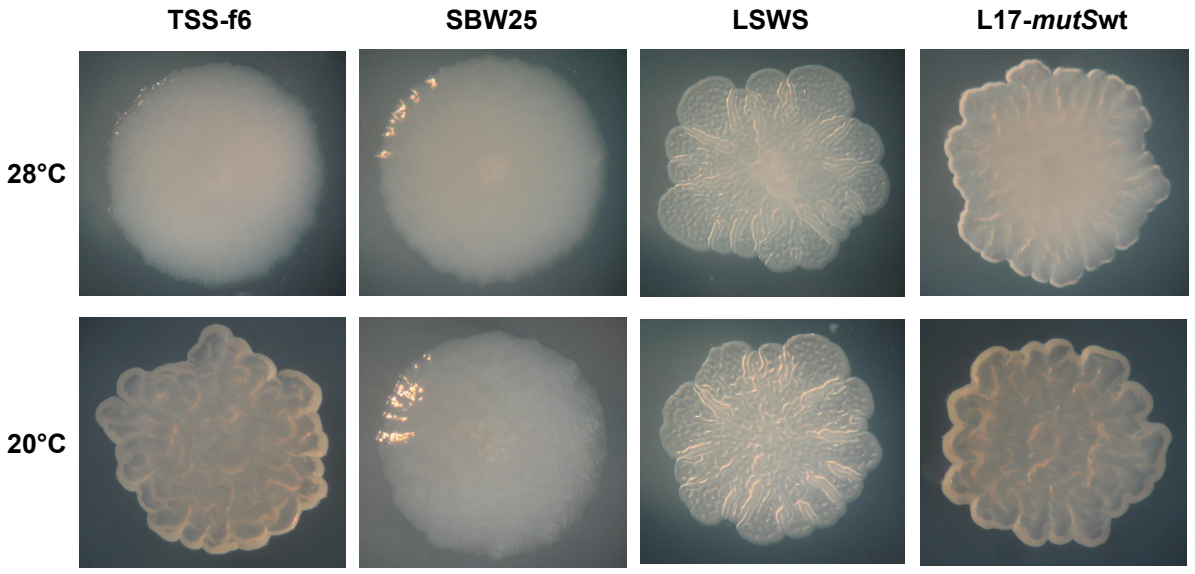

Figure 3.1 Colony morphology phenotypes at the temperatures of 28 and 20°C. The colony morphology of TSS-f6, SBW25, LSWS and L17-*mutS*wt; individual colonies observed on KB agar plates incubated at either 28 or 20°C for 3 days. TSS-f6 with the distinct phenotypes of SM at 28°C and WS at 20°C.

The TSS-f6 colony morphology was stably maintained upon prolonged restreaking (every 2-3 days for 2 weeks, from initial plates at both 28 and 20°C, with alternation in temperature). The origin of the cells or the number of times restreaked and alternated incubation temperature had no influence – the colonies always appeared distinctly smooth at 28°C and wrinkly at 20°C. To further confirm this phenotype, the morphology of overnight culture spots on KB plates were observed as seen in Figure 3.2 below; also demonstrating the phenotypes of SM at 28°C and WS at 20°C. The extent to which overnight cultures were grown (between 16-20 hours at 28°C) also had no effect on the resulting TSS-f6 phenotype.

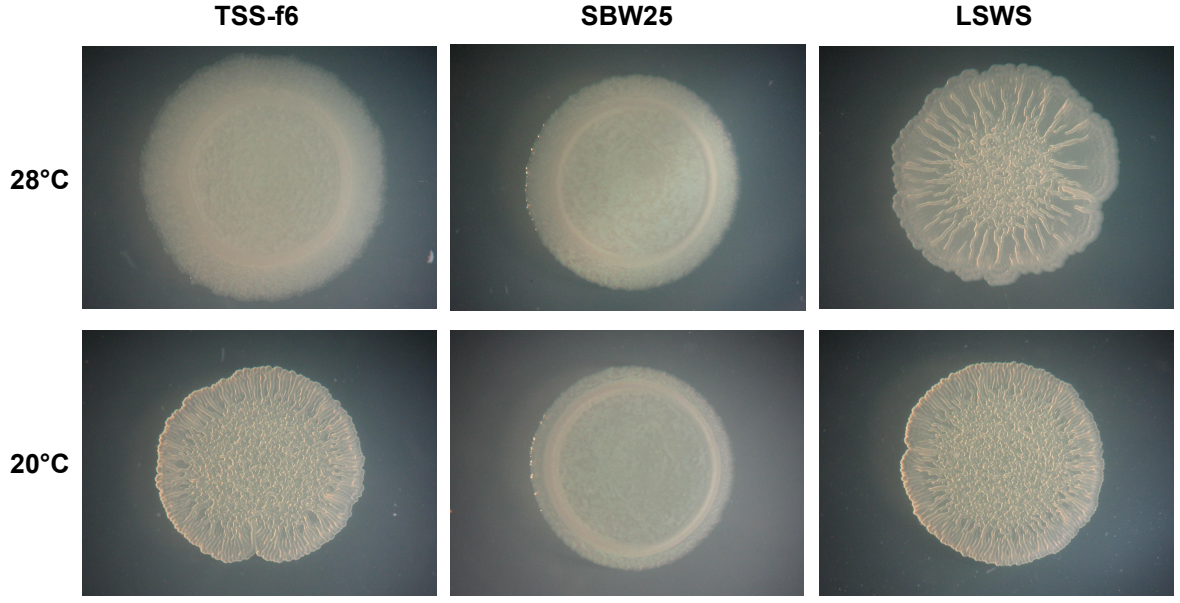

Figure 3.2 Morphology phenotypes of overnight culture spots at the temperatures of 28 and 20°C. The morphology of TSS-f6, SBW25 and LSWS; observed of 5 µl spots of overnight culture on KB agar plates incubated at either 28 or 20°C for 1 day. TSS-f6 with the distinct phenotypes of SM at 28°C and WS at 20°C.

To visually demonstrate the TSS-f6 phenotype, overnight culture spots were also observed on KB plates containing the Congo red stain, with the incubation temperature of plates alternated between 28 and 20°C (every 2 days, beginning at either temperature, 8 days total). As seen in Figure 3.3 below there is a defined difference in the Congo red binding of TSS-f6 at 28 and 20°C as compared to SBW25 – the WS colony morphology phenotype at 20°C appearing red in colour. As the cells grew and expanded outwards with the alternation of temperature, the WS at 20°C is observed as red rings and the SM at 28°C as rings without the red colour (although turning a pale-red colour over time as seen on the SBW25 plate)

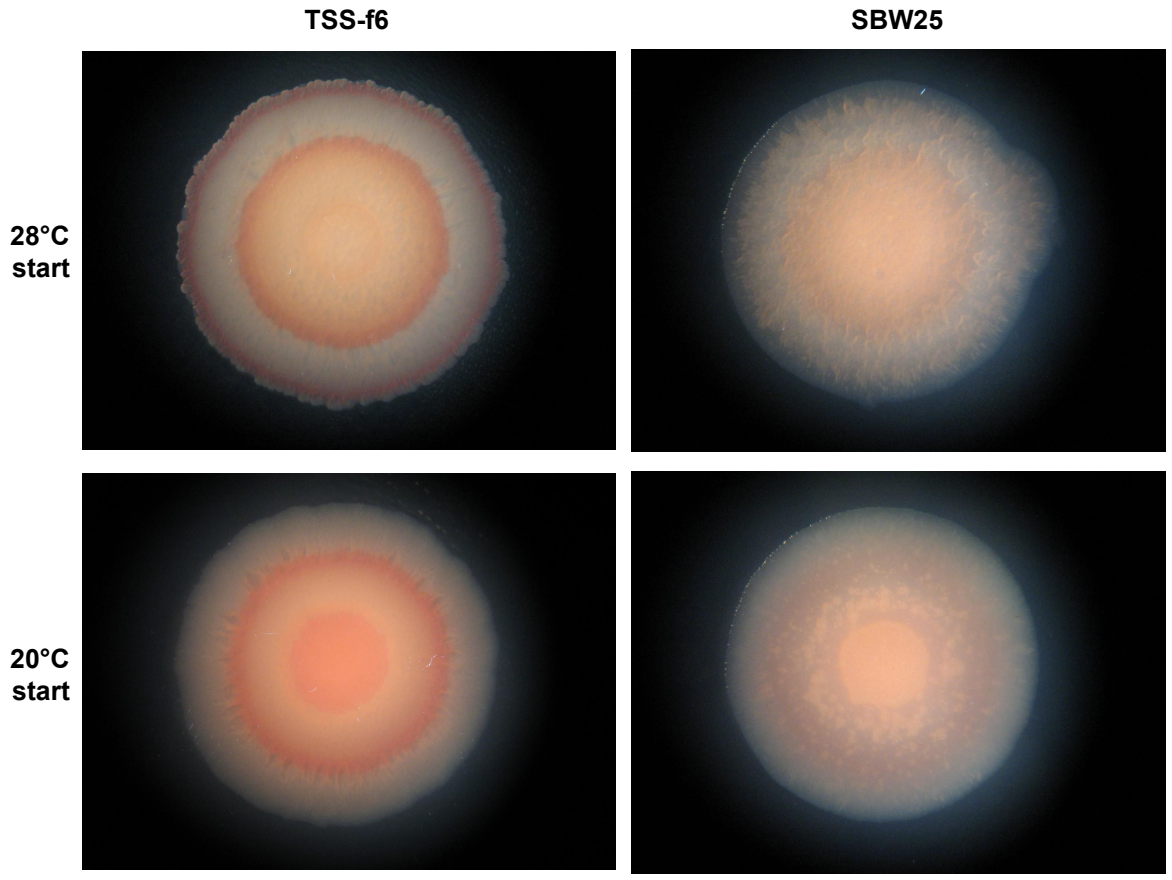

Figure 3.3 Morphology phenotypes of overnight culture spots on Congo red plates with alternation in incubation temperature. The morphology and Congo red binding of TSS-f6 and SBW25; observed of 2 µl spots of overnight culture on KB agar plates containing Congo red stain, incubated for 2 days at the alternating temperatures of 28 and 20°C (for 8 days total). TSS-f6 with a red ring observable from the WS phenotype at 20°C and no red colour from the SM phenotype at 20°C.

3.1.1.2 Other colony phenotypes

TSS-f6 was also seen to give a distinctive colony phenotype at the incubation temperature of 20°C, as seen in Figure 3.4 below. After 3 or 4 days of incubation on KB plates a 'lumpy' mucoid coating often began to cover the colony, almost completely covering the colony by day 6 (and hiding the WS colony phenotype underneath). The TSS-f6 coating shows visual similarity to the colanic acid-based capsules seen by Beaumont et al. (2009) – evolved stochastic switching strains of *P. fluorescens* SBW25 with populations exhibiting an ON-OFF switch for expression of capsulation (Gallie, 2010; Gallie et al., 2015). To investigate whether this coating in TSS-f6 is correlated with a similar capsulation, a capsule staining assay was complete; refer to Section 3.1.3.

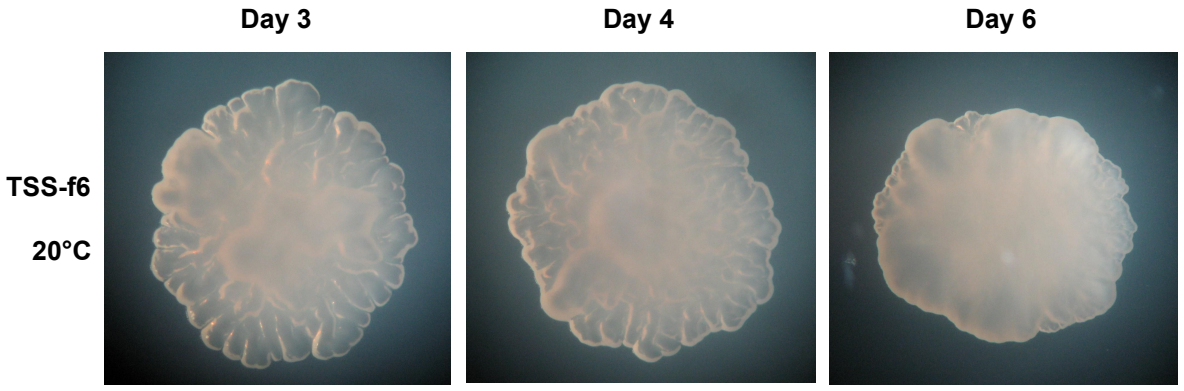

Figure 3.4 Colony morphology phenotype of TSS-f6 at 20°C over 6 days. The colony morphology of TSS-f6; individual colonies observed on KB agar plates incubated at 20°C for 6 days. Formation of a mucoid coating over the colony often observed after 3-4 days, showing visual similarity to colanic acid-based capsules.

3.1.1.3 Potential environmental cues

The possibility that a range of different environmental cues might affect the colony phenotype in TSS-f6 was considered. Various changes were made to KB agar media and the environmental conditions of incubation. Alterations made to pH level, agarose percentage, and salt concentration showed no obvious response (P. Remigi & D. Rexin, unpublished data). An increase in incubation temperature to as high as 32°C also did not demonstrate any effect, neither did decreasing the temperature (although such changes were difficult to observe, as non-optimal temperature hindered the general cell growth). The growth of TSS-f6 on depleted media (described in Section 2.2.1.1) showed a minor response, with a slight wrinkly texture observed on overnight culture spots grown at 28°C; though this was not considered a significant effect. More work is required to devise a method of investigating the potential effect of altering oxygen levels or evoking oxygen starvation.

3.1.1.4 Genotypes ancestral to TSS-f6

To confirm the emergence of the developmental switch in TSS-f6, the colony morphology of the ancestral genotypes were also examined. The origin of TSS-f6 and the ancestral genotypes in the continuation of the Hammerschmidt et al. (2014) life cycle experiment are shown in Figure 3.5 below. There was no observation of environmentally-responsive phenotypes for the following ancestral genotypes: Line 17, L17-*mutS*wt, and the f2 ancestors (f2-5.2, f2-6.1 & f2-6.2). The temperature-sensitivity was observed in the direct f2 ancestor (f2-7.1) in only some cells of the SM pool, this was expected as this line is the origin of

TSS-f6. From this, it is clear that the final mutation resulting in the TSS-f6 phenotype switch occurred at some point between the ancestor f2-6.2 and f6-7.2, that was not present in the previous ancestors.

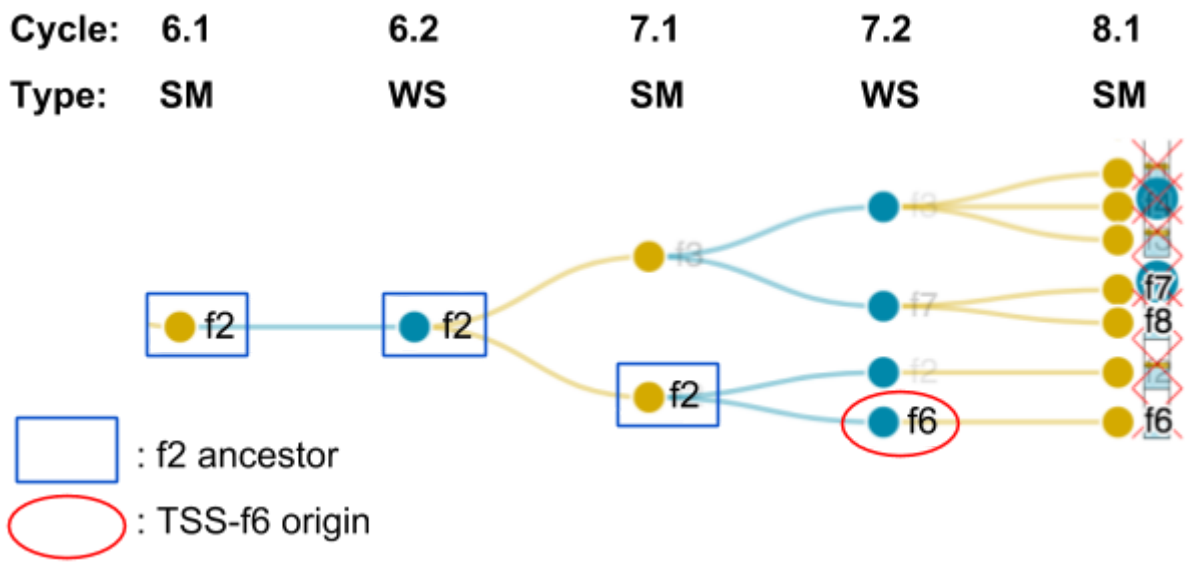

Figure 3.5 Diagram of lineage selection and continuation of the life cycle experiment showing the origin of TSS-f6 and ancestral genotypes. The TSS-f6 strain was isolated after cycle 7 phase II (7.2), from the continuation of the life cycle experiment with Line 17-*mut*Swt in small microcosms. During cycle 7 the f2 ancestor was used to seed both f2 and f6 lines, with reproduction the result of extinction of another replicate line. No environmentally-responsive phenotypes observed for the ancestral genotypes f2 6.1 & 6.2; only in TSS-f6 and some cells of the f2 7.1 ancestor (origin of TSS-f6).

3.1.2 Niche preference in static broth

3.1.2.1 Mat formation

The niche preference indicated by mat formation ability in static broth microcosm was investigated as described in Section 2.2.1.2. The formation of mats were observed in replicate cultures of TSS-f6 at both 28°C and room temperature (RT, to approximate 20°C), and comparisons made with SBW25 and the ancestral genotype L17-*mut*Swt. As seen in Figure 3.6 below, TSS-f6 demonstrates a unique niche preference at 28 and 20°C incubation: at 20°C a 'webbed' texture mat forms at the surface of the broth, while at 28°C a thick 'milky' texture mat begins to form even after 1 day of incubation. The TSS-f6 webbed mat at 20°C resembles the L17-*mut*Swt ancestral mat at 28°C, with very little cell growth observed

throughout the rest of the microcosm broth phase. The TSS-f6 thick milky mat at 28°C does not resemble the ancestor, with substantial cell growth throughout the microcosm. This differs from SBW25, that has no mat formation after 2 days incubation, and more cell growth throughout the microcosm.

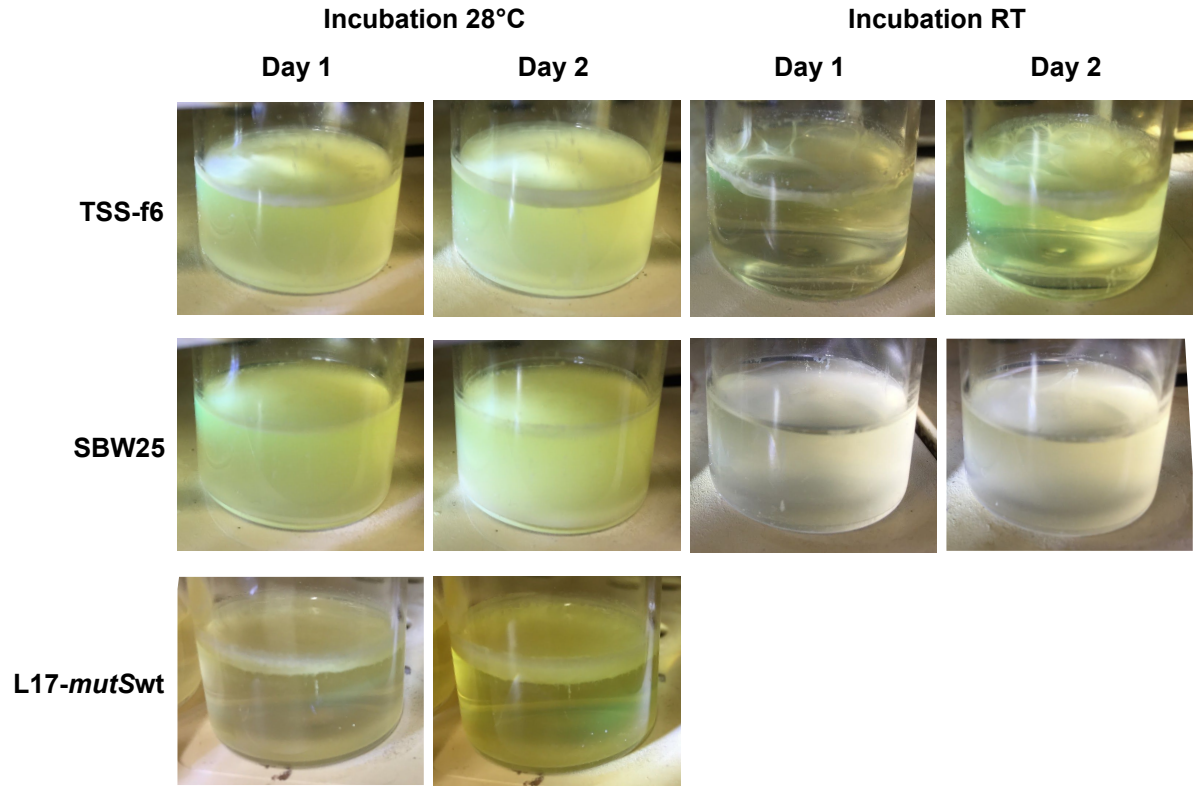

Figure 3.6 Niche preference of TSS-f6 with incubation at 28°C and room temperature. The mat formation ability of TSS-f6, SBW25, and L17-*mutS*wt; mats observed in static KB broth incubated at either 28°C or room temperature for 2 days. TSS-f6 with the unique mat formation ability, a thick milky mat observable at 28°C and a webbed mat at room temperature.

To further compare the niche preference of TSS-f6 and SBW25 at 28°C in the context of the life cycle experiment, time lapse images of mat formation were captured over 6 days – shown in Figure 3.7 below. TSS-f6 began to form a thick milky mat at the broth surface by Day 2 of incubation at 28°C, while SBW25 did not form any mat until Day 4. At Day 2 for TSS-f6 the cells in the broth were located both at the surface forming a mat and spread throughout the broth phase, and for SBW25 all cells were throughout the broth with no mat formation. This demonstrates a clear difference in the niche preference of TSS-f6 and SBW25 at 28°C. Even though TSS-f6 demonstrates the SM colony morphology phenotype at 28°C on KB plates, this phenotype is not carried through in the KB static broth in which it appears to act as a WS

type. TSS-f6 thus alters its phenotype – revealing the capacity to colonise the air-liquid interface, in response to some environmental cue encountered within static broth microcosms.

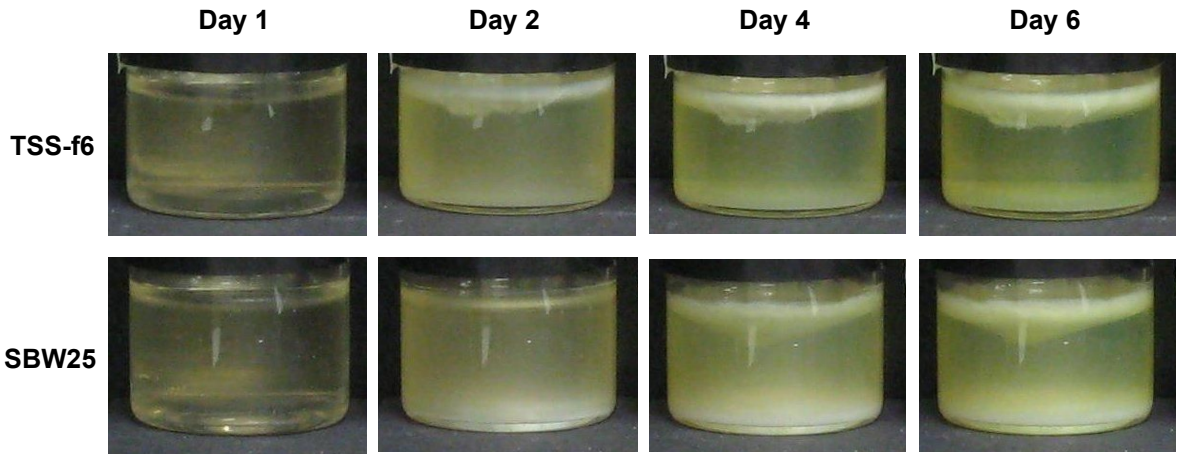

Figure 3.7 Niche preference of TSS-f6 over 6 days incubation at 28°C. The mat formation ability of TSS-f6 and SBW25; mats observed in static KB broth incubated at 28°C for 6 days. TSS-f6 with a thick milky mat forming by Day 2 incubation, while for SBW25 a mat forms by Day 4.

3.1.2.1 Evolution of WS phenotypes

To further investigate the niche preference of TSS-f6 at 28°C, static broths were plated each day over 6 days of incubation, to check whether WS phenotypes were evolving. This was completed for TSS-f6, the smooth SBW25, and smooth f2 ancestor. From the plating of broth samples at Day 1 and 2 all strains remained SM in colony morphology (after 2 days mutations then start to accumulate). For TSS-f6, by Day 6 no WS types evolved – the colonies remaining completely homogenous for the SM colony phenotype at 28°C. For SBW25, by Day 3 the plated static broths demonstrated the evolution of WS types, and by Day 6 various phenotypes were present (SM, small SM, large WS, small WS & fuzzy); the same occured in the f2 ancestor (though no large WS types were observed). This result indicates that the mat formed by SBW25 after 3 days incubation in static broth is likely the result of the evolution of WS types, while the mat formed by TSS-f6 at 28°C is the result of the SM types (as observed by colony morphology on plates) with no evolution of other types observed.

The inability for TSS-f6 to evolve WS types at 28°C over 6 days indicates that it either may be no longer able to evolve this phenotype due to destruction of the mutational pathways, or that it does not need to evolve the WS types as it is already capable of forming a mat. As

TSS-f6 forms a strong mat at 28°C, and the SM f2 ancestor is able to evolve WS types (though only of the smaller variety) while TSS-f6 cannot, gives support for the later. It is likely that TSS-f6 is already fulfilling the niche of colonisation of the air-liquid interface and thus there is no selective pressure for the evolution of WS types. Overall this confirms that while TSS-f6 demonstrates the distinct SM colony morphology at 28°C, it is able to form a mat and act like a WS type at the surface of static broth microcosms. It may be concluded that TSS-f6 at 20°C has the WS colony phenotype and mat production with niche preference for the ALI, while at 28°C it has the SM colony phenotype with an indistinct niche preference.

3.1.3 Capsule staining

The India ink capsule staining assay was employed to investigate production of capsules in TSS-f6. This was performed on TSS-f6 and select TSS-f6 transposon mutants (transposon mutagenesis described later in Section 3.3.1). TSS-f6 displayed capsulation of approximately 5% (greater than SBW25), while the transposon mutants had varying levels of capsulation from approximately 20% to as high as 99% capsulation. This result indicates that the formation of this lumpy coating on TSS-f6 at 20°C is likely due to capsulation, and suggests that the developmental switch may have some link to known mechanisms of stochastic switching in SBW25 (Beaumont et al., 2009; Gallie et al., 2015; Remigi et al., 2018).

3.2 Mutational History of TSS-f6

The mutational history of TSS-f6 was derived by whole-genome sequencing of TSS-f6, and the ancestral genotypes L17-*mutS*wt and f2; as described in Section 2.2.6.2. The full list of mutations identified in these genotypes are provided in Appendix 1. Sequencing was also obtained of TSS-f6 from colony scrapings grown at both 28 and 20°C, to identify any mutational difference in the SM or WS colony cells grown at the different temperatures.

3.2.1 TSS-f6 mutations

The mutations identified to be unique to the TSS-f6 genotype as compared to the most recent f2 ancestor are detailed in Table 3.1 below. There were two mutations found in TSS-f6: a substitution (V441G) in the methyl-acceptor domain of *wspA*, resulting in the expansion of a G tract from 5 to 7 residues; and a 9 bp in-frame duplication (470_472dupNLT) in the GGDEF domain of *pflu0458*.

Gene	Protein function[a]	Mutation[b]	Effect[c]	Domain[d]
wspA	Signal transduction; methyl-accepting chemotaxis	T>G	Substitution (V441G); G tract expansion (5 → 7)	MCPsignal (methyl acceptor)
pflu0458	Signal transduction; histidine kinase; EAL & GGDEF domain	dup 9bp	9 bp duplication in-frame (470_472dupNLT)	GGDEF

Table 3.1 Mutations unique to cDNA of the TSS-f6 genotype. [a] Protein function refers to the predicted function of the putative gene product. [b] Mutation refers to the nucleotide sequence change. [c] Effect refers to the amino acid sequence change of the protein, and the description of the mutation effect. [d] Domain refers to the predicted protein domain of the mutation (NCBI CDD, significant expect value).

The *wspA* mutation is of great interest as the *wsp* operon has major involvement in the WS phenotype of *P. fluorescens* SBW25, with WspA predicted to be a membrane-bound methyl-accepting chemotaxis protein (Bantinaki et al., 2007). In models developed of the *wsp* system in *Pseudomonas*, WspA is theorised to act as a chemoreceptor that detects extracellular signals on a surface during bacterial chemotaxis, resulting in the phosphorylation of WspR (upon interaction with *wsp* pathway); the phosphorylated WspR DGC then catalysing the synthesis of c-di-GMP and thus biofilm production (Bantinaki et al., 2007; O'Connor et al., 2012). The role of WspA as a chemotaxis receptor provides a potential link to the temperature-sensitivity of TSS-f6 – and more specifically to the possibility of oxygen sensing. In TSS-f6, the substitution in *wspA* results in the expansion of a G tract specifically in the MCP domain (containing putative MCP methylation sites), this may potentially alter the detection and transduction of environmental signals.

The other mutation in *pflu0458* unique to TSS-f6 is also of interest – Pflu 0458 containing both an active EAL domain and an inactive GGDEF domain (lacking the enzymatic GGDEF motif), likely functioning as a PDE in c-di-GMP degradation (Lind et al., 2015). It is unclear the effect of a 9 bp duplication in-frame in the non functional GGDEF domain of *pflu0458*.

Although mutations in this gene have been identified in WS mutants of *P. fluorescens* SBW25 in numerous other studies (Lind et al., 2015; Farr, 2015; Barnett, 2016).

3.2.1.1 Temperature-dependant mutations

From sequencing of TSS-f6 colonies grown at 28 and 20°C, no mutational differences were identified. Therefore no temperature-dependant mutations were found in TSS-f6 that may be involved in the environmentally-responsive phenotype. Although it is possible that these potential mutations are not discoverable from short-read Illumina data; more information may be available using long-read sequencing, for example large structural variants from de novo genome assembly or epigenetic modifications like DNA methylation.

3.2.2 f2 ancestor mutations

The mutations identified as unique to the f2 ancestor (f2-6.2) genotype as compared to Line 17-*mut*Swt are detailed in Table 3.2 below. There were two mutations found in the f2 ancestor: a substitution (T104N) in the ligand-binding chemoreceptor domain of *wspA*; and a substitution (H70L) in the histidine-containing phosphotransfer signaling domain of *wspE*.

Gene	Protein function[a]	Mutation[b]	Effect[c]	Domain[d]
wspA	Signal transduction; methyl-accepting chemotaxis	C>A	Substitution (T104N)	LBD (chemoreceptor)
wspE	Signal transduction; two-component system, histidine kinase; response regulator	A>T	Substitution (H70L)	CheA - HPT (signalling)

Table 3.2 Mutations unique to cDNA of the f2 ancestral genotype. [a] Protein function refers to the predicted function of the putative gene product. [b] Mutation refers to the nucleotide sequence change. [c] Effect refers to the amino acid sequence change of the protein, and the description of the mutation effect. [d] Domain refers to the predicted protein domain of the mutation (NCBI CDD, significant expect value).

Both these mutations in the *wsp* operon are of interest due to their involvement in the WS phenotype. In f2, the substitution in *wspA* results in one amino acid change to the ligand-binding domain; WspA functioning as a membrane-bound chemoreceptor protein (described previously). The substitution in *wspE* results in one amino acid change to the signalling domain; WspE functioning as a hybrid histidine kinase (activated by WspA), and response regulator causing the phosphorylation of WspR (Bantinaki et al., 2007). As only two

mutations were identified in the f2 ancestor after going through 6 extra generations of the life cycle experiment, it is possible that one or both of these mutations are reversible to allow the transition from WS to SM at one mutational locus (or potentially that there were other mutations not identified).

3.2.3 Line 17-*mutS*wt ancestor mutations

The mutations identified to be unique to the *wsp* operon of the Line 17-*mutS*wt ancestral genotype as compared to the SBW25 reference are given in Table 3.3 below; the full list of L17-*mutS*wt mutations are provided in Appendix 1. There were a total of 75 mutations preexisting in the L17-*mutS*wt background of TSS-f6 – those in the *wsp* operon were focused on due to their role in the WS phenotype. There were three mutations identified in the wsp operon of L17-*mutS*wt: a substitution (D253Y) in the histidine kinase domain of *wspA*; a 9 bp in-frame deletion (37_39delAEV) in the signal transduction domain of *wspB*; and a substitution (I295S) in the response regulator domain of *wspF*. This gives a total of 6 mutations to the *wsp* operon of TSS-f6 – *wspA* (x3), *wspE* (x1), *wspB* (x1) and *wspF* (x1). The extensive changes to this important operon will likely have a great influence on the TSS-f6 expression of *wss* and the WS phenotype.

Gene	Protein function[a]	Mutation[b]	Effect[c]	Domain[d]
wspA	Signal transduction; methyl-accepting chemotaxis	G>T	Substitution (D253Y)	Tar - HAMP (histidine kinase)
wspB	Signal transduction; chemotaxis; scaffold protein	del 9bp	9 bp deletion in-frame (37_39delAEV)	CheW (signal transduction)
wspF	Signal transduction; methylesterase; response regulator	T>G	Substitution (I295S)	CheB (response regulator)

Table 3.3 Mutations unique to *wsp* operon of the Line 17-*mutS*wt ancestral genotype. [a] Protein function refers to the predicted function of the putative gene product. [b] Mutation refers to the nucleotide sequence change. [c] Effect refers to the amino acid sequence change of the protein, and the description of the mutation effect. [d] Domain refers to the predicted protein domain of the mutation (NCBI CDD, significant expect value).

3.3 Suppressor Analysis

Suppressor analysis was achieved by transposon mutagenesis using IS-Ω-km/hah, as described in Section 2.2.4. This was performed for TSS-f6 to identify the specific genes underlying the environmentally-responsive phenotype. Screening was completed with TSS-f6 in parallel at 28°C (SM suppressed) and 20°C (WS suppressed). A second round of transposon mutagenesis screening was then completed using two selected transposon mutants from the initial screens, with the transposon removed using the Cre-*lox* system (Giddens et al., 2007): WS TSS-f6-*wspE*mut at 28°C (WS suppressed) and SM TSS-f6-*wspE*mut at 20°C (SM suppressed). For all screens, the phenotype of each mutant was checked at both incubation temperatures to ensure that the temperature-sensitivity was being suppressed, and only the true revertants with no observation of switching in phenotype were retained. The full details of each transposon mutant obtained from the four transposon mutagenesis screens are provided in Appendix 2.

3.3.1 Transposon mutagenesis of TSS-f6

The transposon mutagenesis of TSS-f6 was performed at 28°C and mutants screened for suppression of the SM phenotype (WS colonies were selected (Screen A)), and at 20°C mutants were screened for loss of the WS phenotype (SM colonies were selected (Screen B)). More than 8,000 colonies were examined in each screen.

3.3.1.1 Screen A: TSS-f6 – SM suppressed at 28°C

The results from Screen A, the transposon mutagenesis of TSS-f6 suppressing SM at 28°C are given in Table 3.4 below – with a total of 29 independent transposon insertions (JS:A 1-29). The cre-mediated excision of the transposon in TSS-f6 mutants resulted in no change in phenotype for mutants of *pflu5960* (JS:A17ΔCre), *wspE* (JS:A9ΔCre & JS:A24ΔCre) and *amrZ* (JS:A3ΔCre), indicating that the transposon insertion in these genes were responsible for the mutant phenotype. No polar effects were observed.

The majority of insertions were located in *pflu5960*, with 17 independent insertions (JS:A 1, 2, 6-8, 11-13, 17-21, 25, & 27-29) in both the GGDEF and EAL domains suppressing the SM

phenotype at 28°C. *pflu5960* encodes a protein with both the GGDEF and EAL domains, predicted to have DGC and PDE activity. Mutations in this gene have been identified in numerous studies with *P. fluorescens*, including WS mutants (Lind et al., 2015; Barnett, 2016), and an evolved line under selection in a carbon-limited environment (Schick et al., 2015). There were also six independent insertions in *amrZ* (JS:A 3-5, 15, 16, 22, & 23) suppressing SM; *amrZ* (also known as *algZ* or *pflu4744*) encodes a predicted DNA-binding protein. AmrZ is considered a global regulator, involved in the transcriptional regulation of alginate synthesis, motility and biofilm formation in *Pseudomonas* (Martínez-Granero et al., 2014). It is known to act as a negative repressor of the *wss* operon, an activator of the alginate gene *algR*, and to interact with flagella regulatory genes (likely repression of *fleQ*); predicted to decrease intracellular levels of c-di-GMP (Giddens et al., 2007; Jones et al., 2014). The expression of *amrZ* is also dependant on the environmental stress sigma factor AlgU (Martínez-Granero et al., 2014). Mutations in this gene have been identified in WS mutants in various studies (Lind et al., 2015; Barnett et al., 2016; Giddens et al., 2007).

Gene[a]	**Ins**[b]	**Size**[c]	**Protein function**[d]	**Domains**[e]
pflu5960	17	554	- EAL & GGDEF domain - DGC and PDE activity	- GGDEF (5) - EAL (4)
amrZ	6	108	- DNA-binding, regulation of transcription - Negative regulator of the *wss* operon	- Arc (1)
wspE	3	755	- Histidine kinase of two-component system - *wsp* operon primary mutational pathway of WS	- CheY (3)
pflu0479	1	293	- Glycosyl transferase, biosynthetic process	- None

Table 3.4 Summary of the transposon insertions in TSS-f6 suppressing the SM phenotype at 28°C. [a] Gene refers to the gene locus of transposon insertion. [b] Ins refers to number of independent insertions. [c] Size refers to the number of amino acid residues. [d] Protein function refers to the predicted function of the putative gene product. [e] Domains refers to the predicted protein domains of the gene insertions (NCBI CDD, significant expect value), specified in brackets if more than one insertion.

Interestingly there were also three independent insertions in *wspE* (JS:A 9, 10, & 24) suppressing the SM phenotype of TSS-f6 at 28°C; WspE the histidine kinase of the *wsp* system, phosphorylating the DGC-encoding *wspR* (Giddens et al., 2007). It is not usual for mutations to the *wsp* operon to suppress the SM phenotype, but rather to suppress WS and produce the SM phenotype. These insertions in *wspE* were also all within the CheY response

regulator domain, in which signals are received from the sensor kinase in the two-component system. There was also a single insertion in *pflu0479*, encoding a glycosyltransferase enzyme. The *pflu0475-0479* gene locus is involved in cell wall modification, with mutations known to cause suppression of the WS phenotype (McDonald et al., 2009). The nearby gene *pflu0478* (or *fuzY*) also encoding a glycosyltransferase has been identified as the main mutational pathway for the fuzzy-spreader (FS) phenotype of *P. fluorescens* SBW25, with mutation causing cell flocculation (Ferguson et al., 2013). FS types give the 'fuzzy' colony morphology, and as demonstrated by Ferguson et al. (2013) form a transient mat the ALI of static broth that repeatedly collapses and reforms (thus giving the appearance of colonisation of the bottom of the microcosm). The observation of transposon insertions from this screen in *pflu5960* and *amrZ* are familiar, while those in *wspE* and *pflu0479* were not to be expected.

3.3.1.2 Screen B: TSS-f6 – WS suppressed at 20°C

The results from Screen B, the transposon mutagenesis of TSS-f6 suppressing WS at 20°C are given in Table 3.5 below – with a total of 36 independent transposon insertions (JS:B 1-36). The cre-mediated excision of the transposon in TSS-f6 mutants produced no change in phenotype for mutants of *wspE* (JS:B22ΔCre & JS:B28ΔCre) and *mutL* (JS:B19ΔCre), with no polar effects observed.

Most of the insertions suppressing the WS phenotype of TSS-f6 at 20°C were located in the *wsp* operon; including five independent insertions in *wspE* (JS:B 16, 22, 27, 28, & 36), two in *wspD* (JS:B 10 & 35) and one in *wspA* (JS:B24). There were also insertions to the *wss* operon, with one in both *wssE* (JS:B31) and *wssB* (JS:B32). The role of the *wsp* and *wss* pathways in the WS phenotype are well understood, thus suppression of the WS phenotype at 20°C is as expected. Furthermore there were various singleton insertions to genes involved in metabolism; including the synthesis of pyrimidines (e.g. *carB* (JS:B11) & *pflu3892* (JS:B14)), and amino acid synthesis and transport (e.g. *phhA* (JS:B33) *pflu5860* (JS:B1), & *pflu2019* (JS:B8)). Those genes relating to the synthesis of pyrimidines and arginine provide a connection to the stochastic switching of capsulation observed by Beaumont et al. (2009) and Gallie et al. (2015). The mutations to genes of the metabolic pathway may result in changes to the global levels of c-di-GMP in the cell, thus influencing DGC/PDE activity and subsequently biofilm formation.

Gene[a]	Ins[b]	Size[c]	Protein function[d]	Domains[e]
wspE	5	755	- Histidine kinase of two-component system - *wsp* operon primary mutational pathway of WS	- CheA (1), HPT (1), HAPTase (2) - CheY (1)
wspD	2	232	- Signal transduction; scaffold protein - *wsp* operon primary mutational pathway of WS	- CheW (2)
wspA	1	540	- Signal transduction; methyl accepting - *wsp* operon primary mutational pathway of WS	- Tar
mutL	3	633	- DNA mismatch repair	- C terminal (2) - Transducer (1)
mutY	1	355	- A/G-specific adenine glycosylase - DNA mismatch repair	- Endonuclease III
wssE	1	1279	- Cellulose synthase operon protein C - *wss* operon structural basis of WS	- CesA
wssB	1	739	- Cellulose synthase catalytic subunit - *wss* operon structural basis of WS	- BcsC
pflu5860	1	457	- Outer membrane porin (OprD), transport	- OprD
carB	1	1073	- Carbamoyl phosphate synthase (CarB) large subunit - Pyrimidine/arginine biosynthesis	- ATP binding
pflu4426	1	145	- Flagellar protein FliO, cell motility	- FliO
pflu3892	1	641	- Biotin carboxylase subunit of acetyl-CoA carboxylase - Pyrimidine synthesis; carbamoyl-phosphate synthesis	- CPS L chain ATP binding
pflu0085	1	684	- GGDEF domain, DGC activity	- GGDEF
pflu2019	1	205	- Amino acid transport	- RhtB
pflu3995	1	502	- ABC-type sugar transport, ATP-binding	- ATPase
pflu4159	1	517	- Ribose transport, ATP-binding	- ABC Carb Monos II
pflu3739	1	333	- ABC transporter substrate-binding	- TauA
phaA	1	559	- Poly-hydroxybutyrate biosynthetic process	- PhaC
pdhR	1	255	- Pyruvate dehydrogenase complex repressor - Transcription regulation	- FadR C terminal
phhA	1	263	- Phenylalanine 4-monooxygenase (PhhA) - Phenylalanine metabolism	- PhhA

Table 3.5 Summary of the transposon insertions in TSS-f6 suppressing the WS phenotype at 20°C. [a] Gene refers to the gene locus of transposon insertion. [b] Ins refers to number of independent insertions. [c] Size refers to the number of amino acid residues. [d] Protein function refers to the predicted function of the putative gene product. [e] Domains refers to the predicted protein domains of the gene insertions (NCBI CDD, significant expect value), specified in brackets if more than one insertion.

Transposon insertions were also found in genes encoding determinants of the DNA mismatch repair (MMR) system, that repairs mutational errors from DNA replication; with three independent insertions in *mutL* (JS:B 5, 18, & 19) and one in *mutY* (JS:B13). The MutL enzyme has weak ATPase activity, while MutY has a more specific enzymatic function with glycosylase activity, recognising and aiding in the repair of G:A (or C:A) mismatches (to G:C) in lesions formed from oxidative damage (Modrich, 1991; Porello et al., 1996). In the MMR system: MutS binds at a mismatched base on DNA and recruits MutL, that aids in the formation of a complex between MutS and MutH; within this complex the activated MutH endonuclease then cleaves the DNA strand at specific hemimethylated sites, allowing for repair of the mismatch (Modrich, 1991). There is an association between TSS-f6 and the MMR system – with it being derived from the hypermutator Line 17 background, having a mutation in the *mutS* gene (later restored to wild type) (Hammerschmidt et al., 2014). Although it is unclear in this case how a mutation in *mutL* or *mutY* could result in suppression of the WS phenotype in TSS-f6.

3.3.1.3 TSS-f6 WS & SM wspE *transposon mutants*

The TSS-f6 transposon mutants with insertion in *wspE* were of interest as they were obtained from both transposon mutagenesis screens – suppressing both SM at 28°C and WS at 20°C. These two mutants selected from either screen with the transposon cre-deleted will be referred to as: WS TSS-f6-*wspE*mut (JS:A9ΔCre) and SM TSS-f6-*wspE*mut (JS:B22ΔCre). The WS & SM TSS-f6-*wspE*mut both contain a mutation to the *wspE* gene, but demonstrate opposite phenotypes (no polar effects were confirmed with cre-mediated excision of the transposon); the same underlying genotype TSS-f6-*wspE*mut therefore having a different phenotype. This was confirmed by whole-genome sequencing of WS & SM TSS-f6-*wspE*mut from colonies grown at both 28 and 20°C (as described in Section 2.2.6.2). The *wspE* transposon insertion was identified from the reads (transposon scar left after cre-deletion), and from the genome alignment no other mutational differences were found between the two mutants, or at either incubation temperature. A second round of mutagenesis was therefore completed with both WS TSS-f6-*wspE*mut and SM TSS-f6-*wspE*mut to further investigate the TSS-f6 developmental switch and the role of *wspE* in this complex system.

3.3.2 Second round transposon mutagenesis

A second round of transposon mutagenesis was performed with WS TSS-f6-*wspE*mut (JS:A9ΔCre) at 28°C and mutants screened for suppression of the WS phenotype (SM colonies were selected (Screen C)), and with SM TSS-f6-*wspE*mut (JS:B22ΔCre) at 20°C and mutants screened for suppression of the SM phenotype (WS colonies were selected (Screen D)). This was achieved in the same way as the initial rounds of mutagenesis, with more than 4,000 colonies examined in each screen.

*3.3.2.1 Screen C: WS TSS-f6-*wspE*mut – WS suppressed at 28°C*

The results from Screen C, the transposon mutagenesis of WS TSS-f6-*wspE*mut suppressing WS at 28°C are given in Table 3.6 below – with a total of 28 independent transposon insertions (JS:C 1-28). The cre-mediated excision of the transposon in WS TSS-f6-*wspE*mut mutants produced no change in phenotype for mutants of *wspA* (JS:C11), *wspC* (JS:C25), *wspD* (JS:C8), *wspE* (JS:C23), *wspR* (JS:C27) and *pflu5960* (JS:C21). No polar effects were observed.

From this second round of screening with WS suppressed in WS TSS-f6-*wspE*mut at 28°C, most of the insertions were as expected to the *wsp* pathway; with seven independent insertions in *wspE* (JS:C 7, 14, 16, 20, 22, 23, & 28), seven in *wspR* (JS:C 4, 9, 12, 17, 18, 24, & 27), four in *wspD* (JS:C 1, 6, 8, & 15), and two in *wspC* (JS:C 19 & 25). It is of interest to point out that compared to the first screen this gave a much simpler result, with fewer singleton insertions; the *wspR* DGC-encoding gene also coming back into the picture (having no insertions in the first screen). Somehow even with a previous mutation in *wspE*, insertions to this gene in WS TSS-f6-*wspE*mut still suppressed the WS phenotype in seven independent cases. There was also another insertion to the MMR system, with one in *mutS* (JS:C13); and curiously one insertion in *pflu5960* (JS:C21), that obtained many insertions when suppressing the SM phenotype.

Gene[a]	Ins[b]	Size[c]	Protein function[d]	Domains[e]
wspE	7	755	- Histidine kinase of two-component system - *wsp* operon primary mutational pathway of WS	- CheA (3), HPT (1), HATPase (2) - CheW (1)
wspR	7	333	- Response regulator of two-component system - *wsp* operon primary mutational pathway of WS	- CheY (4) - GGDEF (3)

wspA	4	540	- Methyl-accepting chemotaxis protein - *wsp* operon primary mutational pathway of WS	- LBD (2) - Tar (1), MCPsignal (1)
wspD	4	232	- Scaffold protein - *wsp* operon primary mutational pathway of WS	- CheW (2)
wspC	2	419	- Methyltransferase - *wsp* operon primary mutational pathway of WS	- CheR (1)
pflu5960	1	554	- EAL & GGDEF domain - DGC and PDE activity	- None
mutS	1	863	- DNA mismatch repair	- MutS
pyrD	1	341	- Dihydroorotate dehydrogenase activity - Pyrimidine biosynthesis	- PyrD
pflu0679	1	767	- Paraquat-inducible protein (PqiB)	- PqiB

Table 3.6 Summary of the transposon insertions in WS TSS-f6-*wspE*mut suppressing the WS phenotype at 28°C. [a] Gene refers to the gene locus of transposon insertion. [b] Ins refers to number of independent insertions. [c] Size refers to the number of amino acid residues. [d] Protein function refers to the predicted function of the putative gene product. [e] Domains refers to the predicted protein domains of the gene insertions (NCBI CDD, significant expect value), specified in brackets if more than one insertion.

*3.3.2.2 Screen D: SM TSS-f6-*wspE*mut – SM suppressed at 20°C*

The results from Screen D, the transposon mutagenesis of SM TSS-f6-*wspE*mut suppressing SM at 20°C are given in Table 3.7 below – with a total of 25 independent transposon insertions (JS:D 1-25). The cre-mediated excision of the transposon in SM TSS-f6-*wspE*mut mutants restored the phenotype for mutants of *pflu5960* (JS:D12), *amrZ* (JS:D8), and *wspR* (JS:D37) indicating polar effects; while produced no change in phenotype for mutants of *wspA* (JS:D1).

In the second round with SM suppressed in SM TSS-f6-*wspE*mut at 20°C, most of the insertions were again in *pflu5960*, with 21 independent insertions (JS:D 2-7, & 11-25). There was also again one insertion in *amrZ* (JS:D8). It is not clear the effect of these mutations, as the SM phenotype was restored upon cre-deletion of the transposon; this indicating that the insertion had polar effects on downstream genes for both *pflu5960* and *amrZ*. There were also more unexpected insertions to the *wsp* operon, with one independent insertion in *wspA* (JS:D1), and one in *wspR* (JS:D9) that also restored the phenotype after cre-deletion.

Gene[a]	Ins[b]	Size[c]	Protein function[d]	Domains[e]
pflu5960	21	554	- EAL & GGDEF domain - DGC and PDE activity	- GGDEF (11) - EAL (5)
amrZ	1	108	- DNA-binding, regulation of transcription - Negative regulator of the *wss* operon	- Arc
wspR	1	333	- Response regulator of two-component system - *wsp* operon primary mutational pathway of WS	- CheY
wspA	1	540	- Methyl-accepting chemotaxis protein - *wsp* operon primary mutational pathway of WS	- LBD
pflu5574	1	341	- Phosphotransferase enzyme	- APH

Table 3.7 Summary of the transposon insertions in SM TSS-f6-*wspE*mut suppressing the SM phenotype at 20°C. [a] Gene refers to the gene locus of transposon insertion. [b] Ins refers to number of independent insertions. [c] Size refers to the number of amino acid residues. [d] Protein function refers to the predicted function of the putative gene product. [e] Domains refers to the predicted protein domains of the gene insertions (NCBI CDD, significant expect value), specified in brackets if more than one insertion.

3.3.3 Phenotypic characterisation of TSS-f6 *wspE* transposon mutants

The phenotype of the two TSS-f6 transposon mutants for *wspE* were characterised as described in Section 2.2.4.3 – WS TSS-f6-*wspE*mut (JS:A9ΔCre) & SM TSS-f6-*wspE*mut (JS:B22ΔCre). The colony morphology and mat formation ability were of interest as a comparison to TSS-f6, and to further understand how the two TSS-f6 *wspE* mutants were obtained with the same genotype and having an opposite phenotype.

The colony morphology phenotype of the TSS-f6 *wspE* transposon mutants are shown in Figure 3.8 below. The WS TSS-f6-*wspE*mut strongly resembles the L17-*mutS*wt ancestor and TSS-f6 at 20°C, with a strong wrinkly colony; while SM TSS-f6-*wspE*mut resembles SBW25 and TSS-f6 at 28°C, with a smooth colony. The mat formation ability and niche perefence of the two mutants are shown in Figure 3.9 below. The WS TSS-f6-*wspE*mut demonstrates niche preference for the ALI, forming a strong webbed mat at both 28°C and room temperature; while the SM TSS-f6-*wspE*mut resembles the TSS-f6 niche preference at 28°C, with colonisation of both the broth and ALI at both incubation temperatures. Therefore the

WS TSS-f6-*wspE*mut is distinctly WS in colony morphology and in static broth, and the SM TSS-f6-*wspE*mut has a clear SM colony morphology but an indistinct niche preference.

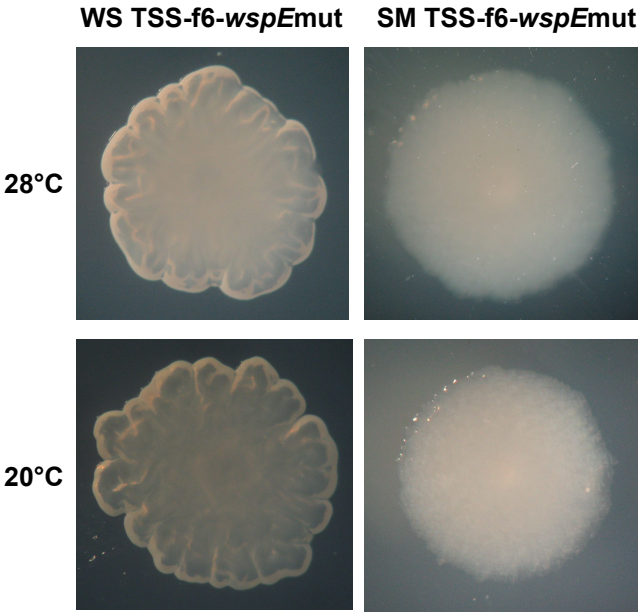

Figure 3.8 Colony morphology phenotypes of TSS-f6 *wspE* transposon mutants at the temperatures of 28 and 20°C. The colony morphology of WS TSS-f6-*wspE*mut and SM TSS-f6-*wspE*mut; the individual colonies observed on KB agar plates incubated at either 28 or 20°C for 3 days.

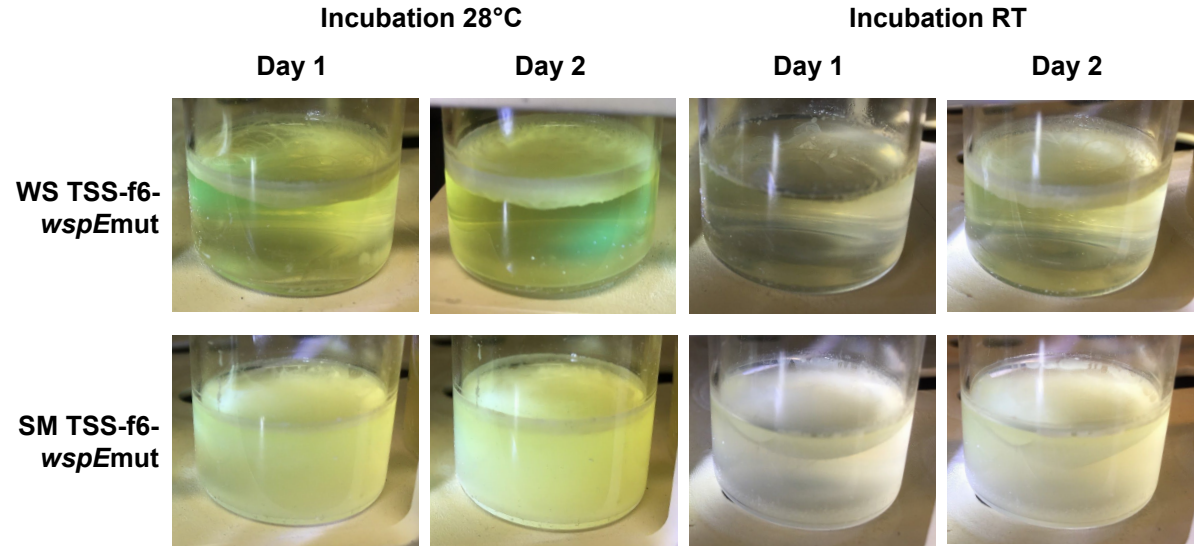

Figure 3.9 Niche preference of TSS-f6 *wspE* transposon mutants. The mat formation ability of WS TSS-f6-*wspE*mut and SM TSS-f6-*wspE*mut; mats observed in static KB broth incubated at either 28°C or room temperature for 2 days.

3.4 Analysis of Mutation Rate

3.4.1 Fluctuation tests

Fluctuation tests were performed to analyse the general spontaneous mutation rate of TSS-f6, compared to SBW25 and the f2 ancestral genotype; as described in Section 2.2.7.1. The results of these experiments estimating mutation rate using resistance to the antibiotics rifampicin (Rif) and nalidixic acid (Nal) are provided in Table 3.8 below; Rif^R (experiment #1) from 12 replicate cultures, and Rif^R & Nal^R (experiment #2) from 16 replicate cultures each. Mutation rate was calculated using the FALCOR fluctuation analysis calculator and MSS-maximum likelihood method (Hall et al., 2009), with the unit: per 10^{-7} mutations, per genome (or cell), per generation.

Selective antibiotic (experiment #)	**Mutation rate (x 10^{-7})** [95% CI]		
	TSS-f6	**SBW25**	**f2 ancestor**
Rif^R (#1)	0.1420 [0.0968; 0.1933]	0.2844 [0.1931; 0.3884]	-
Rif^R (#2)	0.1343 [0.0968; 0.1761]	0.1911 [0.1332; 0.2564]	0.1569 [0.1089; 0.2112]
Nal^R (#2)	2.4083 [2.1264; 2.7031]	0.7729 [0.6176; 0.9407]	3.6227 [3.1895; 4.0759]

Table 3.8 Fluctuation analysis of mutation rate in TSS-f6. The mutation rate (per 10^{-7} mutations/ genome/generation) and 95% confidence interval estimated using resistance to the antibiotic rifampicin (Rif^R) or Nalidixic acid (Nal^R) of TSS-f6, SBW25 and f2 ancestor; calculated from fluctuation tests using the FALCOR fluctuation analysis calculator and MSS-maximum likelihood method.

From the first experiment using Rif^R, the mutation rate (per 10^{-7} mutations/ genome/generation) of TSS-f6 was estimated as 0.1420, and SBW25 as 0.2844; this indicating that TSS-f6 has a slightly reduced mutation rate compared to SBW25 – though not statistically significant as the 95% CI overlaps. From the second experiment using Rif^R, the mutation rate of TSS-f6 was estimated as 0.1343, SBW25 as 0.1911, and f2 as 0.1569; this demonstrates no statistical difference in the mutation rate of these strains. While in the first experiment using Nal^R, the mutation rate of TSS-f6 was estimated as 2.4083, SBW25 as

0.7729, and f2 as 3.6227; this conversely demonstrating that TSS-f6 and the f2 ancestor may have an elevated mutation rate as compared to SBW25.

As the estimation of mutation rate using Rif and Nal resistance gave opposing results, the use of these antibiotics in fluctuation tests and the basis of resistance were considered. Resistance to rifampicin is most commonly due to mutation in the *rpoB* gene (1348 residues), encoding the RNA polymerase β-subunit; the level of resistance dependant on the mutational site (Taniguchi et al., 1996). Though there is also some evidence for Rif^R based on membrane permeability; notably in *P. fluorescens* a plasmid-mediated resistance mechanism has been identified likely involving the efflux of rifampicin (Chandrasekaran & Lalithakumari, 1998). While for nalidixic acid, resistance is due to mutation in the genes *gyrB* (806 residues) or *gyrA* (885 residues), encoding the A and B subunits of DNA gyrase (Yamagishi et al., 1986); with Nal resistance being far lesser characterised. It is useful to note that TSS-f6 does not harbour any existing mutations to any of the Rif^R or Nal^R genes, as confirmed by whole-genome sequencing. For fluctuation tests, rifampicin resistance is better understood and more often used in the literature to estimate mutation rates; based on this, using Rif^R was considered more trustworthy than Nal^R. Therefore from the results with Rif, there is no evidence that the general mutation rate of TSS-f6 genotype is elevated or that it statistically differs from SBW25 or the f2 ancestor.

3.4.2 G tract expansion or contraction

The guanine tracts (G tracts) of genes of interest in the *wss* and *wsp* operons were sequenced to investigate the potential of mutational expansion or contraction of these loci in TSS-f6 or select transposon mutants; as described in Section 2.2.7.2. There was no change observed to the length of G tracts in *wssE*, *wssJ*, *wspC* & *wspR* in TSS-f6 (from overnight cultures), and no changes to the G tracts in *wssE* & *wspR* in TSS-f6, WS TSS-f6-*wspE*mut, SM TSS-f6-*wspE*mut, and the ancestral genotypes L17-*mutS*wt & f2 (from colony scrapings grown at 28 and 20°C). The lack of evidence for changes to the G tracts in TSS-f6 indicates that the environmentally-responsive phenotype is likely not related to the mutational expansion or contraction of these known G tracts in the *wss* and *wsp* operons, as seen in the Line 17 *mutS*-dependant genetic switch (Hammerschmidt et al., 2014).

The TSS-f6 transposon mutants with insertion in the *mutL* and *mutY* genes were also of interest, as mutation to the DNA mismatch repair system often results in an elevated mutation rate, and this hypermutability may result in secondary mutations in the genome. Therefore in the TSS-f6 *mut* mutants the G tracts of interest were checked for evidence of these secondary mutations, that may be causing the suppression of the WS phenotype (rather than the *mutL* or *mutY* mutation in itself). The results are provided in Table 3.9 below; with the G tracts in *wssE*, *wssJ*, *wspC* and *wspR* sequenced in TSS-f6, the TSS-f6 transposon mutants for *mutL* (JS:B 5, 18, & 19) & *mutY* (JS:B13), and the WS TSS-f6-*wspE*mut transposon mutant for *mutS* (JS:C13). There were some changes observed in the TSS-f6 *mut* mutants, though not in all of them. In the TSS-f6 mutant for *mutL* (JS:B5) there was expansion of the G tract by one residue in *wssE* (5 → 6 G's), and by one residue in *wspR* (7 → 10 G's); and in the WS TSS-f6-*wspE*mut mutant for *mutS* (JS:C13) there was contraction of the G tract by one residue in *wspR* (7 → 6 G's). These changes to G tracts in the TSS-f6 *mut* mutants may explain the observance of these unexpected insertions when suppressing the WS in TSS-f6 by transposon mutagenesis. The SM phenotype of these mutants may not be a direct result of the *mut* system mutation, but rather of the secondary mutations in other genes such as these G tracts, due to the resulting hypermutability of a mutation to the MMR system. From the evidence, this may explain at least the two transposon mutants – TSS-f6-*mutL*mut (JS:B5) and WS TSS-f6-*wspE*mut-*mutS*mut (JS:C13).

Genotype	**G tract length**			
	wssE (5 G's)	***wssJ*** (5 G's)	***wspC*** (5 G's)	***wspR*** (7 G's)
TSS-f6	WT	WT	WT	WT
TSS-f6- *mutL*mut (JS:B5)	**+1**	WT	WT	**+1**
TSS-f6- *mutL*mut (JS:B18)	WT	WT	WT	WT
TSS-f6- *mutL*mut (JS:B19)	WT	WT	WT	WT
TSS-f6- *mutY*mut (JS:B13)	WT	WT	WT	WT
WS TSS-f6-*wspE*mut-*mutS*mut (JS:C13)	WT	WT	WT	**−1**

Table 3.9 Guanine tracts lengths in TSS-f6 and *mut* transposon mutants. The lengths of specific guanine tracts (G tract) in the *wss* and *wsp* operons of TSS-f6 and select TSS-f6 *mut* transposon mutants, as determined by sequencing. No changes were observed in the G tracts of TSS-f6; with expansion or contraction observed in TSS-f6 mutants for *mutL* & *mutS*.

Chapter 4: Discussion

4.1 Environmentally-Responsive Phenotype of TSS-f6

The TSS-f6 genotype of *P. fluorescens* SBW25 was derived from a continuation of the Hammerschmidt et al. (2014) life cycle experiment with Line 17-*mutS*wt, passed through 6 further generations of the life cycle (P. Remigi & D. Rexin, unpublished data). TSS-f6 demonstrates an environmentally-responsive ability to change colony morphology phenotype. This transition occurs in a temperature-sensitive manner, from colonies incubated at 28°C having the smooth phenotype and at 20°C the wrinkly phenotype. Although temperature is not the relevant environmental cue, as during the life cycle experiment it was held constant at the optimal of 28°C. The effect of temperature likely mimics that of some other environmental factor – of particular interest is oxygen; under Henry's law the level of dissolved oxygen decreases as temperature increases. It may be hypothesised that at 28°C the growth of *P. fluorescens* SBW25 is maximal; cells within colonies likely grow and divide rapidly, depleting oxygen, and thus cells will experience low levels of oxygen. Conversely, at 20°C the growth is reduced, and oxygen levels within colonies are likely to be higher. Therefore in TSS-f6 the SM phenotype at 28°C may correlate with low oxygen levels, and the WS phenotype at 20°C with high oxygen levels. This influence of environmental oxygen is also supported by the niche preference in static broth – with TSS-f6 at 28°C forming a strong WS mat at the air-liquid interface, in correlation with high oxygen availability.

Within the context of the Hammerschmidt et al. (2014) experiment, oxygen is a major factor driving evolution of the life cycle that transitions between the soma-like WS types and germ-like SM types (Rainey & Kerr, 2010; Libby & Rainey, 2013). Over time, oxygen is eliminated from static broth microcosms due to the metabolic activities of planktonic SM types; thus setting the conditions that provide selective pressure for the evolution of mat-forming WS types. The evolved WS types gain maximal access to oxygen at the ALI, though their success is short-lived due to the presence of SM types within the mat that result in its collapse. Upon collapse of the mat, oxygen again becomes available throughout the

broth phase, which in turn reestablishes the conditions that favour evolution of WS types (Rainey & Kerr, 2010) – this is the basis of the life cycle. If the life cycle transitioning between the WS and SM states were to come under developmental control, then evolving a mechanism that allows responsiveness to environmental oxygen would be a potential way to achieve this. There may be conceived a genotype that expresses the WS phenotype when oxygen is abundant and the SM phenotype when oxygen levels fall below some threshold, allowing the transition through the life cycle without any need for mutational change. The next step is to consider for the TSS-f6 genotype how such a developmental switch may operate, and to produce a model to account for the genetic basis of the environmental responsiveness and resulting change in phenotype.

4.2 Model for the TSS-f6 Developmental Switch

The stability of the change in colony morphology phenotype of TSS-f6 at the two environmental conditions assumes that the environmentally-responsive phenotype has a decipherable GPM, and that the underlying mechanism is under developmental regulation. At first view, the hypothesis would be that the TSS-f6 developmental switch is the result of a genetic change that establishes a genotype responsive to the environment: expressing the WS phenotype at low oxygen levels (or 20°C) and SM phenotype at high oxygen levels (or 28°C). One must now consider whether the experimental evidence provides support – that the TSS-f6 phenotype is based solely on developmental processes.

4.2.1 Mutational background and environmental sensing

It is first necessary to confirm that the TSS-f6 environmentally-responsive phenotype is under developmental regulation, and that there is no genetic difference between the two phenotypic states. From whole-genome sequencing of TSS-f6 colonies grown at both 28 and 20°C there were no mutational differences identified throughout the genome at the two environmental conditions. No differences were also observed from the sequencing of specific G tracts in the *wsp* and *wss* operons. There was no evidence of a general elevated mutation rate in TSS-f6

from fluctuation tests, the mutation rate not differing from that of SBW25 or the f2 ancestor. Therefore no heritable genetic basis of the TSS-f6 phenotype was immediately evident from this data, thus it is reasonable to refer to the capacity to transition in phenotype as a 'developmental switch'.

Whole-genome sequencing also revealed the mutational history of TSS-f6, and subsequently the genetic basis of the environmentally-responsive phenotype. Due to the hypermutator background of Line 17 numerous existing mutations were identified in the *wsp* operon including: two substitutions in *wspA*, one substitution in *wspE*, one 9 bp deletion in *wspB* and one substitution in *wspF*. There were two mutations identified to be unique to the TSS-f6 genotype (and not the f2 ancestral genotype) that are necessary for the developmental switch: a substitution in the methyl-acceptor domain of *wspA* (expanding a G tract from 5 to 7 residues), and a 9 bp duplication in the GGDEF domain of *pflu0458*. The mutational change to these genes must somehow contribute to the TSS-f6 phenotype, either mediating the mechanism of sensing and responding to an environmental cue, or the transition in phenotype from the WS to SM colony morphology.

4.2.1.1 WspA as an oxygen sensor

Although TSS-f6 is observed as temperature-sensitive, it is hypothesised that the level of oxygen is the significant aspect of the environmental condition that is being sensed. The SM phenotype at the higher temperature of 28°C may correlate with low levels of oxygen, and the WS phenotype at 20°C with high levels of oxygen. The *wspA* gene is likely important in the environmental sensing ability of TSS-f6, as WspA acts as a membrane-bound chemotaxis receptor specific for the *wsp* pathway (Bantinaki et al., 2007). It has been previously demonstrated that WspA senses environmental signals by interaction at the ligand-binding domain and methyl-acceptor sites, and that signal transduction is activated by the sensing of growth on a surface including cell-cell contact (Güvener & Harwood, 2007). From computational predictions of protein-protein networks it has also been predicted that WspA is the only chemoreceptor to interact with the *wsp* pathway (Ortega et al., 2017).

In TSS-f6, the mutation in the *wspA* methyl-acceptor domain may allow WspA to sense the environmental cue of oxygen, and respond by signal transduction through the *wsp* pathway resulting in the differential phosphorylation of WspR. A simple model may be considered: at

high oxygen levels (or 20°C) WspA will phosphorylate WspR resulting in c-di-GMP production, biofilm formation, and the WS phenotype; while at low oxygen levels (or 28°C) WspA does not activate WspR resulting in no c-di-GMP production, and the SM phenotype. This model holds for the colony morphology phenotype of TSS-f6, though the indistinct niche preference in static broth may also be explained – at low oxygen levels (or 28°C) there still remains sufficient oxygen on the surface of the broth at the ALI for WspA to sense, resulting in the phosphorylation of WspR, c-di-GMP production and the formation of a mat. The ability of WspA to sense the levels of environmental oxygen and produce a response could potentially relate to reversible changes in patterns of DNA methylation at methylation sites in *wspA*, or differences in binding at the ligand-binding receptor (Bantinaki et al., 2007). To produce a model sufficient to explain the TSS-f6 environmentally-responsive phenotype and developmental switch, further information is required, notably the results of suppressor analysis.

4.2.2 Suppressor analysis and activation pathways

The suppressor analysis achieved by two rounds of transposon mutagenesis with TSS-f6 suppressing the WS and SM phenotype at either 28 or 20°C, revealed the activation pathways and important genes involved in the environmentally-responsive phenotype. The transposon insertion in the following genes were identified to suppress the WS colony morphology: the *wsp* operon (*wspE*, *wspD* & *wspA*; *wspR* & *wspC* from second round), the *wss* operon (*wssE* & *wssB*), the MMR system (*mutL* & *mutY*; *mutS* from second round), and various genes related to metabolism and transport. And to suppress the SM colony morphology: *pflu5960*, *amrZ*, *pflu0479*, and *wspE* (also *wspA* from second round). From these results, various hypotheses will be outline to explain the phenotypes of WS at 20°C and SM at 28°C, and the mutational activation pathways underlying the TSS-f6 developmental switch.

4.2.2.1 Hypothesis: WS at 20°C

The WS phenotype of TSS-f6 at 20°C generally makes sense regarding what is known about this system, with insertions in the *wsp* and *wss* operon suppressing this phenotype. The *wss* operon is the structural basis of the WS phenotype, encoding the cellulose synthase machinery required to produce acetylated cellulose; overproduction of this resulting in cells

able to stick together and thus the formation of a biofilm (Spiers et al., 2003). The *wsp* operon is the primary mutational pathway for the WS phenotype, the gene products controlling activation of the DGC-containing WspR that synthesises c-di-GMP; high c-di-GMP levels activating the production of cellulose by the *wss* operon, and thus biofilm formation (Bantinaki et al., 2007). Therefore in TSS-f6, mutation to genes in the *wsp* and *wss* operon will result in the suppression of the WS phenotype by decreasing c-di-GMP levels or preventing formation of the cellulose synthase complex, thus preventing the expression of *wss* and cellulose production. The insertions in genes relating to metabolism and transport may be explained by their effect on the global intracellular levels of the c-di-GMP secondary messenger – though not directly relevant to the mechanism of the switch. The *mut* MMR system insertions lead to speculation, so will later be taken into consideration.

The TSS-f6 WS phenotype at 20°C may therefore be explained in the following model: the WspA methyl-accepting chemoreceptor detects the high levels of environmental oxygen and activates the WspE histidine kinase (linked by WspB & WspD, and controlled by methylation from WspC & WspF), this results in the phosphorylation of WspR and production of c-di-GMP by the DGC activity; high c-di-GMP levels activate the *wss* operon and the overproduction of acetylated cellulose, this cell-cell glue enabling the cells to form a biofilm and thus the WS colony morphology and niche preference is observed.

4.2.2.2 Hypothesis: SM at 28°C

The SM phenotype of TSS-f6 at 28°C may be explained with a more complex model, linking the genes *amrZ*, *pflu5960*, and *wspE* to regulation of the *wss* operon and production of cellulose. The involvement of these genes in maintaining the SM phenotype indicates that a simple model with the chemoreceptor WspA sensing oxygen and resulting in the differential methylation of WspR is not enough – *amrZ*, *pflu5960*, and *wspE* must come into play to explain the TSS-f6 environmentally-responsive phenotype. The *amrZ* gene product is a global transcriptional regulator of motility, alginate synthesis, and biofilm formation in *Pseudomonas* (Martínez-Granero et al., 2014). AmrZ is also known to be a negative repressor of the *wss* operon, with the expression correlated with decreased levels of intracellular c-di-GMP (Jones at al., 2014). *pflu5960* has the GGDEF and EAL domains, Pflu 5960 predicted to have PDE activity (DGC inactive), and thus the ability to break down the

c-di-GMP secondary messenger. The mutations to *amrZ* and *pflu5960* will therefore result in suppression of the SM phenotype by increasing levels of c-di-GMP.

While the *wspE* gene encodes the WspE hybrid histidine kinase/response regulator; the histidine kinase transduces signals, and the response regulator receives signals by the acceptance of phosphoryl groups and mediates a cellular response. In models of the *wsp* pathway, WspE is activated by the WspA chemoreceptor, and transfers phosphoryl groups to WspR (Bantinaki et al., 2007; O'Connor et al., 2012). To explain the role of *wspE*, it may be considered that the *wsp* pathway in TSS-f6 has been rewired due to the number of underlying mutations, resulting in the WspE histidine kinase not only transferring phosphoryl groups to WspR but also to other recievers. It is plausible that due to the mutational rewiring of TSS-f6, WspE may be communicating with both WspR and Pflu 5960 – the target of signal transduction and acceptor of phosphoryl groups from WspE dependant on the environmental conditions and sensing by WspA. This alteration to the *wsp* signal transduction and role of WspE may help to explain how TSS-f6 transposon mutants were obtained with insertions in *wspE* suppressing both the WS and SM phenotype (refer to WS & SM TSS-f6-*wspE*mut). Therefore in this case the mutation to *wspE* may suppress the SM phenotype by preventing the transfer of phosphoryl groups to Pflu 5960, this will increase c-di-GMP levels by decreasing the PDE activity of Pflu 5960, and potentially preventing activation of the AmrZ negative regulator.

The TSS-f6 SM phenotype at 28°C may therefore be explained in the following model: the WspA methyl-accepting chemoreceptor detects the low levels of environmental oxygen and activates the WspE histidine kinase; WspE then preferentially transfers phosphoryl group to Pflu 5960, this results in the degradation of c-di-GMP by PDE activity; the negative regulator AmrZ is also activated by Pflu 5960 (or an unknown environmental stress signal) giving a further decrease to c-di-GMP levels; the low level of c-di-GMP prevents activation of the *wss* operon and production of cellulose, thus no biofilm is formed and the SM colony morphology and niche preference (except at the ALI of static broth) is observed.

4.2.2.3 Dilemma of the TSS-f6 wspE *mutants*

The two models outlined above regarding the TSS-f6 environmentally-responsive phenotype provide a role for WspE, though this still does not explain the phenotypes of the WS & SM

TSS-f6-*wspE*mut. Here we face a major dilemma – the same genotype TSS-f6 with a mutation disrupting *wspE* (transposon scar left after cre-deletion, no polar effects confirmed) resulting in either the WS or SM phenotype, when derived from the transposon mutagenesis of TSS-f6 at 28 or 20°C respectively. Although highly unlikely, perhaps due to unknown mechanisms the transposon insertion did not disrupt the *wspE* gene completely, and some functionality remained; though this still does not explain how a mutation in *wspE* may result in opposite phenotypes – this is altogether unexpected. This leads to the questioning of our original assumption that the TSS-f6 phenotype is under complete developmental regulation, rather than having some mutational basis; for example in the case of the Line 17 *mutS*-dependent genetic switch (Hammerschmidt et al., 2014). For the TSS-f6-*wspE*mut genotype to have both the WS and SM phenotype suggests that there must be some other heritable genetic (or epigenetic) change to the genotype that has not been found from the methods of whole-genome sequencing used; this unidentified mutational difference may also be contributing to the environmentally-responsive phenotype of TSS-f6. This strange result in combination with the observation of transposon insertions to the DNA mismatch repair system (*mutL*, *mutY* & *mutS*), leads to the deliberation of an alternative model, to be discussed in the next section.

4.2.3 Significance of the MMR system

Involvement of the DNA mismatch repair (MMR) system in the TSS-f6 phenotype must be taken into consideration, with insertions to the *mutL* and *mutY* genes (and *mutS* from the second round) obtained from the transposon mutagenesis of TSS-f6 in which the WS phenotype was suppressed. The MMR system repairs mutations due to errors in DNA replication or DNA damage from environmental agents or metabolic processes, thus maintaining the fidelity of DNA. In this system the MutL enzyme has weak ATPase activity, and assists in a general manner in the formation of a complex with MutH & MutS at a mismatched base on DNA for repair. While MutY has a specific function in aiding the repair of G:A mismatches (to G:C) in DNA lesions resulting from oxidative damage (Modrich, 1991). The insertions to these *mut* genes in TSS-f6 may either be explained by the MMR system having a direct effect on maintaining the WS phenotype at high oxygen levels (or 20°C), or an indirect effect with the hypermutability resulting in secondary mutations that

themselves suppress WS. The direct and indirect effect of mutations in *mutL* and *mutY* will each be examined for TSS-f6, and how this may fit into the model for the environmentally-responsive phenotype.

4.2.3.1 Hypothesis: MMR system and oxygen

The direct effect of the MMR system speculates that the *mutL* and *mutY* genes are essential to the WS phenotype of TSS-f6 at 20°C. Under the proposed model for TSS-f6, the environmental cue for the transition in phenotype is the level of environmental oxygen sensed by WspA. Oxygen (O_2) may result in DNA damage and oxidative stress in cells at both high and low levels in the environment. In conditions of hyperoxia (high O_2), mutagenesis may be induced by the extensive production of reactive oxygen species; while in hypoxia (low O_2), the lack of oxygen and effect of this on metabolic processes may hinder the repair of DNA damage, and also potentially produce reactive oxygen species (Chandel & Scott Budinger, 2007; Yuan et al., 2000). From this knowledge, a potential new model may be presented for the TSS-f6 environmentally-responsive phenotype relating to DNA damage, high/low levels of oxygen, and activity of the MMR system. It may be hypothesised that in TSS-f6 there is a bias for mutation in a specific genetic contingency loci – specifically for the expansion and contraction of G tracts in genes of the *wss* and *wsp* operons, as seen by Hammerschmidt et al. (2014). Under this model TSS-f6 will have a high mutation rate, and DNA damage in these contingency loci due to reactive oxygen species, or perhaps other unknown mechanisms.

The TSS-f6 SM phenotype at 28°C may therefore be explained in the following model: WspA senses low oxygen levels; the MMR system and *mutL* and *mutY* are inactive due to the hypoxic conditions, and the DNA damage in *wss* or *wsp* G tracts is not repaired; the G tract mutation causes WS to be repressed and thus the SM phenotype is observed. And the TSS-f6 WS phenotype at 20°C: WspA senses high oxygen levels; the MMR system and *mutL* and *mutY* are active, and repair the DNA damage in *wss* or *wsp* G tracts; WS is expressed and thus the WS phenotype is observed. This model would explain how the mutations to *mutL* and *mutY* result in suppression of the WS phenotype at 20°C, which is also appropriate given the specific function of MutY in G:A oxidative damage repair.

4.2.3.2 Alternate hypothesis: Secondary mutations

Although it is interesting to consider this potential model for the TSS-f6 phenotypic switching mediated by the MMR system, it is still a long shot to fully endorse this model. The experimental results do not provide any support – no temperature-sensitive mutations or the expansion and contraction of known G tracts were identified in TSS-f6. The alternate hypothesis of the indirect effect of the MMR system may be more plausible, with mutations to *mutL* and *mutY* resulting in a general elevated mutation rate in TSS-f6. This hypermutability may then result in secondary mutations at other genetic loci that cause the suppression of WS, therefore not the *mut* mutation directly. This is supported by the results of G tract sequencing in the TSS-f6 transposon mutants for the *mut* genes, with expansion or contraction of the G tracts in *wspR* and *wssE* identified in the mutants with insertions in *mutL* and *mutS*. Therefore the MMR system may play a role in the TSS-f6 phenotype, but it is more likely that it is just due to an indirect effect on the WS phenotype by the repair of mutations in G tracts.

4.2.4 Final model for the TSS-f6 developmental switch

It is evident that the TSS-f6 environmentally-responsive phenotype is very complex; from all the evidence available at present, a simple model was constructed to explain the genetic basis of the TSS-f6 developmental switch. A diagrammatic summary of this model is provided in Figure 4.1 below, subsequently explaining the WS phenotype at 20°C and the SM phenotype at 28°C. This model was based on the assumption that the phenotype is under developmental regulation, dependant on developmental processes and an interaction with the environment. Though this is still under speculation, due to the observation of TSS-f6 *wspE* mutants with opposite phenotypes, and the potential involvement of the DNA mismatch repair system.

The final model for the TSS-f6 developmental switch is explained as follows. The chemoreceptor WspA (with mutation) senses the level of oxygen in the environment – high O_2 at 20°C and low O_2 at 28°C; WspA then activates the histidine kinase WspE. Due to rewiring of the *wsp* pathway in TSS-f6, WspE is able to interact and send phosphoryl groups (℗) to both WspR and Pflu 5960. At high O_2 levels (20°C, ALI at 28°C): WspE phosphorylates the DGC-containing WspR, the DGC activity produces the c-di-GMP secondary messenger; the high c-di-GMP levels result in activation of the *wss* operon (ON),

overproduction of acetylated cellulose, biofilm formation, and the WS colony morphology of TSS-f6. At low O_2 levels (28°C): WspE phosphorylates the DGC/PDE-containing Pflu 5960, the PDE activity degrades c-di-GMP and causes activation of the AmrZ regulator; AmrZ also negatively regulates the *wss* operon; the low c-di-GMP levels result in repression of the *wss* operon (OFF), no biofilm formation, and the SM colony morphology of TSS-f6.

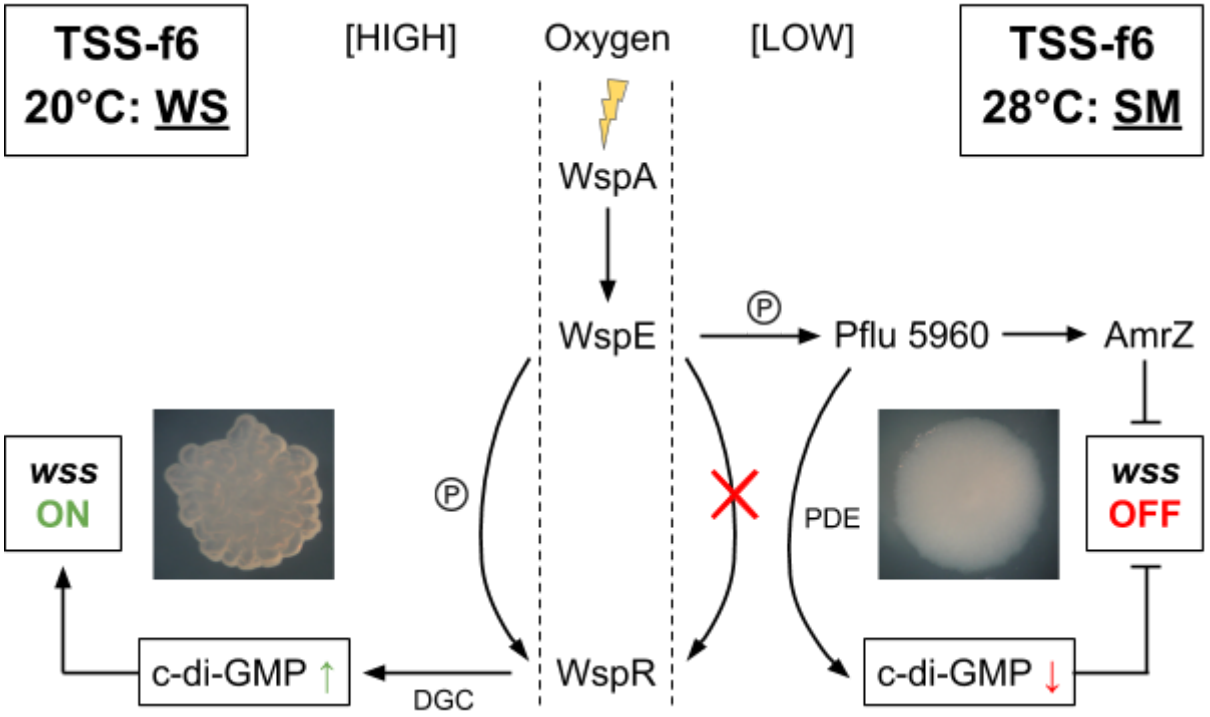

Figure 4.1 Model for the genetic basis of the TSS-f6 developmental switch. The WspA chemoreceptor senses the level of environmental oxygen, and activates the WspE histidine kinase. At 20°C (high O_2): WspE phosphorylates WspR, DGC-activity increases c-di-GMP levels, and the *wss* operon ON results in the WS phenotype. At 28°C (low O_2): WspE phosphorylates Pflu 5960, PDE-activity increases c-d-GMP levels, AmrZ is activated and represses *wss*, and the *wss* operon OFF results in the SM phenotype.

4.3 Concluding Remarks

4.3.1 Conclusion

The work reported in this thesis describes the undertaking of a genetic dissection of an environmentally-responsive phenotype of *P. fluorescens* SBW25, evolved from an

experimental exploration of the origins of multicellularity (Hammerschmidt et al., 2014). The TSS-f6 genotype has evolved the capacity to transition between the soma-like SM and germ-like WS phases of the life cycle, under regulation by developmental processes (P. Rainey, personal communication, January 24, 2018). On the face of it, this appears to be be based on mechanisms that allow sensing of environmental levels of oxygen, and consequently the changing of phenotype. From the mutational background of TSS-f6, the substitution identified in the methyl-acceptor domain of *wspA* is likely important; the WspA chemoreceptor hypothesised to sense oxygen levels in the environment. The suppressor analysis investigation also defined the activation pathways and set of genes necessary for the expression of the WS phenotype at 20°C and the SM phenotype at 28°C in TSS-f6. These were identified as: WS phenotype – the *wsp* operon, *wss* operon, and MMR system (*mutL* & *mutY*); SM phenotype – *pflu5960*, *amrZ*, and *wspE*. Strikingly from this analysis, mutations to the *wspE* gene in TSS-f6 generated opposing phenotypes from transposon mutagenesis, allowing suppression of both the WS at 20°C and the SM at 28°C. The only interpretation of this unexpected result is that there is some heritable genetic (or epigenetic) difference between the genotype at the two environmental conditions and phenotypic states. It also leads to the consideration that the TSS-f6 environmentally-responsive phenotype is not under complete developmental regulation – that some other unknown mechanisms may be at play here. It is tempting to invoke a role for the DNA mismatch repair system, though the experimental evidence does not provide direct support for this. Therefore a simple model was constructed for the TSS-f6 developmental switch, to provide the most rational explanation given the wide range of experimental results; refer to Figure 4.1 in Section 4.2.4.

In the evolutionary origin of multicellular life, for the transition in Darwinian individuality required the emergence of reproduction at the level of the cell collective (Godfrey-Smith, 2009). It is unclear how this occurred, though it has been argued that it required a life cycle in which the transitioning between single cell and collective phases were integrated by a developmental program (Ratcliff et al., 2017). The work completed for the TSS-f6 genotype provided a unique opportunity to gain mechanistic insight into the emergence of a nascent life cycle under developmental regulation. In contrast to the *mutS*-dependent genetic switch described previously by Hammerschmidt et al. (2014), the TSS-f6 developmental switch took

it one step further – demonstrating an environmentally-responsive ability to transition through the life cycle, likely based on a developmental program.

4.3.2 Future directions

There is most definitely more work to be done to better characterize the TSS-f6 genotype, and to test the predictions of the model constructed for the developmental switch. The first obvious missing piece of evidence is the confirmation that oxygen is the significant cue behind the TSS-f6 environmentally-responsive phenotype. This may be investigated with the use of oxygen probes, and comparison of growth under different levels of environmental oxygen; for example using oxygen-controlled chambers to produce hypoxic and hyperoxic conditions. The model predicts that increasing O_2 levels will result in the WS phenotype, and that decreasing O_2 levels will result in the SM phenotype. If the hypothesis also holds that the correlation between temperature and oxygen is based on cell growth within colonies, it may be predicted that increasing the temperature will give the similar result as decreasing it (low growth rate giving increased O_2 levels and the WS phenotype); this may be tested experimentally. The niche preference of TSS-f6 could be explored further, including a comparison of the strength of the types of mat formed at 28 and 20°C; for example an experiment may be taken out using glass beads placed as weights on mats to test durability. The mat formed by 'WS types' of TSS-f6 at 28°C (with the SM colony morphology) could also be compared to other WS types using competition experiments; for example by the equal inoculation of static broths with TSS-f6 and a true WS type (e.g. L17-*mutS*wt or LSWS), followed by fitness tests. This mat may also be further examined by Calcofluor staining, to give an indication of the levels of cellulose production by TSS-f6 cells in the mat at the ALI of static broths at 28 and 20°C.

Regarding the understanding of the genetic basis of the TSS-f6 developmental switch, there is further investigation to be complete. Importantly, is solving the dilemma of the TSS-f6 *wspE* mutants having both the WS and SM phenotype, and the involvement of the MMR system in the TSS-f6 phenotype. For the WS & SM TSS-f6-*wspE*mut, the assembly of genomes from Nanopore long-read sequencing (or hybrid assembly with short-read data) may reveal mutational differences that were not found in the Illumina short-read assembly alone. The involvement of *wspE* could also be explored by the deletion of the entire *wspE* gene by

site-directed mutagenesis, in the two *wspE* mutants and TSS-f6 colonies at both 28 and 20°C. If the deletion of *wspE* in TSS-f6 grown at either temperature also results in the opposite phenotypes – then something truly strange is going on here. The same could be complete for the DNA mismatch repair genes, with the deletion of *mutL* and *mutY* in TSS-f6, and examination of the effect on phenotype.

To provide further support for the model of the TSS-f6 developmental switch requires the construction of important mutations in the TSS-f6 genotype and ancestral genotypes. Most importantly is to reconstruct the TSS-f6 *wspA* mutation in the most recent f2 ancestor, Line 17 *mutS*wt ancestor, and SBW25 – to confirm the role of WspA in the sensing of environmental oxygen. As this mutation in *wspA* establishes a G tract of 7 residue length, the significance of this should be investigated for the TSS-f6 phenotype; for example this G tract could be sequenced in depth to find evidence for mutational expansion or contraction. The roles of the *pflu5960, amrZ*, and *wspE* genes in both the TSS-f6 environmentally-responsive phenotype and general WS phenotype may be explored by the specific mutation or deletion of these genes in TSS-f6, ancestral genotypes and SBW25. There are also two other temperature-sensitive genotypes of *P. fluorescens* SBW25 derived from lines of the Hammerschmidt et al. (2014) life cycle experiment (TSS-g11 & TSS-c4), also discovered by chance as with TSS-f6. The characterisation and suppressor analysis of these other environmentally-responsive phenotypes would be useful as a comparison to TSS-f6, and may provide support for the model of the developmental switch. Whole-genome sequencing would reveal if they have a shared mutational background (e.g. *wspA*), and transposon mutagenesis if the underlying activation pathways are similar (e.g. *pflu5960*, *wspE* & *amrZ*).

An important point should be made here about the design of the Hammerschmidt et al. (2014) life cycle experiment – that it does not allow for the discovery of these environmentally-responsive genotypes. This experiment does select for the ability to transition through the life cycle, with the evolution of WS and SM types driven by the environmental factor of oxygen; it thus provides the conditions that may select for evolution of genotypes responsive to oxygen, but due to the experimental design it does not allow them to persist (with phenotypic screening for WS colonies at 28°C). Therefore it is evident that

the design of the life cycle experiment should be reconsidered for the future, and that there is a range of further work to follow through from that completed in this thesis.

Bibliography

Alberch, P. (1991). From genes to phenotype: Dynamical systems and evolvability. *Genetica, 84*(1), 5-11.

Bantinaki, E., Kassen, R., Knight, C. G., Robinson, Z., Spiers A. J., & Rainey, P. B. (2007). Adaptive divergence in experimental populations of Pseudomonas fluorescens. III. Mutational origins of wrinkly spreader diversity. *Genetics, 176*, 441-453. doi:10.1534/genetics.106.069906.

Barnett, M. B. (2015). *Evolution of the Genotype-Phenotype Map* (Master's thesis, Massey University, Auckland, New Zealand). Retrieved from: http://mro.massey.ac.nz/handle/10179/8339

Barrick Lab. (2017). *Protocols Fluctuation Tests*. Retrieved from: http://barricklab.org/twiki/bin/view/Lab/ProtocolsFluctuationTests

Bateson, W. (1909). *Mendel's Principles of Heredity*. Cambridge, United Kingdom: Cambridge University Press.

Beaumont, H. J. E., Gallie, J., Kost, C., Ferguson, G. C., & Rainey, P. A. (2009). Experimental evolution of bet hedging. *Nature, 462*, 90-93. doi:10.1038/nature08504.

Calcott, B., & Sterelny, K. (2011). *The Major Transitions in Evolution Revisited*. Cambridge, MA: The MIT Press.

Chandel, N. S., & Scott Budinger, G. R. (2007). The cellular basis for diverse responses to oxygen. *Free Radical Biology and Medicine, 42*(2), 165-174. doi:10.1016/j.freeradbiomed.2006.10.048

Chandrasekaran, S., & Lalithakumari, D. (1998). Plasmid-mediated rifampicin resistance in Pseudomonas fluorescens. *Journal of Medical Microbiology, 47*, 197-200.

Christen, B., Christen, M., Paul, R., Schmid, F., Folcher, M., Jenoe, P., ... Jenal, U. (2006). Allosteric control of cyclic di-GMP signaling. *The Journal of Biological Chemistry, 281*(42), 32015-32024.

Ciliberti, S., Martin, O. C., & Wagner, A. (2007). Innovation and robustness in complex regulatory gene networks. *PNAS, 104*(34), 13591-13596.

Coggan, K. A., & Wolfgang, M. C. (2012). Global regulatory pathways and cross-talk control Pseudomonas aeruginosa environmental lifestyle and virulence phenotype. *Current Issues in Molecular Biology, 14*, 47-70.

Continenza, B. (2009). The Darwinian view of life. In Minelli, A., & Contrafatto, G. *Biological Science Fundamentals and Systematics* (Vol. 1, pp. 277-285). Oxford, United Kingdom: Eolss Publishers Co. Ltd.

Conway Morris, S. (1998). *The Crucible of Creation: The Burgess Shale and the Rise of Animals*. Oxford, England: Oxford University Press.

Darwin, C. (1859). *On the Origin of Species by Means of Natural Selection* (1st ed.) London, England: John Murray.

Das, S., Noe, J. C., Paik, S., & Kitten, T. (2005). An improved arbitrary primed PCR method for rapid characterization of transposon insertion sites. *Journal of Microbiological Methods, 63*, 89-94. doi:10.1016/j.mimet.2005.02.011.

Deatherage, D. E., Barrick, J. E. (2014). Identification of mutations in laboratory-evolved microbes from next-generation sequencing data using breseq. *Methods in Molecular Biology, 1151*, 165-188.

De Monte, S., & Rainey, P. B. (2014). Nascent multicellular life and the emergence of individuality. *Journal of Biosciences, 39*(2), 237-248. doi:10.1007/s12038-014-9420-5.

Dobzhansky, T (1937). *Genetics and the Origin of Species*. Columbia University Biological Series. New York: Columbia University Press.

Drake, J. W., Charlesworth, B., Charlesworth, D., & Crow, J. F. (1998). Rates of spontaneous mutation. *Genetics, 148*(4), 1667-1686.

Farr, A. (2015). *Formalist features determining the tempo and mode of evolution in Pseudomonas fluorescens SBW25* (Doctoral thesis, Massey University, Auckland, New Zealand). Retrieved from: http://mro.massey.ac.nz/handle/10179/7215

Ferguson, G. C., Bertels, F., & Rainey, P. B. (2013). Adaptive divergence in experimental populations of Pseudomonas fluorescens. V. Insight into the niche specialist fuzzy spreader compels revision of the model Pseudomonas radiation. *Genetics, 195*, 1319-1335. doi:10.1534/genetics.113.154948.

Fisher, R. A. (1930). *The Genetical Theory of Natural Selection*. Oxford, United Kingdom: The Clarendon Press.

Foster, P. L. (2006). Methods for determining spontaneous mutation rates. *Methods in Enzymology, 409*, 195-213. doi:10.1016/S0076-6879(05)09012-9.

Gallie, J., Libby, E., Bertels, F., Remigi, P., Jendresen, C. B., Ferguson, G. C., … Rainey, P. B. (2015). Bistability in a metabolic network underpins the de novo evolution of colony switching in Pseudomonas fluorescens. *PLOS Biology 13*(3). doi:10.1371/journal.pbio.1002109

Gallie, J. (2010). *Evolutionary and molecular origins of a phenotypic switch in Pseudomonas fluorescens SBW25* (Doctoral thesis, Massey University, Auckland, New Zealand). Retrieved from: http://mro.massey.ac.nz/handle/10179/1215

Giddens, S. R., Jackson, R. W., Moon, C. D., Jacobs, M. A., Zhang, X., Gehrig, S. M., & Rainey, P. B. (2007). Mutational activation of niche-specific genes provides insight into regulatory networks and bacterial function in a complex environment. *PNAS, 104*(46), 18247-18252. doi:10.1073/pnas.0706739104.

Gompel, N., & Prud'homme, B. (2009). The causes of repeated genetic evolution. *Developmental Biology, 332*, 36-47. doi:10.1016/j.ydbio.2009.04.040.

Gould, S. J., & Eldredge, N. (1977). Punctuated equilibria: the tempo and mode of evolution reconsidered. *Paleobiology, 3*, 115-151.

Gould, S. J. (1977). *Ontogeny and Phylogeny*. MA, US: Harvard University Press.

Gould, S. J. (1989). *Wonderful Life: The Burgess Shale and the Nature of History*. New York, NY: W. W. Norton & Company.

Gould, S. J. (2002). *The Structure of Evolutionary Theory*. MA, US: Harvard University Press.

Goymer, P., Kahn, S. G., Malone, J. G., Gehrig, S. M., Spiers A. J., & Rainey, P. B. (2006). Adaptive divergence in experimental populations of Pseudomonas fluorescens. II. Role of the GGDEF regulator WspR in evolution and development of the wrinkly spreader phenotype. *Genetics, 173*, 515-526. doi:10.1534/genetics.106.055863.

Güvener, Z. T., & Harwood, C. S. (2007). Subcellular location characteristics of the Pseudomonas aeruginosa GGDEF protein, WspR, indicate that it produces cyclic-di-GMP in response to growth on surfaces. *Molecular Microbiology, 66*(6), 1459-1473. doi:10.1111/j.1365-2958.2007.06008.x.

Hall, B. M., Ma, C., Liang, P., & Singh, K. K. (2009). Fluctuation analysis calculator (FALCOR): A web tool for the determination of mutation rate using Luria-Delbruck fluctuation analysis. *Bioinformatics, 25*, 12, 1564-1565.

Hammerschmidt, K., Rose, C. J., Kerr, B., & Rainey, P. B. (2014). Life cycles, fitness decoupling and the evolution of multicellularity. *Nature, 515*, 75-79. doi:10.1038/nature13884.

Henderson, I. R., Owen, P., & Nataro, J. P. (1999). Molecular switches - the ON and OFF of bacterial phase variation. *Molecular Microbiology, 33*(5), 919-932.

Hengge, R. (2009). Principles of c-di-GMP signalling in bacteria. *Nature Reviews Microbiology, 7*, 263-273. doi:10.1038/nrmicro2109.

Huxley, J. (1942). *Evolution: The Modern Synthesis*. London, United Kingdom: Allen & Unwin.

Jones, C. J., Newsom, D., Kelly, B., Irie, Y., Jennings, L. K., Xu, B., ... Wozniak, D. J. (2014). ChIP-seq and RNA-seq reveal an AmrZ-mediated mechanism for cyclic di-GMP synthesis and biofilm development by Pseudomonas aeruginosa. *PLOS Pathogens, 10*(3). doi:10.1371/journal.ppat.1003984.

Kussel, E., & Leibler, S. (2005). Phenotypic diversity, population growth, and information in fluctuating environments. *Science, 309*, 2075-2078. doi:10.1126/science.1114383.

Lewontin, R. C. (1970). The units of selection. *Annual Review of Ecology and Systematics, 1*, 1-18. doi:10.1146/annurev.es.01.110170.000245.

Libby, E., & Rainey, P. B. (2013a). A conceptual framework for the evolutionary origins of multicellularity. *Physical Biology, 10*(3). doi:10.1088/1478-3975/10/3/035001.

Libby, E., & Rainey, P. B. (2013b). Eco-evolutionary feedback and the tuning of proto-developmental life cycles. *PLOS ONE, 8*(12). doi:10.1371/journal.pone.0082274.

Lind, P. A., Farr, A. D., & Rainey, P. B. (2015). Experimental evolution reveals hidden diversity in evolutionary pathways. *eLife, 4*. doi:10.7554/eLife.07074.

Luria, S. E., & Delbrück, M. (1943). Mutations of bacteria from virus sensitivity to virus resistance. *Genetics, 28*, 491-511.

Malthus, T. R. (1798). *An Essay on the Principle of Population* (1st ed.). London, England: J. Johnson.

Manoil, C. (2000). Tagging exported proteins using Escherichia coli alkaline phosphatase gene fusions. *Methods in Enzymology, 326*, 35-47.

Marchler-Bauer, A., Lu, S., Anderson, J. B., Chitsaz, F., Derbyshire, M. K., DeWeese-Scott, C., ... Gwadz, M. (2011). CDD: a Conserved Domain Database for the functional annotation of proteins. *Nucleic Acids Research, 39*, D225-229.

Martínez-Granero, F., Redondo-Nieto, M., Vesga, P., Martín, M., & Rivilla, R. (2014). AmrZ is a global transcriptional regulator implicated in iron uptake and environmental adaption in P. fluorescens F113. *BMC Genomics, 15*(237).

Maynard Smith, J., & Szathmáry, E. (1995). *The Major Transitions in Evolution*. Oxford, UK: Oxford University Press.

Mayr, E (1942). *Systematics and the Origin of Species, from the Viewpoint of a Zoologist*. Cambridge: Harvard University Press.

McDonald, M. J., Gehrig, S. M., Meintjes, P. L., Zhang, X., & Rainey, P. B. (2009). Adaptive divergence in experimental populations of Pseudomonas fluorescens. IV. Genetic constraints guide evolutionary trajectories in a parallel adaptive radiation. *Genetics, 183*, 1041-1053. doi:10.1534/genetics.109.107110.

Michod, R. E., & Roze, D. (2001). Cooperation and conflict in the evolution of multicellularity. *Heredity, 86*, 1-7. doi:10.1046/j.1365-2540.2001.00808.x.

Modrich, P. (1991). Mechanisms and biological effects of mismatch repair. *Annual Review of Genetics, 25*, 229-53.

Ortega, D. R., Fleetwood, A. D., Krell, T., Harwood, C. S., Jensen, G. J., & Zhulin, I. B. (2017). Assigning chemoreceptors to chemosensory pathways in Pseudomonas aeruginosa. *PNAS, 114*(48), 12809-12814. doi:10.1073/pnas.1708842114.

Oster, G., & Alberch, P. (1982). Evolution and bifurcation of developmental programs. *Evolution, 36*(3), 444-459. doi:10.1111/j.1558-5646.1982.tb05066.x.

O'Connor, J. R., Kuwada, N. J., Huangyutitham, V., Wiggins, P. A., & Harwood, C. S. (2012). Surface sensing and lateral subcellular localization of WspA, the receptor in a chemosensory-like system leading to c-di-GMP production. *Molecular Microbiology, 86*(3), 720-729. doi:10.1111/mmi.12013.

Pigluicci, M. (2007). Do we need an extended evolutionary synthesis? *Evolution, 61*(12), 2743-2749. doi:10.1111/j.1558-5646.2007.00246.x.

Pigluicci, M. (2010). Genotype–phenotype mapping and the end of the 'genes as blueprint' metaphor. *Philosophical Transactions of the Royal Society B, 365*, 557-566. doi:10.1098/rstb.2009.0241.

Porello, S. L., Williams, S. D., Kuhn, H., Michaels, M. L., & David, S. S. (1996). Specific recognition of substrate analogs by the DNA mismatch repair enzyme MutY. *Journal of the American Chemical Society, 118*, 10684-10692.

Rainey, P. B., & Bailey, M. J. (1996). Physical and genetic map of the Pseudomonas fluorescens SBW25 chromosome. *Molecular Microbiology, 19*(3), 521-533.

Rainey, P. B., & Kerr, B. (2010). Cheats as first propagules: A new hypothesis for the evolution of individuality during the transition from single cells to multicellularity. *BioEssays, 32*, 872-880. doi:10.1002/bies.201000039

Rainey, P. B., & Rainey, K. (2003). Evolution of cooperation and conflict in experimental bacterial populations. *Nature, 425*, 72-74.

Rainey, P. B., & Travisano, M. (1998). Adaptive radiation in a heterogeneous environment. *Nature, 394*, 69-72.

Rainey, P. B. (1999). Adaptation of Pseudomonas fluorescens to the plant rhizosphere. *Environmental Microbiology, 1*(3), 243-257.

Ratcliff, W. C., Herron, M., Conlin, P. L., & Libby, E. (2017). Nascent life cycles and the emergence of higher-level individuality. *Philosophical Transactions of the Royal Society B, 372*. doi:10.1098/rstb.2016.0420.

Remigi, P., Ferguson, G. C., De Monte, S., & Rainey, P. B. (2018). Pyrimidine starvation activates a bistable phenotypic switch leading to ribosome provisioning and rapid exit from stationary phase. *bioRxiv*. doi:10.1101/244129

Rosche, W. A., & Foster, P. L. (2000). Determining mutation rates in bacterial populations. *Methods, 20*(1), 4-17.

Saavedra, J. T., Schwartzman, J. A., & Gilmore, M. S. (2017). Mapping transposon insertions in bacterial genomes by arbitrarily primed PCR. *Current Protocols in Molecular Biology, 118*(15). doi:10.1002/cpmb.38.

Schick, I., Bailey, S. F., & Kassen, R. (2015). Evolution of fitness trade-offs in locally adapted populations of Pseudomonas fluorescens. *The American Naturalist, 186*(S1), S48-S59.

Silby, M. W., Cerdeño-Tárraga, A. M., Vernikos, G. S., Giddens, S. R., Jackson, R. W., Preston, G. M., … Thomson, N. R. (2009). Genomic and genetic analyses of diversity and plant interactions of Pseudomonas fluorescens. *Genome Biology, 10*(R51).

Simpson, G. G. (1944) *Tempo and Mode in Evolution*. New York: Columbia University Press.

Spiers, A. J., Bohannon, J., Gehrig, S. M., & Rainey, P. B. (2003). Biofilm formation at the air–liquid interface by the Pseudomonas fluorescens SBW25 wrinkly spreader requires an acetylated form of cellulose. *Molecular Microbiology, 50*(1), 15-27. doi:10.1046/j.1365-2958.2003.03670.x.

Spiers, A. J., Kahn, S. G., Bohannon, J., Travisano, M., & Rainey, P. B. (2002). Adaptive divergence in experimental populations of Pseudomonas fluorescens. I. Genetic and phenotypic bases of wrinkly spreader fitness. *Genetics, 161*, 33-46.

Stern, D. L., & Orgogozo, V. (2009). Is genetic evolution predictable? *Science, 323*(5915), 746-751.

Szathmáry, E., & Maynard Smith, J. (1995). The major evolutionary transitions. *Nature, 374*, 227-232. doi: 10.1038/374227a0.

Taniguchi, H., Aramaki, H., Nikaido, Y., Mizuguchi, Y., Nakamura, N., Koga, T., & Yoshida, H. (1996). Rifampicin resistance and mutation of the rpoB gene in Mycobacterium tuberculosis. *FEMS Microbiology Letters, 144*, 103-108.

Travisano, M., Mongold, J. A., Bennett, A. F., & Lenski, R. E. (1995). Experimental tests of the roles of adaptation, chance, and history in evolution. *Science, 264*(5194), 87-90.

Wagner, G. P., & Altenberg, L. (1996). Perspective: complex adaptations and the evolution of evolvability. *Evolution, 50*(3), 967-976.

West-Eberhard, M. J. (1989). Phenotypic plasticity and the origins of diversity. *Annual Review of Ecology, Evolution, and Systematics, 20*, 249-78.

Winsor, G. L., Griffiths, E. J., Lo, R., Dhillon, B. K., Shay, J. A., & Brinkman, F. S. (2016). Enhanced annotations and features for comparing thousands of Pseudomonas genomes in the Pseudomonas genome database. *Nucleic Acids Research, 44*(Database issue). doi:10.1093/nar/gkv1227.

Wolpert, L., & Szathmáry, E. (2002). Evolution and the egg. *Nature, 420*, 745-.

Yamagishi, J., Yoshida, H., Yamayoshi, M., & Nakamura, S. (1986). Nalidixic acid-resistant mutations of the gyrB gene of Escherichia coli. *Molecular Genetics and Genomics, 204*, 367-373.

Yuan, J., Narayanan, L., Rockwell, S., & Glazer, P. M. (2000). Diminished DNA repair and elevated mutagenesis in mammalian cells exposed to hypoxia and low pH. *Cancer Research, 60*(16), 4372-4376.

Appendices

Appendix 1: Mutational history of TSS-f6

#[a]	Gene	Annotation	Mutation	Change[b]	Freq[c]	P-value[d]	Residue[e]	Protein effect[f]
1	*pflu0458*	GGDEF/EAL domain protein	Insertion	+ GTCA GGTTG	87.2	1.8×10^{-183}	469	9 bp duplication (D → DNLT)
2	*wspA*	methyl-accepting chemotaxis protein	SNP	T → G	100.0	1.0×10^{-213}	441	Substitution (V → G)
3	*pflur18*	23S ribosomal RNA	SNP	T → C	97.9	6.7×10^{-8}	-	-

Table 1. Mutations identified in TSS-f6 from whole-genome sequencing. [a] # refers to the number of the mutation. [b] Change refers to the nucleotide sequence change. [c] Freq refers to the variant frequency (%). [d] P-value refers to the variant P-value. [e] Residue refers to the amino acid residue number of the mutation in the protein. [f] Protein effect refers to the change to the amino acid code of the protein.

#[a]	Gene	Annotation	Mutation	Change[b]	Freq[c]	P-value[d]	Residue[e]	Protein effect[f]
1	*wspA*	methyl-accepting chemotaxis protein	SNP	C → A	98.1	5.8×10^{-315}	104	Substitution (T → N)
2	*wspE*	chemotaxis-related two-component system, sensor kinase	SNP	A → T	98.6	7.1×10^{-202}	70	Substitution (H → L)

Table 2. Mutations identified in f2 ancestor from whole-genome sequencing. [a] # refers to the number of the mutation. [b] Change refers to the nucleotide sequence change. [c] Freq refers to the variant frequency (%). [d] P-value refers to the variant P-value. [e] Residue refers to the amino acid residue number of the mutation in the protein. [f] Protein effect refers to the change to the amino acid code of the protein.

#[a]	Gene	Annotation	Mutation	Change[b]	Freq[c]	P-value[d]	Residue[e]	Protein effect[f]
1	19 bp↓ *pflu0046*	-	Insertion	G(4) + G	100.0	1.0×10^{-80}	-	-
2	*pflu0046*	hydrolase	SNP	A → G	100.0	$2.5\text{x}10^{-22}$	142	None
3	*fic*	cell filamentation protein	SNP	C → T	97.7	$2.7\text{x}10^{-129}$	164	None
4	*gpmI*	phosphoglycero mutase	SNP	C → G	100.0	4.0×10^{-47}	300	Substitution (A → P)
5	*glnA*	glutamine synthetase	SNP	C → T	98.2	5.5×10^{-161}	310	Substitution (G → S)
6	*hutU*	urocanate hydratase	SNP	C → T	97.2	3.6×10^{-111}	356	Substitution

								(R → C)
7	*pflu0541*	hypothetical protein	Insertion	G(6) + G	97.8	1.1×10^{-126}	331	Frame Shift
8	*ureA*	urease subunit gamma	SNP	C → T	97.8	4.5×10^{-131}	89	Substitution (G → S)
9	*prmA*	ribosomal protein L11 methyltransferase	SNP	G → A	100.0	7.9×10^{-97}	259	None
10	*dppA1*	dipeptide ABC transporter substrate-binding protein	SNP	T → C	100.0	5.0×10^{-166}	494	Substitution (D → G)
11	*pflu0872*	modulation of DNA gyrase-like protein	SNP	A → G	97.7	6.8×10^{-121}	410	None
12	17 bp↓ *pflu0872*	-	Insertion	+ C	94.1	1.7×10^{-39}	-	-
13	*pflu0917*	exported peptidase	Insertion	G(5) + G	100.0	3.2×10^{-218}	173	Frame Shift
14	*hprA*	glycerate dehydrogenase	SNP	A → G	100.0	3.2×10^{-102}	239	None
15	56 bp↓ *lpxC*	-	Deletion	T(10) − T	97.8	2.7×10^{-56}	-	-
16	*pflu1093*	fimbrial outer membrane usher protein	Insertion	G(8) + G	83.3	1.1×10^{-50}	660	Frame Shift
17	12 bp↓ *pflu1191*	-	Deletion	T(9) − T	100.0	1.3×10^{-17}	-	-
18	*wspA*	methyl-accepting chemotaxis protein	SNP	G → T	100.0	3.2×10^{-116}	253	Substitution (D → Y)
19	*wspB*	chemotaxis-like protein	Deletion	− GCCG AAGTG	100.0	2.5×10^{-58}	37	Deletion (− AEV)
20	*wspF*	chemotaxis-specific methylesterase	SNP	T → G	96.0	2.5×10^{-71}	295	Substitution (I → S)
21	*pflu1490*	GntR family transcriptional regulator	SNP	A → G	100.0	1.3×10^{-61}	81	None
22	*pflu1593*	hypothetical protein	Insertion	G(7) + G	97.7	1.1×10^{-116}	33	Frame Shift
23	*pflu1668*	polysaccharide biosynthesis-related membrane protein	Insertion	G(6) + G	93.8	1.7×10^{-131}	502	Frame Shift
24	*kdpB*	potassium-transporting ATPase subunit B	SNP	C → T	97.1	1.4×10^{-104}	397	None
25	*pflu1849*	two-component system sensor kinase	Insertion	G(8) + G	95.2	2.1×10^{-49}	39	Frame Shift
26	3 bp↑ *pflut43*	-	SNP	T → A	93.3	9.5×10^{-39}	-	-
27	1 bp↑ *pflut43*	-	Insertion	+ A	100.0	1.6×10^{-45}	-	-
28	*gabD2*	succinate-semialdehyde dehydrogenase	SNP	A → G	100.0	5.0×10^{-134}	414	None
29	*pflu1990*	transporter-like membrane	SNP	C → T	100.0	2.5×10^{-167}	371	Substitution

		protein						(G → S)
30	5 bp↑ *pflu2000*	-	SNP	A → G	98.0	3.1×10^{-162}	-	-
31	38 bp↓ *pflu2019*	-	SNP	G → A	98.5	2.7×10^{-213}	-	-
32	*pflu2041*	ABC transporter substrate-binding protein	SNP	A → G	100.0	1.6×10^{-119}	4	Substitution (V → A)
33	*pflu2079*	polysaccharide exported-related lipoprotein	SNP	C → T	100.0	3.2×10^{-78}	87	Substitution (D → N)
34	*pflu2156*	hypothetical protein	SNP	A → G	95.1	6.5×10^{-111}	88	Substitution (S → P)
35	9 bp↑ *pflu2167*	-	SNP	A → G	100.0	1.3×10^{-119}	-	-
36	*pflu2267*	two-component system fusion protein	SNP	A → G	100.0	1.0×10^{-87}	1,059	None
37	*pflu2295*	methyl-accepting chemotaxis protein	SNP	A → G	100.0	2.0×10^{-57}	363	Substitution (D → G)
38	52 bp↓ *pflu2296*	-	Insertion	G(7) + G	97.7	6.8×10^{-121}	-	-
39	*pflu2381*	hypothetical protein	Insertion	G(9) + G	85.7	2.1×10^{-53}	364	Frame shift
40	*pflu2732*	hypothetical protein	SNP	C → T	95.0	4.0×10^{-62}	254	None
41	*pflu2743*	ABC transporter permease	SNP	G → A	100.0	2.0×10^{-84}	50	None
42	*pflu2807*	nicotinamide mono-nucleotide transporter	SNP	A → G	91.7	2.8×10^{-89}	167	Substitution (L → P)
43	*pflu2947*	ABC transporter peri-plasmic binding protein	SNP	C → T	100.0	4.0×10^{-65}	283	Substitution (G → R)
44	45 bp↓ *pflu3031*	-	Insertion	C(6) + C	100.0	5.0×10^{-108}	-	-
45	*pflu3049*	oxidoreductase	SNP	C → T	100.0	5.0×10^{-136}	120	Truncation
46	*pflu3130*	sensory box GGDEF/ EAL domain-containing protein	SNP	T → C	100.0	1.0×10^{-58}	275	None
47	22 bp↓ *pflu3155*	-	Deletion	− CC	100.0	1.6×10^{-41}	-	-
48	18 bp↓ *pflu3157*	-	Insertion	C(8) + C	92.9	6.0×10^{-84}	-	-
49	*pflu3409*	methyl-accepting chemotaxis protein	SNP	T → C	96.4	1.1×10^{-85}	187	None
50	*pflu3426*	bifunctional reductase	SNP	G → A	96.2	8.2×10^{-67}	642	Substitution (E → K)
51	*pflu3488*	hypothetical protein	Insertion	C(6) + C(2)	100.0	6.3×10^{-82}	102	Frame Shift
52	15 bp↓	-	SNP	A → G	96.9	8.0×10^{-196}	-	-

	pflu3647							
53	*pflu3728*	ribose ABC transporter ATP-binding protein	SNP	C → T	97.5	4.0×10^{-116}	35	Substitution (S → L)
54	*pflu3951*	substrate-binding periplasmic protein	Insertion	C(7) + C	85.7	9.0×10^{-29}	210	Frame shift
55	*pflu4017*	amino acid ABC transporter permease	Insertion	C(7) + C	98.2	1.8×10^{-158}	25	Frame Shift
56	*pflu4042*	pyridine nucleotide-disulfide oxidoreductase	Insertion	C(6) + C	97.5	2.0×10^{-104}	236	Frame Shift
57	*pflu4306*	GGDEF/GAF domain sensory box protein	SNP	G → C	100.0	1.0×10^{-62}	135	Substitution (A → P)
58	*pflu4466*	patatin-like phospholipase	Insertion	C(5) + C	100.0	1.0×10^{-108}	331	Frame Shift
59	*pflu4600*	regulatory protein	SNP	T → C	100.0	2.0×10^{-96}	157	Substitution (Y → C)
60	*pflu4769*	hypothetical protein	SNP	G → A	100.0	1.6×10^{-125}	576	Substitution (A → T)
61	30 bp↑ *pflu4801*	-	SNP	T → C	96.8	1.9×10^{-189}	-	-
62	*pflu4976*	HlyD family secretion protein	Deletion	C(8) − C	100.0	4.0×10^{-51}	304	Frame Shift
63	27 bp↓ *pflu5147*	-	Insertion	C(7) + C	100.0	6.3×10^{-162}	-	-
64	*pflu5210*	signaling-related membrane protein	SNP	G → A	100.0	1.0×10^{-99}	207	Substitution (P → L)
66	*pflu5210*	signaling-related membrane protein	SNP	T → G	100.0	1.0×10^{-140}	27	Substitution (T → P)
67	*pflu5213*	exodeoxyribonuclease V subunit beta	SNP	G → A	96.0	6.3×10^{-69}	627	None
68	*pflu5329*	sensory box GGDEF/ EAL domain-containing protein	SNP	T → C	97.4	3.0×10^{-121}	970	Substitution (F → L)
69	*pflu5329*	sensory box GGDEF/ EAL domain-containing protein	SNP	C → T	100.0	1.3×10^{-214}	1,194	Truncation
70	*rpe*	ribulose-phosphate 3-epimerase	SNP	G → A	100.0	2.5×10^{-172}	159	Substitution (R → C)
71	*pflu5629*	TonB-dependent membrane protein	SNP	G → A	100.0	7.9×10^{-159}	732	Substitution (G → S)
72	*pflu5883*	hypothetical protein	SNP	G → A	100.0	1.6×10^{-129}	52	Substitution (D → N)
73	*pflu5883*	hypothetical protein	SNP	G → A	97.1	1.4×10^{-208}	105	Substitution (G → S)
74	*pflu5978*	hypothetical protein	SNP	T → C	97.8	4.6×10^{-125}	36	Substitution (Y → H)

75	*pflu6104*	hypothetical protein	SNP	G → A	100.0	4.0×10^{-135}	632	None

Table 2. Mutations identified in f2 ancestor from whole-genome sequencing. [a] # refers to the number of the mutation. [b] Change refers to the nucleotide sequence change. [c] Freq refers to the variant frequency (%). [d] P-value refers to the variant P-value. [e] Residue refers to the amino acid residue number of the mutation in the protein. [f] Protein effect refers to the change to the amino acid code of the protein.

Appendix 2: Transposon mutants of TSS-f6

#[a]	Phenotype[b]	BLAST[c]	Pflu	Gene	Annotation	Ins[d]	Domain[e]
1	Wrinkly	0	5960	*pflu5960*	EAL/GGDEF domain-containing protein	40	None
2	Wrinkly	0	5960	*pflu5960*	EAL/GGDEF domain-containing protein	40	None
3	Wrinkly+	3.0×10^{-79}	4744	*amrZ*	DNA-binding protein	30	Arc repressor
4	Wrinkly+	2.0×10^{-79}	4744	*amrZ*	DNA-binding protein	106	None
5	Wrinkly+	8.0×10^{-173}	4744	*amrZ*	DNA-binding protein	73	None
6	Wrinkly	0	5960	*pflu5960*	EAL/GGDEF domain-containing protein	19	None
7	Wrinkly	6.0×10^{-90}	5960	*pflu5960*	EAL/GGDEF domain-containing protein	327	EAL
8	Wrinkly	2.0×10^{-84}	5960	*pflu5960*	EAL/GGDEF domain-containing protein	156	GGDEF
9	Wrinkly	7.0×10^{-40}	1223	*wspE*	chemotaxis-related two-component system, sensor kinase	660	CheY
10	Wrinkly	2.0×10^{-05}	1223	*wspE*	chemotaxis-related two-component system, sensor kinase	618	CheY
11	Wrinkly	2.0×10^{-06}	5960	*pflu5960*	EAL/GGDEF domain-containing protein	74	None
12	Wrinkly	1.0×10^{-86}	5960	*pflu5960*	EAL/GGDEF domain-containing protein	184	GGDEF
13	Wrinkly	0	5960	*pflu5960*	EAL/GGDEF domain-containing protein	40	None
14	Wrinkly	1.0×10^{-12}	5699	*pflu5699*	Hypothetical protein	186	Unknown
15	Wrinkly+	1.0×10^{-86}	4744	*amrZ*	DNA-binding protein	120 bp↑	None
16	Wrinkly+	0	4744	*amrZ*	DNA-binding protein	8	None
17	Wrinkly	6.0×10^{-85}	5960	*pflu5960*	EAL/GGDEF domain-containing protein	205	GGDEF
18	Wrinkly	1.0×10^{-31}	5960	*pflu5960*	EAL/GGDEF domain-containing protein	60	None
19	Wrinkly	0	5960	*pflu5960*	EAL/GGDEF domain-containing protein	493	EAL
20	Wrinkly	1.0×10^{-13}	5960	*pflu5960*	EAL/GGDEF domain-containing protein	276	GGDEF
21	Wrinkly	6.0×10^{-60}	5960	*pflu5960*	EAL/GGDEF domain-containing protein	41	None
22	Wrinkly+	6.0×10^{-30}	4744	*amrZ*	DNA-binding protein	65	None

23	Wrinkly+	2.0×10^{-09}	4744	*amrZ*	DNA-binding protein	77	None
24	Wrinkly	0	1223	*wspE*	chemotaxis-related two-component system, sensor kinase	688	CheY
25	Wrinkly	2.0×10^{-04}	5960	*pflu5960*	EAL/GGDEF domain-containing protein	397	EAL
26	Wrinkly	1.0×10^{-17}	0479	*pflu0479*	glycosyl transferase	251	None
27	Wrinkly	0	5960	*pflu5960*	EAL/GGDEF domain-containing protein	240	GGDEF
28	Wrinkly	0	5960	*pflu5960*	EAL/GGDEF domain-containing protein	76	None
29	Wrinkly	4.0×10^{-79}	5960	*pflu5960*	EAL/GGDEF domain-containing protein	527	EAL

Table 1. Screen A: Transposon mutants obtained from transposon mutagenesis of TSS-f6 at 28°C (SM → WS). [a] # refers to the number of the transposon mutant (JS:A#); all being independent transposon insertions. [b] Phenotype refers to the colony morphology at 28°C; Wrinkly+ indicating a strong wrinkly colony. [c] BLAST refers to the expect value for the BLAST nucleotide sequence search. [d] Ins refers to the amino acid residue number of the transposon insertion. [e] Domain refers to the predicted protein domain of the insertion (NCBI CDD, significant expect value).

#[a]	Phenotype[b]	BLAST[c]	Pflu	Gene	Annotation	Ins[d]	Domain[e]
1	Smooth	3.0×10^{-18}	5860	*pflu5860*	hypothetical protein	233	OprD
2	Smooth	2.0×10^{-156}	0396	*phaA*	poly(3-hydroxyalkanoate) polymerase	362	PhaC
3	Smooth	0	1915	*pflu1915*	hypothetical protein	395	None
4	Smooth	0.044	4413	*pflu4413*	chemotaxis-specific methylesterase	155	None
5	Smooth	4.0×10^{-100}	0518	*mutL*	DNA mismatch repair protein	540	MutL C terminal
6	Smooth	5.0×10^{-161}	2094	*pflu2094*	hypothetical protein	106	NADB
7	Smooth	9.0×10^{-69}	2663	*pflu2663*	putative exported fatty acid cis/trans isomerase	396	CTI
8	Smooth	9.0×10^{-137}	2019	*pflu2019*	amino acid transporter-like protein	29	RhtB
9	Smooth	2.0×10^{-99}	4478	*pflu4478*	glutathione peroxidase	113	TRX
10	Smooth	1.0×10^{-97}	1222	*wspD*	chemotaxis-like protein	209	CheW
11	Smooth	1.0×10^{-7}	5265	*carB*	carbamoyl phosphate synthase large subunit	708	ATP binding
12	Smooth	0	4426	*pflu4426*	flagellar protein FliO	110	FliO
13	Smooth	1.0×10^{-127}	0323	*mutY*	A/G-specific adenine glycosylase	76	Endonuclease III
14	Smooth	0	3892	*pflu3892*	biotin carboxylase subunit of acetyl-CoA carboxylase	139	CPS L chain ATP binding
15	Smooth	9.0×10^{-19}	0085	*pflu0085*	hypothetical protein	649	GGDEF
16	Smooth	2.0×10^{-11}	1223	*wspE*	chemotaxis-related two-component system, sensor kinase	171	CheA

17	Smooth	4.0×10^{-82}	2489	*pflu2489*	hypothetical protein	225	PEP mutase
18	Smooth	1.0×10^{-16}	0518	*mutL*	DNA mismatch repair protein	262	MutL transducer
19	Smooth	0	0518	*mutL*	DNA mismatch repair protein	479	MutL C terminal
20	Smooth	6.0×10^{-130}	0978	*pflu0978*	hypothetical protein	136	Unknown
21	Smooth	4.0×10^{-142}	3995	*pflu3995*	sugar transporter ATP-binding protein	119	ATPase
22	Smooth	2.0×10^{-31}	1223	*wspE*	chemotaxis-related two-component system, sensor kinase	81	HPT
23	Smooth	0	4159	*pflu4159*	ribose transporter ATP-binding protein	332	ABC Carb Monos II
24	Smooth*	1.0×10^{-140}	1219	*wspA*	methyl-accepting chemotaxis protein	186	Tar
25	Smooth*	6.0×10^{-105}	3331	*pflu3331*	hypothetical protein	191	EamA
26	Smooth*	8.0×10^{-93}	5277	*pdhR*	pyruvate dehydrogenase complex repressor	242	FadR C terminal
27	Smooth*	3.0×10^{-14}	1223	*wspE*	chemotaxis-related two-component system, sensor kinase	469	HATPase
28	Smooth*	5.0×10^{-165}	1223	*wspE*	chemotaxis-related two-component system, sensor kinase	741	CheY
29	Smooth*	2.0×10^{-54}	3739	*pflu3739*	ABC transporter substrate-binding protein	129	TauA
30	Smooth*	0.043	4319	*pflu4319*	leucine rich-repeat protein	22	None
31	Smooth*	2.0×10^{-69}	0304	*wssE*	cellulose synthase operon protein C	159	BcsC
32	Smooth*	3.0×10^{-78}	0301	*wssB*	cellulose synthase catalytic subunit	386	CESA
33	Smooth*	2.0×10^{-141}	4458	*phhA*	phenylalanine 4-monooxygenase	189	PhhA
34	Smooth*	2.0×10^{-153}	3120	*pflu3120*	cytochrome b561	101	CybB
35	Smooth*	4.0×10^{-47}	1222	*wspD*	chemotaxis-like protein	163	CheW
36	Smooth*	5.0×10^{-130}	1223	*wspE*	chemotaxis-related two-component system, sensor kinase	379	HATPase

Table 2. Screen B: Transposon mutants obtained from transposon mutagenesis of TSS-f6 at 20°C (WS → SM). [a] # refers to the number of the transposon mutant (JS:B#); all being independent transposon insertions. [b] Phenotype refers to the colony morphology at 20°C; Smooth* indicating a smooth colony with a semi-wrinkly center. [c] BLAST refers to the expect value for the BLAST nucleotide sequence search. [d] Ins refers to the amino acid residue number of the transposon insertion. [e] Domain refers to the predicted protein domain of the insertion (NCBI CDD, significant expect value).

#[a]	Phenotype[b]	BLAST[c]	Pflu	Gene	Annotation	Ins[d]	Domain[e]
1	Smooth	1.0×10^{-75}	1222	*wspD*	chemotaxis-like protein	38	None
2	Smooth	1.2×10^{-01}	4603	*pyrD*	dihydroorotate dehydrogenase 2	112	PyrD
3	Smooth	6.0×10^{-29}	0679	*pflu0679*	paraquat-inducible protein	1547	PqiB
4	Smooth	5.0×10^{-95}	1225	*wspR*	chemotaxis-related two component system response regulator	47	CheY
5	Smooth	0	1222	*wspD*	chemotaxis-like protein	35	None
6	Smooth	2.0×10^{-34}	1219	*wspA*	methyl-accepting chemotaxis protein	494	MCPsignal
7	Smooth	4.0×10^{-13}	1223	*wspE*	chemotaxis-related two-component system, sensor kinase	99	HPT
8	Smooth	1.0×10^{-79}	1222	*wspD*	chemotaxis-like protein	143	CheW
9	Smooth	6.0×10^{-18}	1225	*wspR*	chemotaxis-related two component system, response regulator	302	GGDEF
10	Smooth	9.0×10^{-31}	1219	*wspA*	methyl-accepting chemotaxis protein	38	LBD
11	Smooth	5.0×10^{-78}	1219	*wspA*	methyl-accepting chemotaxis protein	304	Tar
12	Smooth	1.0×10^{-54}	1225	*wspR*	chemotaxis-related two component system, response regulator	85	CheY
13	Smooth	4.0×10^{-60}	1164	*mutS*	DNA mismatch repair protein MutS	806	MutS
14	Smooth	6.0×10^{-112}	1223	*wspE*	chemotaxis-related two-component system, sensor kinase	196	CheA
15	Smooth	2.0×10^{-13}	1222	*wspD*	chemotaxis-like protein	183	CheW
16	Smooth	9.0×10^{-139}	1223	*wspE*	chemotaxis-related two-component system, sensor kinase	580	CheW
17	Smooth	1.0×10^{-104}	1225	*wspR*	chemotaxis-related two component system, response regulator	81	CheY
18	Smooth	5.0×10^{-118}	1225	*wspR*	chemotaxis-related two component system, response regulator	34	CheY
19	Smooth	0	1221	*wspC*	chemotaxis-related methyltransferase	419	None
20	Smooth	2.0×10^{-79}	1223	*wspE*	chemotaxis-related two-component system, sensor kinase	276	CheA
21	Smooth	2.0×10^{-16}	5960	*pflu5960*	EAL/GGDEF domain-containing protein	289	None
22	Smooth	1.0×10^{-25}	1223	*wspE*	chemotaxis-related two-component system, sensor kinase	439	HATPase
23	Smooth	3.0×10^{-60}	1223	*wspE*	chemotaxis-related two-component system, sensor kinase	298	CheA
24	Smooth	4.0×10^{-29}	1225	*wspR*	chemotaxis-related two component system, response regulator	322	GGDEF
25	Smooth	2.0×10^{-66}	1221	*wspC*	chemotaxis-related methyltransferase	199	CheR

26	Smooth	2.0×10^{-89}	1219	*wspA*	methyl-accepting chemotaxis protein	117	LBD
27	Smooth	2.0×10^{-70}	1225	*wspR*	chemotaxis-related two component system, response regulator	245	GGDEF
28	Smooth	5.0×10^{-147}	1223	*wspE*	chemotaxis-related two-component system, sensor kinase	372	HATPase

Table 3. Screen C: Second round transposon mutants obtained from transposon mutagenesis of WS TSS-f6-*wspE*mut (JS:A9ΔCre) at 28°C (WS → SM). [a] # refers to the number of the transposon mutant (JS:C#); all being independent transposon insertions. [b] Phenotype refers to the colony morphology at 28°C. [c] BLAST refers to the expect value for the BLAST nucleotide sequence search. [d] Ins refers to the amino acid residue number of the transposon insertion. [e] Domain refers to the predicted protein domain of the insertion (NCBI CDD, significant expect value).

#[a]	Phenotype[b]	BLAST[c]	Pflu	Gene	Annotation	Ins[d]	Domain[e]
1	Wrinkly+	3.0×10^{-82}	1219	*wspA*	methyl-accepting chemotaxis protein	116	LBD
2	Wrinkly+	0	5960	*pflu5960*	EAL/GGDEF domain-containing protein	38	None
3	Wrinkly+	2.0×10^{-86}	5960	*pflu5960*	EAL/GGDEF domain-containing protein	320	EAL
4	Wrinkly+	0	5960	*pflu5960*	EAL/GGDEF domain-containing protein	523	EAL
5	Wrinkly+	7.0×10^{-112}	5960	*pflu5960*	EAL/GGDEF domain-containing protein	249	GGDEF
6	Wrinkly+	3.0×10^{-7}	5960	*pflu5960*	EAL/GGDEF domain-containing protein	273	GGDEF
7	Wrinkly+	0	5960	*pflu5960*	EAL/GGDEF domain-containing protein	3 bp↓	None
8	Wrinkly+	2.0×10^{-6}	4744	*amrZ*	DNA-binding protein	59	Arc repressor
9	Wrinkly+	9.0×10^{-26}	1225	*wspR*	chemotaxis-related two component, system response regulator	37	CheY
10	Wrinkly+	2.0×10^{-36}	5574	*pflu5574*	phosphotransferase	187	APH
11	Wrinkly+	3.0×10^{-16}	5960	*pflu5960*	EAL/GGDEF domain-containing protein	279	GGDEF
12	Wrinkly+	0	5960	*pflu5960*	EAL/GGDEF domain-containing protein	438	EAL
13	Wrinkly+	0	5960	*pflu5960*	EAL/GGDEF domain-containing protein	246	GGDEF
14	Wrinkly+	2.0×10^{-62}	5960	*pflu5960*	EAL/GGDEF domain-containing protein	203	GGDEF
15	Wrinkly+	2.0×10^{-47}	5960	*pflu5960*	EAL/GGDEF domain-containing protein	131	GGDEF
16	Wrinkly+	2.0×10^{-52}	5960	*pflu5960*	EAL/GGDEF domain-containing protein	373	EAL
17	Wrinkly+	0	5960	*pflu5960*	EAL/GGDEF domain-containing protein	39	None
18	Wrinkly+	2.0×10^{-43}	5960	*pflu5960*	EAL/GGDEF domain-containing protein	276	GGDEF
19	Wrinkly+	2.0×10^{-78}	5960	*pflu5960*	EAL/GGDEF domain-containing protein	186	GGDEF
20	Wrinkly+	0	5960	*pflu5960*	EAL/GGDEF domain-containing protein	45	None
21	Wrinkly+	2.0×10^{-47}	5960	*pflu5960*	EAL/GGDEF domain-containing protein	201	GGDEF

22	Wrinkly+	5.0×10^{-17}	5960	*pflu5960*	EAL/GGDEF domain-containing protein	392	EAL
23	Wrinkly+	4.0×10^{-29}	5960	*pflu5960*	EAL/GGDEF domain-containing protein	59	None
24	Wrinkly+	5.0×10^{-18}	5960	*pflu5960*	EAL/GGDEF domain-containing protein	250	GGDEF
25	Wrinkly+	3.0×10^{-10}	5960	*pflu5960*	EAL/GGDEF domain-containing protein	273	GGDEF

Table 4. Screen D: Second round transposon mutants obtained from transposon mutagenesis of SM TSS-f6-*wspE*mut (JS:B22ΔCre) at 20°C (SM → WS). [a] # refers to the number of the transposon mutant (JS:D#); all being independent transposon insertions. [b] Phenotype refers to the colony morphology at 20°C; Wrinkly+ indicating a strong wrinkly colony. [c] BLAST refers to the expect value for the BLAST nucleotide sequence search. [d] Ins refers to the amino acid residue number of the transposon insertion. [e] Domain refers to the predicted protein domain of the insertion (NCBI CDD, significant expect value).